AD_____

Award Number: W81XWH-04-1-0183

TITLE: Mechanistic Studies of Oligonucleotide Aptamers with Potent Antiproliferative and Pro-apoptotic Activity against Prostate Cancer Cells

PRINCIPAL INVESTIGATOR: Paula J. Bates, Ph.D.

CONTRACTING ORGANIZATION: University of Louisville
Louisville, KY 40292-0001

REPORT DATE: May 2007

TYPE OF REPORT: Final

PREPARED FOR: U.S. Army Medical Research and Materiel Command
Fort Detrick, Maryland 21702-5012

# REPORT DOCUMENTATION PAGE

*Form Approved*
*OMB No. 0704-0188*



| **1. REPORT DATE** *(DD-MM-YYYY)* | **2. REPORT TYPE** | **3. DATES COVERED** *(From - To)* |
|---|---|---|
| 01-05-2007 | Final | 1 May 2004 – 30 Apr 2007 |

**4. TITLE AND SUBTITLE**

Mechanistic Studies of Oligonucleotide Aptamers with Potent Antiproliferative and Pro-apoptotic Activity against Prostate Cancer Cells

**5a. CONTRACT NUMBER**

**5b. GRANT NUMBER**
W81XWH-04-1-0183

**5c. PROGRAM ELEMENT NUMBER**

**6. AUTHOR(S)**

Paula J. Bates, Ph.D.

E-Mail: paula.bates@louisville.edu

**5d. PROJECT NUMBER**

**5e. TASK NUMBER**

**5f. WORK UNIT NUMBER**

**7. PERFORMING ORGANIZATION NAME(S) AND ADDRESS(ES)**

University of Louisville
Louisville, KY 40292-0001

**8. PERFORMING ORGANIZATION REPORT NUMBER**

**9. SPONSORING / MONITORING AGENCY NAME(S) AND ADDRESS(ES)**
U.S. Army Medical Research and Materiel Command
Fort Detrick, Maryland 21702-5012

**10. SPONSOR/MONITOR'S ACRONYM(S)**

**11. SPONSOR/MONITOR'S REPORT NUMBER(S)**

**12. DISTRIBUTION / AVAILABILITY STATEMENT**
Approved for Public Release; Distribution Unlimited

**13. SUPPLEMENTARY NOTES**

**14. ABSTRACT** G-rich oligos (GROs) are a novel class of protein-binding aptamers that selectively inhibit the proliferation of cancer cells. One of the GROs, named AS1411 (formerly AGRO100), is currently in human clinical trials for the treatment of advanced cancers. The GROs specifically target nucleolin, a multifunctional protein that is present at high levels in prostate cancer cells, but it is not yet fully understood how binding of GROs to nucleolin inhibits cancer cell proliferation. The purpose of the project was to explore the mechanism of the AS1411 anticancer effects. The specific hypothesis being tested was that AS1411 binds to nucleolin and modulates its protein-protein interactions, leading to alterations in nucleolin function and pleiotropic biological effects. The results of this study support the validity of that hypothesis. Numerous proteins that bind to nucleolin and/or AS1411 were identified and many were found to be altered in prostate cancer cells treated with AS1411. Several novel activities of AS1411 and previously unknown complexes of nucleolin were identified. For example, AS1411 blocked NF-kappaB signaling by affecting a nucleolin complex containing NEMO/IKKgamma, and upregulation of tumor suppressor geneST7 was linked to redistribution of a PRMT5-nucleolin complex. These new data indicate AS1411 affects the trafficking of a subset of nucleolin complexes.

**15. SUBJECT TERMS**
AGRO100, AS1411, therapeutics, aptamers, oligonucleotides,
drug discovery, novel molecular target, antisense, chemotherapy, pharmacology, cell cycle arrest

| **16. SECURITY CLASSIFICATION OF:** | | | **17. LIMITATION OF ABSTRACT** | **18. NUMBER OF PAGES** | **19a. NAME OF RESPONSIBLE PERSON** |
|---|---|---|---|---|---|
| **a. REPORT** | **b. ABSTRACT** | **c. THIS PAGE** | | | **19b. TELEPHONE NUMBER** *(include area code)* |
| U | U | U | UU | 87 | USAMRMC |

**Table of Contents**

INTRODUCTION

The purpose of this research project was to further elucidate the mechanism of a novel class of G-rich oligonucleotides (GROs) that have antiproliferative activity against prostate cancer and other malignant cell lines [1]. One of these GROs, named AS1411 (previously known as AGRO100) is currently being tested in clinical trial for the treatment of advanced cancers. In Phase I trials, it was found to be very well tolerated (no adverse effects in any patients) and exhibited promising clinical activity, including objective responses in some patients with metastatic cancer [2,3]. In cultured cancer cells, the biological activity of GROs is correlated with their ability to bind to a multifunctional cellular protein called nucleolin [1]. However, it is not known precisely how binding of GRO to nucleolin leads to inhibition of cancer cell proliferation. Surprisingly, there are no obvious changes in the levels or localization of nucleolin in cells treated with AS1411. Therefore, our hypothesis is that GROs alter the protein-protein interactions of nucleolin leading to pleiotropic effects on cell biology. Cellular responses to GRO treatment include cell cycle arrest, inhibition of DNA replication and induction of cell death [4]. Recently, while investigating othe GRO-associated proteins, we discovered that AS1411 forms a complex with NEMO (an essential mediator of NF-κB acyivation, which is also known as IKKγ). Furthermore, preliminary data showed that AS1411 inhibits NF-κB activity in HeLa cells. This activity was considered particularly significant because NF-κB signaling is frequently deregulated in advanced prostate cancer [5-7] and its constitutive activation may contribute to therapeutic resistance [8].

BODY

The progress on each task outlined in the original Statement of Work is detailed below:

AIM 1: Confirm GRO-mediated inhibition of NF-kappa B activation in prostate cancer cells and investigate the mechanism of this effect.

(A) Examine NF-kappa B activation in untreated, control-treated, or GRO-treated DU145 prostate cancer cells, with or without TNF alpha stimulation. Activation will be assayed by EMSA and kappa B-driven luciferase expression. Test the sensitivity of untreated or GRO-treated cells to TNF-induced cell death. (Months 1-3)

(B) Investigate molecules in the NF-kappa B pathway to determine at what molecular level the signal transduction is blocked by GROs. Experiments will include assays to examine I-kappa B-alpha phosphorylation and stability, and nuclear translocation and transcriptional activity of NF-kappa B. (Months 4-6)

(C) Identify the molecular interactions or functions of NEMO that are inhibited by binding to GRO. Functions to be tested will include: kinase activity of IKK complex, interaction of NEMO with IKK-beta, oligomerization of NEMO, phosphorylation of NEMO and IKK-beta, NEMO plasma membrane translocation and binding to TNF receptor. (Months 7-12)

(D) Determine the specificity of GROs in terms of NF-kappa B signaling. Examine if GROs block NF-kappa B signaling induced by stimuli other than TNF-alpha, and whether they block other similar pathways. Determine if the extent of NF-kappa B inhibition by a series of GROs correlates with their antiproliferative activity. (Months 13-18)

*Results:* Parts (A) and (B) were completed in year 1. We demonstrated that **AS1411 (previously called AGRO100) could inhibit both TNFα-induced and constitutive activity of NF-κB in DU145 prostate cancer cells**. This inhibition was **due to inactivation of the IκB kinase (IKK) complex**, as shown by assays to determine kinase activity of IKK and to monitor the presence of phosphorylated

IκBα in GRO-treated cells. These results were written up for publication and submitted to. During Year 2, in response to criticisms of the original manuscript, it was necessary to repeat many of the experiments (biotin-oligo precipitations, IKK activity assays, phospho-IkB westerns and EMSAs) in order to obtain quantitative data. This took a considerable time, but the results validated the original data and the **manuscript was accepted for publication in *Molecular Cancer Therapeutics*** (Girvan *et al*., Appendix 1). To complete part (A), we carried out MTT assays to determine the effect of TNFα with or without pre-incubation with GRO for short (0.5 – 4 h) or longer (24 – 72 h) times. However, we did not find any significant induction of cell death in DU145 cells by TNFα at concentrations up to 20 ng/ml, either in the presence or absence of GRO (data not shown). The experiments for part (C) were carried out during year 2. As described in the *Molecular Cancer Therapeutics* paper (Appendix 1), we have demonstrated by two methods that **the kinase activity of IKK is blocked in cells treated with GRO**. We also showed that **the presence of GRO increases the association between NEMO and nucleolin in the cytoplasm** (see Figure 5 in *MCT* paper) and preliminary data (see Figure 1, Supporting Data) suggest a slight reduction in the amount of NEMO associated with IKKβ. Therefore, our hypothesis is that **NEMO is sequestered in a complex with nucleolin, which abrogates the kinase activity of the IKK complex** (see Figure 6 in *MCT* paper). The experiments proposed for part (D) were initiated in Year 3. In an attempt to facilitate this aim, we purchased a reporter cell line with stable expression of NF-κB-driven luciferase, but, unfortunately, we encountered some technical difficulties and were not able to get results quickly. In the meantime, it became apparent that, while inhibition of NF-kappaB likely contributes to AS1411 activity, nucleolin is the primary mediator of its effects, so we decided to concentrate more on Aim 3.

AIM 2: Examine the role of nucleolin in NF-kappa B signaling.

(A) Investigate nucleolin binding to NEMO in untreated, control-treated, or GRO-treated DU145 prostate cancer cells, with or without TNF alpha stimulation. (Months 19-21)

(B) Examine the levels and localization of nucleolin at various times following stimulation with TNF-alpha or other NF-kappa B activating treatments. (Months 22-24)

(C) Test the hypothesis that nucleolin is involved in transporting NEMO to the TNF receptor. (Months 25-27)

(D) Test the hypothesis that ligation of plasma membrane nucleolin activates NF-kappa B signaling. (Months 28-30)

(E) Determine the effect of nucleolin down-regulation on NF-kappa B activation. This will include the use of the following approaches (which have been previously used to validate nucleolin): expression of antisense nucleolin RNA, nucleolin-directed antisense oligonucleotides and siRNA. (Months 31-36)

*Results:* This aim was completed during Year 2 of the project. Our experiments are described in detail in the **appended excerpt from Allicia Girvan's Ph.D. dissertation** (see Figures 15 -17, Appendix 2) and the results are described briefly here. To investigate the NEMO-nucleolin interaction, we carried out immunoprecipitation (IP) of NEMO at specified times after stimulation with TNFα, followed by western blotting for nucleolin. We found that there was a **transient increase in the interaction between nucleolin and NEMO at 5 - 30 minutes after addition of TNFα**, whereas the interaction returned to its original level by 60 minutes (Figure 16, Appendix 2). For part (B), we prepared nuclear and S100 fractions at specified times after stimulation with TNFα, followed by western blotting for nucleolin. In this experiment, we observed **relocalization of nucleolin from the nucleus to the cytoplasm after 15 minutes with TNFα** (Figure 17, Appendix 2). To address part (C), we carried out IP for TNFR1 and blotted for nucleolin. There was no specific precipitation of nucleolin (data not

shown), and so it is unlikely that this hypothesis is correct. To test the hypothesis proposed in part (D), experiments were carried out to determine the effect of pre-incubation with a nucleolin monoclonal antibody. Preliminary results, which are shown in Figure 2 (Supporting Data), suggest that **ligation of plasma membrane nucleolin by a monoclonal antibody may activate NF-κB signaling**. Part (E) was pursued, using nucleolin siRNA, which is probably the most specific and efficacious method for down-regulating nucleolin. After first confirming specific knockdown of nucleolin by the siRNA, luciferase assays were carried out to determine the effect of siRNA on the activity of NF-κB, as described in Appendix 2. Surprisingly, we found that **knockdown of nucleolin using siRNA causes an increase in NF-κB activity** (Figure 15, Appendix 2).

AIM 3: Capture and identify nucleolin-interacting proteins from untreated and GRO-treated prostate cancer cells in order to identify the molecular interactions of nucleolin that are altered by GRO.

(A) Optimize transfection of construct encoding FLAG-tagged nucleolin and assess expression of FLAG-nucleolin in DU145 prostate cancer cells. (Months 1-3)

(B) Transfect DU145 cells with FLAG-nucleolin construct and capture nucleolin-interacting proteins from untreated cells, and cells treated with GRO or control oligonucleotide. Analyze samples by one- and two-dimensional electrophoresis. Identify selected bands/spots by mass spectrometry techniques. (Months 4-9)

(C) Identify molecular interactions that are specifically blocked (or induced) by GRO treatment. Confirm these results in cells by co-immunoprecipitation experiments. (Months 10-12)

(D) Using gel filtration chromatography, isolate nucleolin-containing multi-protein complexes that are specifically affected by GROs (including the nucleolin-NEMO complex). Analyze components using proteomics techniques. (Months 13-18)

*Results:* We completed parts (A) and (B) during Years 1 and 2, using mass spectrometry analysis of proteins precipitated by FLAG-tagged nucleolin or endogenous protein. **We identified forty nucleolin-interacting proteins, many of which were previously unknown**. At least ten of these interactions have now been confirmed by western blotting of immunoprecipitates with appropriate antibodies. This technique was also used to determine the effect of AS1411 on the interactions and we observed that **many nucleolin-associated proteins had altered nuclear/cytoplasmic distribution in AS1411-treated prostate cancer cells**. Interestingly, some proteins displayed a nuclear-to-cytoplasmic shift, while others were altered in the other direction (*i.e.* cytoplasmic-to-nuclear), perhaps indicating that the **trafficking of nucleolin complexes may be affected by AS1411**. Details of these studies (which constitute part C of this task) are provided in the draft manuscript, which is attached (Teng *et al.*, draft manuscript, Appendix 3). Part (D) was pursued during Years 2 and 3. This task was modified slightly to focus on a specific nucleolin-containing complex that was clearly affected by AS1411. This complex contained protein arginine methyltransferase 5 (PRMT5), a Type II methyltransferase that catalyzes the formation of symmetric dimethylarginines (sDMA). We found that **nucleolin can specifically associate with PRMT5 in both the nucleus and cytoplasm of DU145 prostate cancer cells**. Morever, **the amount of PRMT5 was significantly increased in the cytoplasm, but decreased in the nucleus of cells treated with AS1411**. This **redistribution of PRMT5 was dependent on nucleolin (it was inhibited in cells pre-treated with nucleolin siRNA)**, as well as the time of exposure and dose of AS1411. In accord with these findings, there was a shift in the levels of proteins bearing sDMA modifications from the nucleus to the cytoplasm. An additional novel finding was that **nucleolin is a substrate for methylation by PRMT5**. Interestingly there was an **AS1411-induced shift in sDMA-modified nucleolin from the nucleus to the cytoplasm**, similar to that for PRMT5, whereas total nucleolin levels were apparently unchanged. This was explained by the fact that **only a small**

**proportion of nucleolin (~5%) is sDMA-modified** (presumably by PRMT5), while most of the PRMT5 (~80%) existed in a complex with nucleolin. Finally, in order to evaluate the biological consequences of these changes, we analyzed the expression of some PRMT5-regulated genes. PRMT5 normally methylates histones, leading to transcriptional repression of its targets, which include NM23, cyclin E2 and ST7. We found that **expression of ST7 and cyclin E2 were increased in AS1411-treated cells, due to decreased levels of promoter-bound PRMT5** (a transcriptional repressor), consistent with the observed nuclear-to-cytoplasmic redistribution. ST7 is a known tumor suppressor and cyclin E2 promotes entry into S phase, so their induction by AS1411 may well contribute to the antiproliferative effects of AS1411 and its ability to induce S phase accumulation of cancer cells. A paper describing some of these results was originally submitted to *Cancer Research* in December 2006. In response to the reviewer's comments, we carried out numerous additional experiments and very recently resubmitted an extensively revised version to *Cancer Research*. We are currently awaiting a decision. Full details of these studies can be found in the revised manuscript, which is attached (Teng *et al.*, submitted manuscript, Appendix 4).

AIM 4: Compare the specific molecular interactions and pathways that are affected by GROs in prostate cancer cells versus normal cells.

(A) For NEMO, nucleolin, and other proteins identified in Aim 3, examine the levels and localization in the following cell lines: DU145 (hormone-independent prostate cancer), PC-3 (hormone-independent prostate cancer), LnCaP (hormone-sensitive prostate cancer), PZ-HPV-7 (transformed prostate epithelial cells), PrEC (normal primary prostate epithelial cells), Hs27 (normal skin fibroblasts). (Months 19-21)

(B) For the same cell lines, examine constitutive and TNF-induced NF-kappa B activation. (Months 22-24)

(C) Evaluate the sensitivity of these cell lines to TNF and GROs. (Months 25-27)

(D) Determine if the same specific molecular interactions (identified in Aims 1-3 as modulated by GROs) are occurring in each cell line, and if they are altered by GROs. (Months 28-36)

*Results:* Because of the many additional experiments that we had to do in order to address reviewer critiques for the two submitted manuscripts (see Appendices 1 and 4), there was insufficient time or resources to carry out all of the planned experiments for Aim 4. Moreover, new data generated during the course of the project suggested a number of reasons why the proposed experiments would be unlikely to shed much light on the cancer-selective activity of AS1411. First of all, in our experience, neither primary nor virally transformed epithelial cells were very representative of normal tissues. For example, we found that the PZ-HPV-7 cells were tetraploid and grew faster than most cancer cell lines, whereas primary epithelial cells had a very high rate of apoptosis in culture. In addition, our ongoing work (funded by NIH) to study the cellular internalization of GROs suggests that AS1411 is taken up selectively in cancer cells (probably mediated by surface nucleolin) compared to normal cells. Thus, preferential uptake is likely to be the primary mechanism for the cancer-selectivity, rather than a difference in downstream events. Therefore, we modified our approach in this task to try to determine if the observed changes are "universal" effects of GROs, *i.e.* if they occur in most types of responsive cells and confirmed that AS1411 could inhibit NF-κB signaling in a total of four responsive cancer cell lines (DU145, A549, HeLa, MCF7). Experiments to determine if redistribution of PRMT5 is also a universal effect of AS1411 are also planned for the future.

*Summary of Progress:* The tasks were pursued as outlined in the original statement of work. Aims 1-4 were completed with a few minor modifications when difficulties were encountered or when new data suggested an alternative approach would be more enlightening. This research resulted in three

manuscripts—one published in *Molecular Cancer Therapeutics*, one currently being reviewed at *Cancer Research*, and one that will soon be submitted—and contributed to the Ph.D. dissertation of a graduate student.

COMPLETED: Aims 1-4

## KEY RESEARCH ACCOMPLISHMENTS

1. Publication of data showing that AS1411 (previously known as AGRO100) inhibits constitutive and TNF-induced NF-κB signaling in prostate cancer cells by binding to NEMO/IKKγ.
2. Publication of data indicating a novel interaction between NEMO/IKKγ and nucleolin, indicating a previously unknown role for nucleolin in NF-κB signaling.
3. Demonstration that nucleolin is a novel binding partner and substrate of PRMT5
4. Discovery that nucleolin plays a previously unknown role in mediating the transport of PRMT5 and its ability to act as a transcriptional repressor.
5. Discovery that PRMT5 distribution is altered in GRO-treated cells, leading to upregulation of PRMT5-repressed genes, such as tumor suppressor ST7.
6. Validation of previously reported nucleolin-protein interactions and identification of additional novel interactions, many of which are altered by GRO.
7. Generation of a new mechanistic model, in which binding of GRO to nucleolin affects the nuclear-cytoplasmic transport of a small subset of nucleolin complexes (containing sDMA-modified nucleolin), leading to pleiotropic biological effects.

## REPORTABLE OUTCOMES

**Manuscripts:**

1. Girvan AC, Teng Y, Casson LK, Thomas SD, Jüliger S, Ball MW, Klein JB, Pierce WM, Barve SS and Bates PJ (2006). AGRO100 Inhibits Activation of Nuclear Factor-κB (NF-κB) by Forming a Complex with NEMO and Nucleolin. *Molecular Cancer Therapeutics* **5**, 1790-1799.
2. Teng Y, Girvan AC, Casson LK, Thomas SD, Qian M, Pierce WM and Bates PJ (2007). Protein Arginine Methyltransferase 5 (PRMT5) Associates with Nucleolin and is Altered in Prostate Cancer Cells Treated with Nucleolin-targeted Aptamer, AS1411. Manuscript submitted to *Cancer Research*.
3. Teng Y, Pierce WM and Bates PJ (2007). Proteomic Analysis of the Effects of Novel Anticancer Aptamer, AS1411, on Nucleolin Complexes in Human Prostate Cancer Cells. Manuscript in preparation.

**Abstracts/ Meeting Presentations:**

1. Bates P, Jueliger S, Girvan A, Teng Y, Casson L, Thomas S, Mi Y, Xu X, Barve S, Miller D and Trent J. Activity and mechanism of AS1411, a novel anti-cancer aptamer that targets nucleolin. *Clin. Cancer. Res.* 2005, 11, 24 Part 2, 9114S (Poster Presentation, AACR Molecular Targets Meeting, Philadelphia, PA, November 2005).
2. Teng Y, Girvan A, Casson L, Thomas S and Bates P. A Role for Protein Arginine Methyltransferase 5 (PRMT5) in the Mechanism of Novel Anticancer Agent, AS1411. *Proceedings of the American Association of Cancer Research 95th Annual Meeting* (Poster Presentation, AACR

Annual Meeting, Washington, DC, April 2006).

3. Teng Y, Pierce WM and Bates PJ. Proteomic studies of nucleolin complexes in prostate cancer cells treated with novel anticancer agent, AS1411. *Proceedings of the American Association of Cancer Research 2007 Annual Meeting* (Poster Presentation, AACR Annual Meeting, Los Angeles, CA, April 2007).

**Degree:**

Allicia Girvan was supported in part by this award and graduated from the University of Louisville with a Ph.D. degree in Biochemistry and Molecular Biology in May 2006.

**Patent Filing:**

Bates, PJ, Girvan AC and Barve SS. "Method for inhibiting NF-kappa B signaling and use to treat or prevent human diseases"

CONCLUSIONS

The first aim of this study was to investigate the significance of our preliminary observation that NEMO/IKKγ (an essential molecule for NF-κB activation) binds to an active GRO (named AS1411). Our research confirmed that AS1411 blocks NF-κB signaling in human prostate cancer cells by binding to NEMO and inhibiting the activity of the IKK complex. In fact, it turned out that these effects were mediated by nucleolin (the protein originally identified as a major target of GROs), which forms a novel complex with NEMO. Therefore, we now believe that, while inhibition of NF-kappaB signaling almost certainly contributes to the anticancer activity of AS1411, nucleolin is the primary and most important mediator of AS1411 effects.

The second aim of our study was to investigate whether nucleolin plays a role in NF-κB signaling. Our results confirmed that nucleolin does indeed play an important role in NF-κB signaling, although it is not yet clear precisely what that role is. Our revised hypothesis is that nucleolin may be involved in the nuclear-cytoplasmic trafficking of NEMO. This theory is based on new insights into the importance of this process in the regulation of NEMO [9] and our findings that nucleolin-associated proteins have altered nuclear:cytoplasmic distributions in GRO-treated cells (see Aim 3). Our finding that nucleolin siRNA increases NF-κB activity suggests that nucleolin may be a negative regulator of NEMO, which would be in accord with our observation that an increased nucleolin-NEMO interaction (in GRO-treated cells) is associated with a decrease in NF-κB signaling.

The third aim was to identify nucleolin-associated proteins and investigate their fate in AS1411-treated prostate cancer cells. This aim resulted in numerous new discoveries about nucleolin and substantial insight into the mechanism of AS1411, which became a major focus of the project. Several previously unknown interactions of nucleolin have been identified during our research and many of the nucleolin-associated proteins have important roles in cancer cell biology or tumor progression. When levels of these proteins were examined in nuclear and S100 extracts from treated prostate cancer cells, we frequently found that the nuclear:cytoplasmic distributions of nucleolin-associated proteins were altered by AS1411, although not always in the same direction. This supports our original hypothesis that GRO alters the molecular interactions of nucleolin, which leads to pleiotropic anticancer effects. Our new data further suggest a new hypothesis that changes in the trafficking function of nucleolin (or,

specifically, of a small subset of nucleolin complexes) may be central to the GRO mechanism. In fact, it is possible that the growth inhibitory and pro-apoptotic effects of GROs in prostate cancer cells can all be explained on the basis of mislocalization of nucleolin-assoiated proteins. Thus, the altered interactions that we have characterized (nucleolin/NEMO and nucleolin/ PRMT5) may be representative of a general mechanism of action for GROs.

The fourth aim was to examine the pathways affected by AS1411 in cancer and normal cells, in order to better understand the tumor-selectivity of AS1411. However, it became clear during the course of the research (due to new data from our laboratory and others) that the selectivity of AS1411 probably derives mostly from its selective uptake in cancer cells, rather than the pathways it affects once inside the cell. It appears that the internalization of AS1411 is mediated by cell surface nucleolin, which is overexpressed on the surface of many cancer cell types (Bates *et al.*, unpublished). On the other hand, many of the nucleolin complexes that we have identified play important roles in cancer persistence or progresssion, so it may be that inhibiting nucleolin by other means would have cancer-specific effects.

In conclusion, our study has identified several new binding partners and physiological roles for nucleolin, thereby revealing new insights into prostate cancer molecular biology. In addition, our research has generated substantial new information about the mechanism of AS1411 and has allowed us to develop a new model for its action, which is shown in the Supporting Data (Figure 3). Our results also support the continued clinical development of nucleolin-targeted agents, such as AS1411, as anticancer agents with a novel mechanism of action that imparts tumor-selective activity.

## REFERENCES


1. Bates PJ, Kahlon JB, Thomas SD, Trent JO, Miller DM. Antiproliferative activity of G-rich oligonucleotides correlates with protein binding. J Biol Chem. 1999, 274(37):26369-77.
2. Laber D, Bates P, Trent J, Barnhart K, Taft B, Miller D. Long term clinical response in renal cell carcinoma patients treated with quadruplex forming oligonucleotides. Clin Cancer Res 2005;11:9088S
3. Miller D, Laber D, Bates P, Trent J, Taft B, Kloecker GH. Extended phase I study of AS1411 in renal and non-small cell lung cancers. Ann Oncol. 2006;17(Suppl 8):ix147-8.
4. Xu X, Hamhouyia F, Thomas SD, Burke TJ, Girvan AC, McGregor WG, Trent JO, Miller DM, Bates PJ. Inhibition of DNA replication and induction of S phase cell cycle arrest by G-rich oligonucleotides. J Biol Chem. 2001, 276(46):43221-30.
5. Gasparian AV, Yao YJ, Kowalczyk D, Lyakh LA, Karseladze A, Slaga TJ, Budunova IV. The role of IKK in constitutive activation of NF-kappaB transcription factor in prostate carcinoma cells. J Cell Sci. 2002, 115(Pt 1):141-51.
6. Suh J, Payvandi F, Edelstein LC, Amenta PS, Zong WX, Gelinas C, Rabson AB. Mechanisms of constitutive NF-kappaB activation in human prostate cancer cells. Prostate. 2002, 52(3):183-200.
7. Chen CD, Sawyers CL. NF-kappa B activates prostate-specific antigen expression and is upregulated in androgen-independent prostate cancer. Mol Cell Biol. 2002, 22(8):2862-70.
8. Baldwin A. Control of oncogenesis and cancer therapy resistance by the transcription factor NF-κB. J Clin Invest. 2001, 107(3): 241-246.
9. Kovalenko A, Wallach D. If the prophet does not come to the mountain: dynamics of signaling complexes in NF-kappaB activation. Mol Cell. 2006 May 19;22(4):433-6.

SUPPORTING DATA

**FIGURE 1: Preliminary data showing effect of oligonucleotides on association of NEMO with IKKβ.**

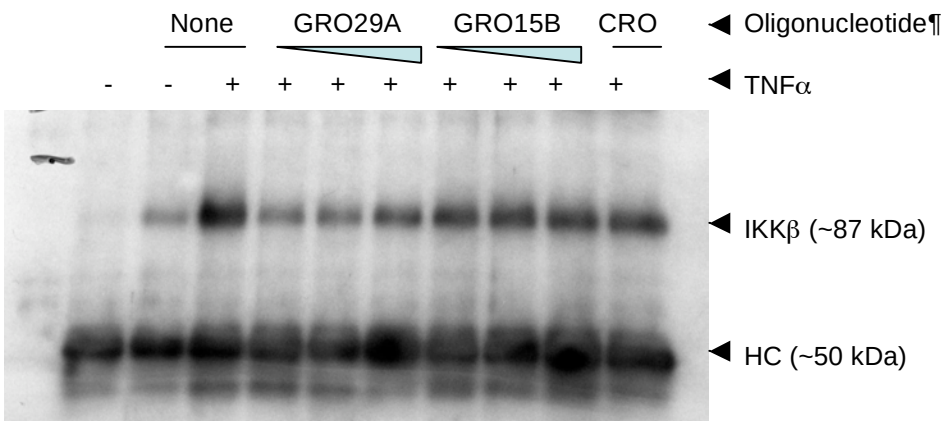


**FIGURE 1:** Cell lysates were prepared from cells that had been stimulated for 2 h with TNFα, following 30 min pre-incubation with various oligonucleotides, as indicated. Lysates were immunoprecipitated using a NEMO monoclonal antibody and then probed for IKKβ. Unfortunately, it was not possible to determine the levels of precipitated NEMO (48 kDa) in this blot due to its proximity to the mouse immunoglobulin heavy chain (HC).
¶ GRO29A is an active GRO and was used at 2.5, 5, and 10 μM final concentrations, whereas GRO15B (used at 2.5, 5, 10 μM) and CRO (10 μM) are control, inactive oligonucleotides.

**FIGURE 2: Preliminary data showing effect of nucleolin antibody on NF-κB transcriptional activity.**

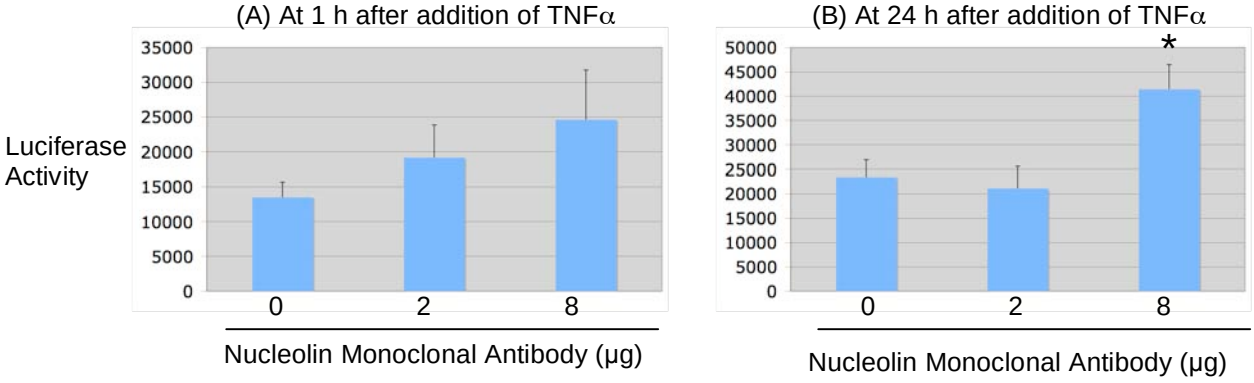


**FIGURE 2:** HeLa cells were transiently transfected with an NF-κB-driven reporter plasmid. After overnight incubation, 0, 2, or 8 μg of nucleolin monoclonal antibody (Santa Cruz MS-3) was added to the culture medium and incubated for 30 min. Recombinant TNFα was then added (for final concentration, 7.5 ng/ml) and incubated for a further 1 h or 24 h before measurement of luciferase activity. At 24 h, the difference between 0 μg and 8 μg of antibody was statistically significant (*, $p<0.05$).

## FIGURE 3

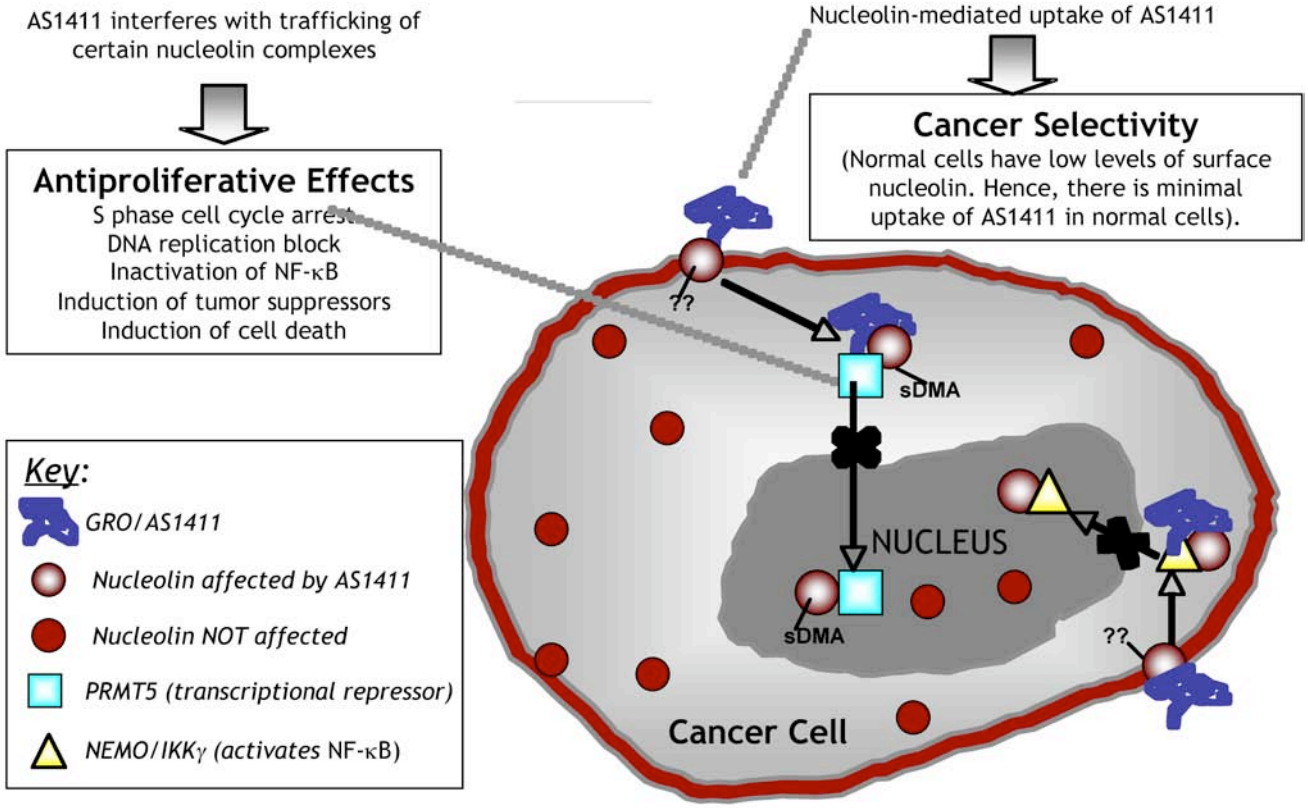


**Model:** It is proposed that GROs such as AS1411 alter the nuclear-cytoplasmic distribution of nucleolin-associated proteins by affecting the shuttling function of nucleolin. This leads to pleiotropic biological effects, due to mislocalization of various proteins. For example, AS1411 leads to inhibition of NF-kB signaling and induction of tumor suppressor genes, due to cytoplasmic sequestration of NEMO and PRMT5, respectively. Many other nucleolin-associated proteins may also be affected and, because nucleolin has many oncogenic roles, the net effect is inhibition of cancer cell proliferation and induction of cell death. However, only a small proportion of the total nucleolin molecules are affected by AS1411, which explains the previously anomalous finding that there is no obvious change in total nuclear/cytoplasmic levels of nucleolin in AS1411-treated cells. It is not yet known if AS1411 binds to a particular form of nucleolin, although we have shown that nucleolin with a certain post-translational modification (symmetric dimethylation of arginine,which is catalyzed by PRMT5) is specifically redistributed by AS1411. The selective effect of AS1411 on cancer cells compared to normal cells is thought to be related to its preferential uptake in cancer cells. Internalization of AS1411 is probably mediated by cell surface nucleolin, which is present at much higher levels on cancer cells compared to normal cells.

APPENDICES

**Appendix 1. Girvan *et al.* (manuscript published in *Molecular Cancer Therapeutics*):**

Girvan AC, Teng Y, Casson LK, Thomas SD, Jüliger S, Ball MW, Klein JB, Pierce WM, Barve SS and Bates PJ (2006).

*AGRO100 Inhibits Activation of Nuclear Factor-κB (NF-κB) by Forming a Complex with NEMO and Nucleolin*

**Appendix 2. Girvan (excerpt from dissertation of Allicia C. Girvan):**

Girvan AC (2006)

*NEMO and Nucleolin: Possible Role for Nucleolin in NF-κB Signaling*

**Appendix 3. Teng *et al.* (manuscript in preparation):**

Teng Y, Pierce WM and Bates PJ (2007).

*Proteomic Analysis of the Effects of Novel Anticancer Aptamer, AS1411, on Nucleolin Complexes in Human Prostate Cancer Cells*

**Appendix 4. Teng *et al.* (re-submitted to *Cancer Research* and currently being reviewed):**

Teng Y, Girvan AC, Casson LK, Thomas SD, Qian MW, Pierce WM and Bates PJ (2007).

*Protein Arginine Methyltransferase 5 (PRMT5) Associates with Nucleolin and is Altered in Prostate Cancer Cells Treated with Nucleolin-targeted Aptamer, AS1411*

# AGRO100 inhibits activation of nuclear factor-κB (NF-κB) by forming a complex with NF-κB essential modulator (NEMO) and nucleolin

**Allicia C. Girvan,[1] Yun Teng,[2] Lavona K. Casson,[2] Shelia D. Thomas,[2] Simone Jüliger,[2] Mark W. Ball,[2] Jon B. Klein,[2] William M. Pierce, Jr.,[3] Shirish S. Barve,[2,3] and Paula J. Bates[1,2]**

**Departments of [1]Biochemistry and Molecular Biology, [2]Medicine, and [3]Pharmacology and Toxicology, James Graham Brown Cancer Center, University of Louisville, Louisville, Kentucky**

## Abstract

**AGRO100, also known as AS1411, is an experimental anticancer drug that recently entered human clinical trials. It is a member of a novel class of antiproliferative agents known as G-rich oligonucleotides (GRO), which are non-antisense, guanosine-rich phosphodiester oligodeoxynucleotides that form stable G-quadruplex structures. The biological activity of GROs results from their binding to specific cellular proteins as aptamers. One important target protein of GROs has been previously identified as nucleolin, a multifunctional protein expressed at high levels by cancer cells. Here, we report that AGRO100 also associates with nuclear factor-κB (NF-κB) essential modulator (NEMO), which is a regulatory subunit of the inhibitor of κB (IκB) kinase (IKK) complex, and also called IKKγ. In the classic NF-κB pathway, the IKK complex is required for phosphorylation of IκBα and subsequent activation of the transcription factor NF-κB. We found that treatment of cancer cells with AGRO100 inhibits IKK activity and reduces phosphorylation of IκBα in response to tumor necrosis factor-α stimulation. Using a reporter gene assay, we showed that AGRO100 blocks both tumor necrosis factor-α-induced and constitutive NF-κB activity in human cancer cell lines derived from cervical, prostate, breast, and lung carcinomas. In addition, we showed that, in AGRO100-treated cancer cells, NEMO is coprecipitated by nucleolin, indicating that both proteins are present in the same complex. Our studies suggest that abrogation of NF-κB activity may contribute to the anticancer effects of AGRO100 and that nucleolin may play a previously unknown role in regulating the NF-κB pathway. [Mol Cancer Ther 2006;5(7):1790–9]**

## Introduction

Many common types of cancer, especially in their advanced stages, do not respond well to traditional chemotherapy agents or may acquire resistance to therapy. Novel agents that work by mechanisms that are different from existing therapies, particularly those that are able to target multiple pathways important for cancer cell survival, may therefore be useful in the treatment of advanced cancer. We have reported previously that certain guanosine-rich phosphodiester oligodeoxynucleotides, termed G-rich oligonucleotides (GRO), have antiproliferative activity against a variety of cancer cell lines (1–4). Furthermore, an active GRO (named GRO29A) can cause cell cycle arrest and induction of cell death in human cancer cell lines but not in non-malignant human cells (4). Following preclinical *in vivo* studies, which showed that it had no detectable toxicity in normal tissues (5), a truncated version of GRO29A, known as AGRO100 (recently renamed AS1411), has been tested in a phase I clinical trial of patients with advanced cancer. The results of this trial were recently presented (6) and indicated that AGRO100 was well tolerated (no serious adverse effects were observed) and had promising clinical activity.

In previous studies, we have examined a series of G-rich sequences to determine a structure-activity relationship and to gain insight into their novel mechanism (1–3). We found that active GROs can have diverse G-rich sequences, but all could adopt folded conformations that are stabilized by G-quartets. However, formation of a stable G-quadruplex was not sufficient for activity. In addition, there was a very good correlation between the biological activity of GROs and their abilities to form a specific complex containing a protein that was identified as nucleolin (1–3). There is strong evidence from UV cross-linking and Southwestern blotting (1) that GROs bind directly to nucleolin rather than interact through an intermediary protein; therefore, we have proposed that nucleolin is the primary target of GROs, such as AGRO100.

Despite their probable target having been identified, the detailed mechanism of action for GROs is not yet fully understood. In part, this is because little is known about the role of nucleolin in cancer biology. Nucleolin protein is expressed at high levels in rapidly proliferating cells, such

Received 9/8/05; revised 5/4/06; accepted 5/16/06.

**Grant support:** Department of Defense Prostate Cancer Research Program grants PC001482 and PC030134 (P.J. Bates), Susan G. Komen Breast Cancer Foundation grant DISS0202095 (P.J. Bates), IMD3 Fellowship (A.C. Girvan and M.W. Ball), and Commonwealth of Kentucky Research Challenge Trust and the Brown Cancer Center.

The costs of publication of this article were defrayed in part by the payment of page charges. This article must therefore be hereby marked advertisement in accordance with 18 U.S.C. Section 1734 solely to indicate this fact.

**Requests for reprints:** Paula J. Bates, University of Louisville, 580 South Preston Street, Delia Baxter Building 321, Louisville, KY 40202-1756. Phone: 502-852-2432; Fax: 502-852-2356.
E-mail: paula.bates@louisville.edu



doi:10.1158/1535-7163.MCT-05-0361

as cancer cells (7), and nucleolin is a major component of a set of cancer prognostic markers (silver-staining nucleolar organizer regions) whose levels are elevated in cancer cells compared with normal or premalignant cells (8, 9). Although it is best known as a nucleolar protein with a role in ribosome biogenesis, nucleolin is in fact a remarkably multifunctional protein that can also be present in the nucleoplasm, cytoplasm, and on the cell surface (10–15). In addition to its multiple functions in ribosome biogenesis (10–12), nucleolin is thought to play a role in numerous cellular processes, including apoptosis (16), signal transduction (14, 17–19), DNA replication (20, 21), mRNA stability (22–24), protein trafficking (13, 25), stress response (26, 27), and telomerase function (28). It has been reported by several research groups that nucleolin binds to G-quadruplex-forming DNA sequences, such as the human telomere (29, 30), immunoglobulin switch regions (31), and rDNA (32), but the significance of these interactions *in vivo* has not yet been determined.

Recently, we identified nuclear factor-κB (NF-κB) essential modulator [NEMO; also known as inhibitor of κB (IκB) kinase (IKK) γ and IKKAP1] as a potential GRO-associated protein following mass spectrometry analysis of proteins that were precipitated when an active biotin-linked GRO was incubated with cancer cell extracts.[4] It was selected for further investigation because of its important role in NF-κB signaling, a pathway that is often deregulated in cancer cells (33–35) and that has been reported previously to be inhibited by polyguanosine sequences (36, 37) via an uncharacterized mechanism. ''NF-κB'' refers to a family of proteins that function as dimeric transcription factors to affect the expression of genes involved in immune and inflammatory responses, cell growth, differentiation, and apoptosis (34, 38, 39). In nonstimulated cells, NF-κB is normally bound to an inhibitor called IκBα, which sequesters it in the cytoplasm in an inactive state. On ligation of an appropriate cell surface receptor [e.g., by tumor necrosis factor-α (TNF-α)], the IKK complex consisting of NEMO, IKKα, and IKKβ becomes activated. This IKK complex then phosphorylates IκBα, leading to its ubiquitination and flagging it for degradation by the 26S proteasome. On degradation of IκBα, NF-κB is released and translocates to the nucleus to activate gene expression. Targets of NF-κB include many antiapoptotic and pro-proliferation genes, and this pathway is constitutively activated in many human cancers (33–35). For this reason, NF-κB and the proteins that control its activation have become interesting targets for cancer drug development (39, 40).

The purpose of the present study was to further investigate the significance of our preliminary observation that NEMO associates with an active GRO. In particular, our aims were to verify that AGRO100 was associated with NEMO in treated cancer cells, to determine the biological consequences of this association, and to investigate the possible role of nucleolin in mediating it.

## Materials and Methods

### Oligodeoxynucleotides

The oligodeoxynucleotides used in the present study were AGRO100, an antiproliferative GRO whose sequence is 5′-d(GGTGGTGGTGGTTGTGGTGGTGGTGG)-3′, and CRO26, an inactive (no antiproliferative activity) control oligonucleotide whose sequence is 5′-d(CCTCCTCCTCC-TTCTCCTCCTCCTCC)-3′. In some experiments, GRO15B, an inactive GRO (1–4) with sequence 5′-d(TTGGGGGGG-GTGGGT)-3′, was used as an additional control. All oligonucleotides had a phosphodiester backbone and, unless otherwise stated, were purchased in the desalted form from Integrated DNA Technologies, Inc. (Coralville, IA) and used without further purification. Oligonucleotides were resuspended in water, sterilized by filtration through a 0.2-μm filter, and then diluted with sterile water to give stock solutions (400–500 μmol/L) that were stored in aliquots at −20°C. For streptavidin precipitation experiments, the following biotin-linked versions of AGRO100, GRO15B, and CRO26 were used: 5′-biotin-d(TTTGGTGG-TGGTGGTTGTGGTGGTGGTGG)-3′, 5′-biotin-d(TTGG-GGGGGGTGGGT)-3′, and 5′-biotin-d(TTTCCTCCTCC-TCCTTCTCCTCCTCCTCC)-3′ (all from Integrated DNA Technologies).

### Cell Culture and Treatment

Cell lines used were HeLa (human cervical cancer), DU145 (human prostate cancer), A549 (human non–small cell lung cancer), MCF-7 (human breast cancer), and Hs27 (nonmalignant human skin fibroblasts), which were obtained from the American Type Culture Collection (Manassas, VA). Cells were grown in a standard incubator in DMEM (Life Technologies, Chicago, IL) supplemented with 10% heat-inactivated (65°C for 20 minutes) fetal bovine serum (Life Technologies) or charcoal-stripped fetal bovine serum (for MCF-7 only; Biomeda, Foster City, CA), 100 units/mL penicillin, and 100 units/mL streptomycin. For the cell proliferation assays (Fig. 1), cells were plated at low density (1,000 or 2,000 cells per well for MCF-7 and Hs27, respectively) in 96-well plates and incubated 18 hours at 37°C to allow adherence. They were treated by addition of AGRO100 directly to the culture medium to give the final concentration indicated in the figure. Cells were incubated for a further 5 days in the presence of oligonucleotide, and then proliferation was determined using the 3-(4,5-dimethylthiazol-2-yl)-2,5-diphenyltetrazolium bromide assay as described previously (1). For other experiments, unless otherwise stated, cells were plated in six-well plates at ~50% confluence and incubated 18 hours to allow adherence and then treated by addition of oligonucleotide directly to the culture medium. Where indicated, TNF-α (R&D Systems, Inc., Minneapolis, MN) was added to the culture medium for a final concentration of 7.5 ng/mL.

### Identification of Candidate GRO-Associated Proteins

Extracts were prepared from HeLa cells as described previously (16). Samples (250 μg) were incubated with a biotin-linked active GRO (GRO29A) or biotin-linked inactive control oligonucleotide (GRO15B), which were

[4] P.J. Bates, A.C. Girvan, J.B. Klein, and W.M. Pierce, Jr., unpublished data.

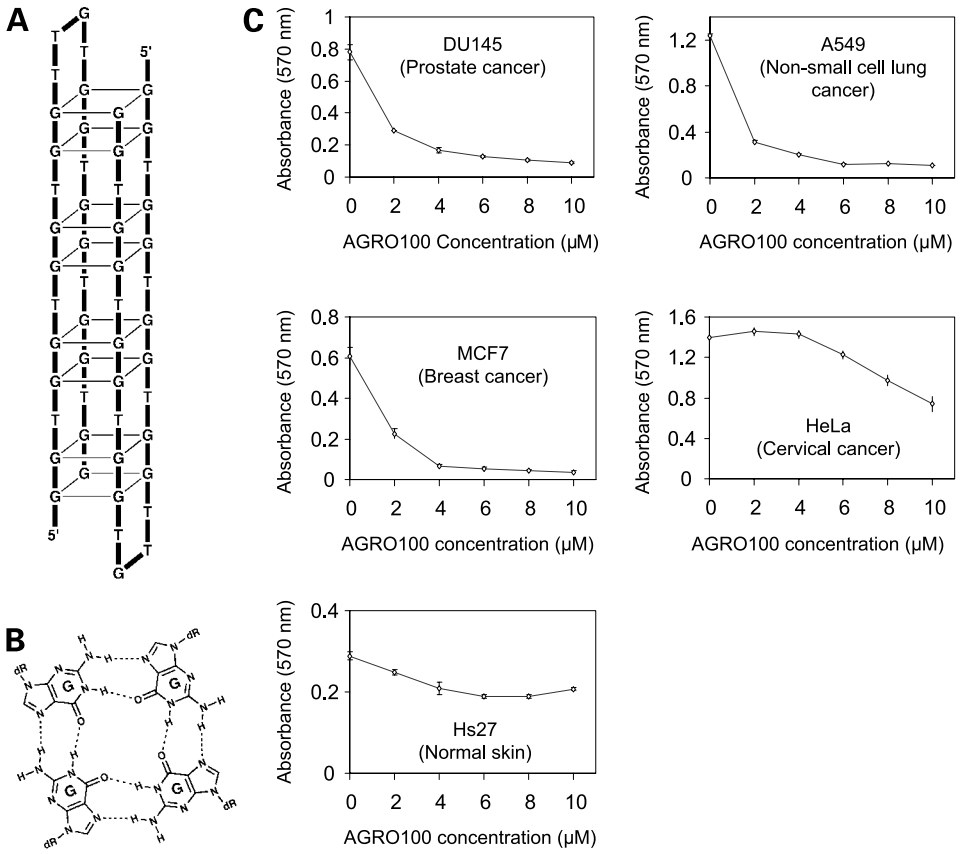


**Figure 1.** Structure and activity of AGRO100. **A,** structure proposed (2) for AGRO100, which comprises two strands of AGRO100 folded in antiparallel orientation to form a bimolecular quadruplex containing eight G-quartets. **B,** G-quartet showing the hydrogen bonding arrangement of the four planar guanosines. **C,** antiproliferative activity of AGRO100 in various human cell lines. Cells were incubated for 5 d following a single treatment with AGRO100 (which was added directly to the medium), and proliferation was measured using a 3-(4,5-dimethylthiazol-2-yl)-2,5-diphenyltetrazolium bromide assay. Identity of the cell line used and its origin. *Y axis,* absorbance at 570 nm, which is directly proportional to the number of viable cells in the sample. *Points,* mean of triplicate samples; *bars,* SE.

previously reported (1). The oligonucleotide-associated proteins were then captured by streptavidin precipitation (Streptavidin MagnaSphere Paramagnetic Particles, Promega, Madison, WI) and electrophoresed on SDS-polyacrylamide (8%) gels. Silver staining was used to identify bands present in the GRO29A-precipitated lane but absent in the control GRO15B lane. These bands were excised, subjected to trypsin digestion, and analyzed by matrix-assisted laser desorption ionization-time of flight mass spectrometry analysis as described previously (41). This analysis identified 18 proteins associated specifically with the active GRO, including NEMO and nucleolin. The other candidate GRO-associated proteins have not yet been verified but are currently under investigation.

### Capture of Biotinylated GRO-Protein Complexes from HeLa Cells

Cells were grown to 50% confluence in T-25 flasks and treated by addition of biotinylated oligonucleotide at a final concentration of 5 μmol/L. After incubation for 2 hours at 37°C, cells were washed extensively with PBS and lysed by addition of 1 mL of lysis buffer [50 mmol/L Tris-HCl (pH 7.4), 150 mmol/L NaCl, 1 mmol/L EDTA, 1% Triton X-100, 0.5% Igepal CA630, complete protease inhibitor cocktail (Roche, Chicago, IL)]. Lysate was added to streptavidin-coated magnetic beads (MagnaBind, Pierce, Rockford, IL) and incubated 10 minutes at room temperature. Beads were captured, and unbound sample was removed. Beads were then washed thrice with 1 mL of immunoprecipitation buffer [0.1 mol/L Tris-HCl (pH 8.0), 1% (v/v) Triton X-100, 1% (w/v) deoxycholate, 0.5% (w/v) SDS, 2 mmol/L phenylmethylsulfonyl fluoride]. Finally, proteins were eluted by addition of 50 μL of loading buffer (1% SDS, 5% 2-mercaptoethanol) and boiled for 5 minutes. Captured proteins were electrophoresed on SDS-polyacrylamide (8%) gels and transferred to polyvinylidene difluoride membranes. Membranes were blocked with 5% nonfat dried milk in PBS plus 0.05% Tween 20 and then incubated with primary antibody in PBS plus 0.05% Tween 20 (1 μg/mL anti-nucleolin or 1 μg/mL anti-NEMO, both from Santa Cruz Biotechnology, Santa Cruz, CA). Following incubation with secondary antibody (0.5 μg/mL anti-mouse horseradish peroxidase conjugated, Santa Cruz Biotechnology), bands were visualized by enhanced chemiluminescence (Amersham Biosciences, Pittsburgh, PA). For densitometric quantitation, the results from three independent experiments were scanned (Epson Expression 1680, Long Beach, CA) and the intensities of bands were determined using ImageQuant 5.2 software (Amersham Biosciences). For each experiment, background (streptavidin precipitated/no oligonucleotide) was subtracted and the intensities were normalized to the value for AGRO100. Error bars shown represent the SE of the normalized results.

### IKK Kinase Assay

HeLa cells were plated in six-well plates as described. After 1 hour of incubation with oligonucleotide, TNF-α was added for a further 30 minutes. Cell lysates were prepared using 0.1 mol/L Tris-HCl (pH 8.0), 1% Triton X-100, 1% deoxycholate, 0.5% SDS, and 2 mmol/L phenylmethylsulfonyl fluoride. The lysates (10 μg) were then assessed for IKK kinase activity as described previously (41) using 2.5 μg of IκBα-glutathione *S*-transferase fusion protein (Santa Cruz Biotechnology) as the substrate. The gels were dried and analyzed by autoradiography or by using a phosphorimager (Typhoon 9400). For densitometric quantitation, the results from three independent experiments (as Typhoon images or scans of autoradiographic film) were analyzed using ImageQuant 5.2 software. For each experiment, intensities were normalized to the positive control (TNF-α stimulated, no oligonucleotide) and the error bars shown represent the SE of the normalized results.

### Detection of Phosphorylated IκBα

HeLa cells were treated exactly as described for the IKK kinase assay. Lysates were prepared by addition of lysis buffer [62.5 mmol/L Tris-HCl (pH 6.8), 2% SDS, 10% glycerol, 50 mmol/L DTT], electrophoresed on 8% polyacrylamide-SDS gels, and transferred to polyvinylidene difluoride membrane. Standard Western blot analysis was then done using anti-phosphorylated IκBα antibody (1 μg/mL; Cell Signaling Technology, Beverly, MA) followed by analysis using anti-β-actin antibody (Sigma-Aldrich, St. Louis, MO) as a control for equal loading. For densitometric quantitation, the results from three independent experiments were scanned and the intensities of the phosphorylated IκBα and the corresponding β-actin bands were determined using ImageQuant 5.2 software. The intensity of each IκBα band was divided by the corresponding β-actin band, and for each experiment, these values were normalized to the positive control (TNF-α stimulated, no oligonucleotide). The error bars shown represent the SE of the normalized results.

### Transient Transfection and Measurement of Luciferase Activity

Cells were plated in 24-well plates at a density of $2 \times 10^4$ per well and transiently transfected with a NF-κB reporter plasmid and an internal control plasmid (described below) using SuperFect reagent (Qiagen, Valencia, CA) according to the manufacturer's protocol. At 24 hours after transfection, oligonucleotide was added directly to the medium for the final concentration indicated. After 1 hour of incubation, recombinant TNF-α was added to the medium for 6 hours (where indicated) and cell lysates were prepared using reporter lysis buffer (Promega). Lysates were added to the substrate reagents supplied in the Dual-Luciferase Reporter System (Promega), and luciferase activity was measured using a luminometer (Zylux Corp., Maryville, TN). The NF-κB reporter plasmid contained tandem repeats of the κB sequence upstream of the minimal SV40 promoter and firefly luciferase gene (BD Biosciences Clontech, Palo Alto, CA). As an internal control to account for variations in transfection efficiency, pRLnull (Promega), which expresses *Renilla* luciferase by basal transcription, was used. Luciferase activities for each sample were calculated as the activity of firefly luciferase divided by *Renilla* luciferase and were normalized to the mean of the control (unstimulated) sample. The error bars shown represent SE, and Student's *t* tests[5] were used to assess the statistical significance of the reduction in activity by AGRO100 compared with the appropriate positive control (no oligonucleotide).

### Electrophoretic Mobility Shift Assay for Detection of NF-κB

HeLa cells were plated in six-well plates as described. After incubation with oligonucleotide for 1 hour, TNF-α was added for a further 2 hours and then nuclear extracts were prepared as described (16). Electrophoretic mobility shift assay analysis, using radiolabeled DNA representing the NF-κB upstream response element and 10 μg nuclear extract, was done using a method that has been described previously (36). Gels were dried and analyzed by autoradiography or by using a phosphorimager (Typhoon 9400). For densitometric quantitation, the results from five independent experiments were analyzed using ImageQuant 5.2 software. For each experiment, these intensities were normalized to the control (TNF-α stimulated, no oligonucleotide) and the error bars shown represent the SE of the normalized results. For these experiments, statistical significance was calculated compared with the control oligonucleotide (CRO26) because samples were normalized to the "no oligonucleotide" samples.

### Immunoprecipitation of Nucleolin

HeLa cells were plated as described. After 1 hour of incubation with oligonucleotide, TNF-α was added for a further 2 hours and then S-100 extracts were prepared (16). The extracts (100 μg) were incubated with 10 μg of anti-nucleolin antibody for 2 hours at 4°C in radioimmunoprecipitation assay buffer [150 mmol/L NaCl, 10 mmol/L Tris-HCl (pH 7.5), 0.1% SDS, 1% Triton X-100, 1% deoxycholate, 5 mmol/L EDTA, 1 mmol/L phenylmethylsulfonyl fluoride, 2 μg/mL leupeptin]. Goat anti-mouse–coated magnetic beads (MagnaBind) were then added to the samples and incubated for 1 hour at 4°C. The beads were captured, and unbound sample was removed by washing thrice with radioimmunoprecipitation assay buffer. The precipitated proteins were eluted from the beads by the addition of SDS sample loading buffer [4% SDS, 2% glycerol, 5% β-mercaptoethanol, 0.75 mol/L Tris-HCl (pH 8.8)] and heating at 65°C for 15 minutes. Western blot analysis, as described above, was then used to detect the presence of NEMO and nucleolin.

## Results

### Antiproliferative Activity of AGRO100

In previous work (1), we have shown that a GRO, named GRO29A, can inhibit proliferation in prostate, breast, and

[5] http://www.physics.csbsju.edu/stats/t-test.html

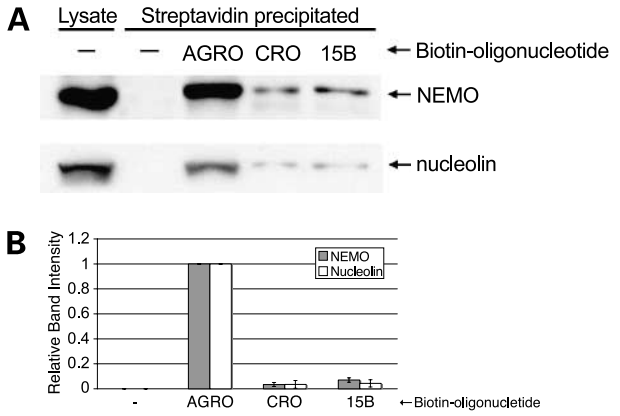


**Figure 2.** NEMO and nucleolin are associated with AGRO100. HeLa cells were treated with biotin-linked AGRO100 (*AGRO*) or biotin-linked control oligonucleotides [CRO26 (*CRO*) or GRO15B (*15B*)] or were untreated (–). After 2 h, cells were lysed under mild conditions and added to streptavidin-coated magnetic beads for precipitation of oligonucleotide-associated proteins. **A,** precipitated proteins were subjected to Western blot analysis to detect the presence of either NEMO or nucleolin. *Left,* nonprecipitated lysate (5 μg) was run for comparison. **B,** quantitative analysis for three independent experiments, where the intensity of bands was determined by densitometry and normalized to the AGRO band as described in Materials and Methods.

cervical cancer cells. Subsequently, we determined that the 3′-amino modification and the three 5′-thymidines of GRO29A are not necessary for nuclease resistance or biological activity (2, 4). Therefore, AGRO100, the oligonucleotide selected for clinical development, lacks these features and is an unmodified 26-mer oligodeoxynucleotide. Thermal denaturation experiments, carried out as described previously (1), indicate that AGRO100 forms a stable structure that melts at 76°C.[6] As shown schematically in Fig. 1, this structure is predicted (2) to be a bimolecular quadruplex that is stabilized by the formation of eight G-quartets. To first verify the antiproliferative activity in the cell lines of interest, AGRO100 was added directly to the culture medium and cells were incubated in the presence of the oligonucleotide for 5 days. This was followed by determination of relative cell number using a colorimetric 3-(4,5-dimethylthiazol-2-yl)-2,5-diphenyltetrazolium bromide assay. As expected, based on our previous studies of GRO29A (1–4), micromolar concentrations of AGRO100 strongly inhibited the proliferation of a variety of human cancer cells but had a lesser effect on Hs27 cells, which are nonmalignant human skin fibroblasts (Fig. 1C).

### NEMO Is an AGRO100-Associated Protein

In preliminary experiments designed to identify candidate proteins that may play a role in GRO activity, we incubated biotin-linked GROs with concentrated HeLa cell extracts *in vitro*. This was followed by streptavidin precipitation, electrophoresis of captured proteins, and mass spectrometry analysis of bands that were precipitated by an active GRO but not a control oligonucleotide. Several specific GRO-associated proteins were identified by this approach, including nucleolin and NEMO (data not shown; see Materials and Methods).

To confirm that complex formation between NEMO and AGRO100 occurs in treated cancer cells, we incubated HeLa cervical carcinoma cells with biotin-linked oligonucleotides, then lysed the cells under mild conditions, and precipitated with streptavidin. Western blot analysis of the streptavidin-precipitated proteins (Fig. 2) revealed that NEMO was precipitated from cells treated with biotin-linked AGRO100 but not from untreated cells. In cells treated with biotin-linked control oligonucleotides (CRO26, an inactive C-rich oligonucleotide, or GRO15B, an inactive GRO), only a very small amount of NEMO was detected. Densitometric analyses (Fig. 2B) of three independent

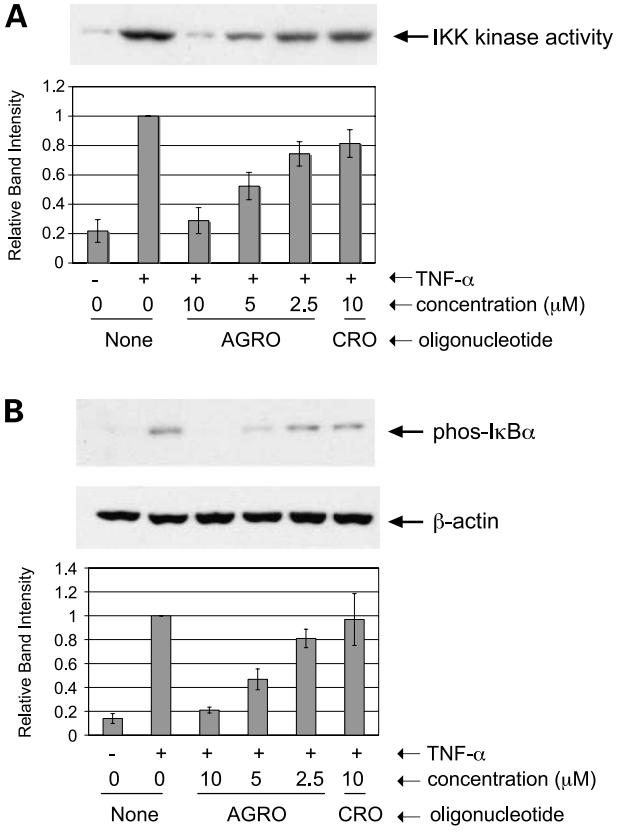


**Figure 3.** AGRO100 inhibits activity of the IKK complex. Lysates were prepared as described from HeLa cells that were treated for 1 h with AGRO100 (*AGRO*) or CRO26 (*CRO*) at the concentrations shown and then stimulated with TNF-α for 30 min. **A,** lysates were used in an IKK kinase assay in the presence of [γ-$^{32}$P]ATP and IκBα-glutathione *S*-transferase as a substrate. *Top,* IKK kinase activity as represented by phosphorylation of precipitated IκBα-glutathione *S*-transferase with $^{32}$P. *Bottom,* quantified IKK kinase activity determined by densitometry of three independent experiments as described in Materials and Methods. **B,** lysates were subjected to Western blot analysis using an antibody specific for the phosphorylated form of IκBα (*phos-IκBα*) to detect IKK-mediated phosphorylation of the endogenous substrate. The blots were stripped and reanalyzed for β-actin. *Bottom,* densitometric analysis of three independent experiments as described in Materials and Methods.

[6] P.J. Bates, unpublished observation.

experiments indicated that the intensity of the NEMO band precipitated by CRO26 or GRO15B was ≤7% compared with the AGRO100 sample. As expected, nucleolin was also specifically precipitated by biotin-linked AGRO100 (Fig. 2).

### Inhibition of IKK Activity in AGRO100-Treated Cells

Because NEMO is essential for function of the IKK complex in the classic pathway of NF-κB signaling (38), we next investigated the effect of AGRO100 treatment on IKK activity. First, we did an IKK kinase assay, which assesses the capability of cell lysates to phosphorylate the IKK substrate IκBα in the presence of radiolabeled ATP. HeLa cells were treated for 1 hour with AGRO100 or CRO26 and then stimulated with TNF-α for 30 minutes. As seen in Fig. 3A, there was significant induction of IKK activity on stimulation with TNF-α in the absence of oligonucleotide. Incubation of cells with AGRO100 abrogated the activation of the IKK complex in a reproducible, dose-dependent manner, whereas treatment with the control CRO26 had little effect. To validate these findings, we next used an additional method to examine the IKK-mediated

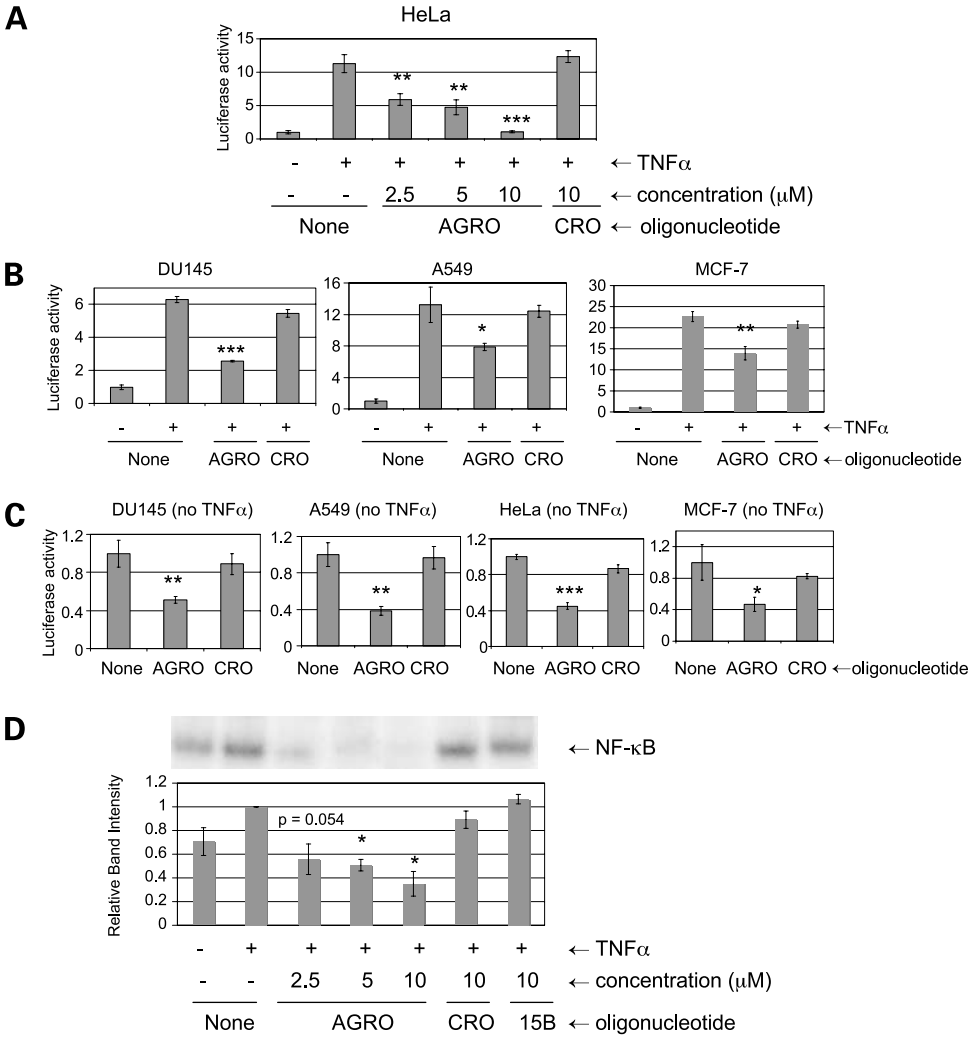


**Figure 4.** AGRO100 inhibits NF-κB transcriptional activity. **A,** HeLa cells were transiently transfected with a NF-κB reporter construct expressing firefly luciferase and a control plasmid expressing *Renilla* luciferase. After 24 h, cells were treated for 1 h with AGRO100 (*AGRO*) or control oligonucleotide, CRO26 (*CRO*), at the concentrations indicated and stimulated for an additional 6 h with TNF-α and luciferase activity was then measured. Luciferase activity was calculated as firefly luciferase activity divided by *Renilla* luciferase activity and shown relative to the unstimulated activity. *Columns,* mean of triplicate experiments; *bars,* SE. Statistical significance for each AGRO100-treated sample compared with control (TNF-α stimulated, no oligonucleotide). *, $P < 0.05$; **, $P < 0.01$; ***, $P < 0.001$. **B,** similar experiments were carried out in the cell lines (*top*) using 10 μmol/L AGRO100 or CRO26. Statistical significance for each AGRO100-treated sample compared with control (TNF-α stimulated, no oligonucleotide). **C,** same assays were carried out in the absence of TNF-α simulation to determine the effect of AGRO100 on constitutive NF-κB activity. Statistical significance for each AGRO100-treated sample compared with control (no oligonucleotide). **D,** nuclear extracts were prepared from HeLa cells that were treated for 1 h with AGRO100 (*AGRO*) or control oligonucleotides, CRO26 (*CRO*) or GRO15B (*15B*), and then stimulated for 2 h with TNF-α. These extracts were analyzed by electrophoretic mobility shift assay using a radiolabeled DNA duplex representing the NF-κB upstream response element to detect the presence of nuclear NF-κB. *Bottom,* densitometric analysis of five independent experiments as described in Materials and Methods and statistical significance for each AGRO100-treated sample compared with control oligonucleotide (*CRO*).

phosphorylation of IκBα. Western blot analysis using an antibody specific for the phosphorylated form of IκBα was done using lysates from cells that had been treated for 1 hour with AGRO100 or CRO26 and then stimulated with TNF-α. The membrane was subsequently stripped and analyzed for β-actin to ensure that equal amounts of protein were loaded and transferred. The results (Fig. 3B) indicated that phoshorylation of IκBα occurred on stimulation with TNF-α but was reproducibly blocked by AGRO100, whereas CRO26 had no effect. These observations correlated well with the results from the IKK kinase assay.

### Inhibition of NF-κB Activation in AGRO100-Treated Cells

Based on the previous result that IKK activity is inhibited, NF-κB signaling would be expected to be blocked in cancer cells treated with AGRO100. To confirm this prediction, we examined the activity of NF-κB in cells that were transiently transfected with a NF-κB-driven luciferase reporter construct. Cells were first transfected for 24 hours with the reporter construct (expressing firefly luciferase) plus an internal control vector (expressing *Renilla* luciferase) and then were treated with AGRO100 or CRO26 for 30 minutes. TNF-α was then added to the medium, and cells were incubated for a further 6 hours followed by measurement of luciferase activity. As shown in Fig. 4A, treatment of HeLa cells with AGRO100 significantly reduced TNF-α-induced NF-κB transcriptional activity in a dose-dependent manner, but treatment with the CRO26 control had no effect on NF-κB-driven luciferase activity. Next, we used the reporter gene assay to determine the effects of AGRO100 treatment on other types of cancer cells. Figure 4B shows that AGRO100 was able to significantly inhibit TNF-α-induced NF-κB activation in cell lines derived from human prostate cancer (DU145), breast cancer (MCF-7), and non–small cell lung cancer (A549). The effect on Hs27 cells was not determined because transfection efficiency in these cells was poor. Furthermore, as shown by similar experiments carried out in the absence of TNF-α, AGRO100 could also significantly inhibit constitutive NF-κB signaling in those cell lines that had significant basal NF-κB activity (Fig. 4C). In either the presence or the absence of TNF-α, there was no effect of AGRO100 on the activity due to the control *Renilla* luciferase plasmid or on cell number, therefore excluding the possibility of nonspecific effects of AGRO100 on transcription, translation, or cell viability (data not shown). Although the inhibitory effects of AGRO100 were highly reproducible (observed in at least three independent experiments for each cell line), we also used a supplementary method that did not depend on cell transfection to confirm our results. An electrophoretic mobility shift assay, using a radiolabeled DNA duplex representing the NF-κB upstream response element and nuclear extracts from HeLa cells stimulated with TNF-α, revealed induction of a band consistent with NF-κB after 2 hours of stimulation. In cells pretreated with the control oligonucleotides (CRO26 or GRO15B), nuclear NF-κB was apparent at levels similar to the cells treated with TNF-α alone. However, when the cells were treated with AGRO100 and then stimulated with TNF-α, the intensity of the NF-κB band was reduced in a dose-dependent manner (Fig. 4D).

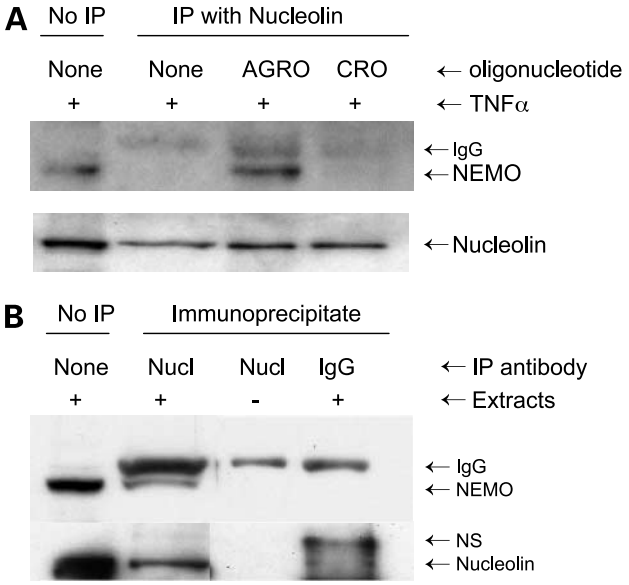


**Figure 5.** Coprecipitation of NEMO by nucleolin in AGRO100-treated cells. **A,** cytoplasmic (S-100) extracts were prepared from HeLa cells that had been treated for 1 h with 10 μmol/L AGRO100 (*AGRO*) or CRO26 (*CRO*) and then stimulated with TNF-α for 30 min. Immunoprecipitation (*IP*) with nucleolin antibody was done, and Western blot analysis was used to assess the presence of NEMO (48 kDa) and nucleolin (which migrates at 110 kDa). *Left,* nonprecipitated extract (5 μg) was run for comparison. **B,** to confirm the specific interaction of NEMO and nucleolin in the absence of AGRO100, a similar experiment was done. *Arrows,* lysates from HeLa cells that were stimulated 30 min with TNF-α were subjected to immunoprecipitation with nucleolin (*NucI*) antibody, and Western blot analysis revealed the presence of NEMO and nucleolin. Mock immunoprecipitation (no cellular extracts; *lane 3*) and immunoprecipitation with nonspecific IgG (*lane 4*) were done in parallel to ensure the specificity of the interaction. *Left,* nonprecipitated lysate (5 μg) was run for comparison. *IgG* and *NS,* unrelated bands that were artifacts of the immunoprecipitation. *IgG,* mouse immunoglobulin heavy chain, ~55 kDa. *NS,* uncharacterized, nonspecific protein.

### Coprecipitation of NEMO and Nucleolin from AGRO100-Treated Cells

Because both nucleolin and NEMO were precipitated by AGRO100, we proceeded to investigate the possibility that these proteins were simultaneously present in the same AGRO100-containing complex within the cell. Immunoprecipitation with nucleolin antibody was done using extracts from cells that had been treated with AGRO100 or CRO26 and then stimulated with TNF-α. The immunoprecipitates were then subjected to Western blot analysis to determine if NEMO was coprecipitated with nucleolin. Figure 5A shows that, in untreated cells or in cells treated with the control oligonucleotide, a very small amount of NEMO was detected in the nucleolin immunoprecipitate. However, when the cells were treated with AGRO100 and then stimulated with TNF-α, substantially more NEMO

coprecipitated with nucleolin, indicating that NEMO, nucleolin, and AGRO100 are present in the same complex. Although we cannot definitively exclude that AGRO100 is bound independently to both proteins, a more likely explanation for this result is that AGRO100 binds directly to nucleolin and stabilizes a protein-protein interaction between nucleolin and NEMO. This idea is supported by the weak interaction between nucleolin and NEMO in untreated cells, the specificity of which was confirmed in additional experiments (Fig. 5B).

## Discussion

It has become clear in recent years that NF-κB signaling is frequently deregulated in many types of cancer (33–35). NF-κB target genes encode a variety of pro-proliferation and antiapoptotic proteins, and it seems likely that malignant cells have acquired constitutive activation of this pathway to bypass the normal physiologic signals that prevent uncontrolled proliferation or to resist apoptosis induced by radiation, chemotherapy, or hormonal agents (33–35). Constitutive NF-κB activation may have particular significance with respect to advanced cancers and their resistance to therapeutic manipulation. For example, constitutive activity of NF-κB was not detected in hormone-responsive prostate cancer cell lines but was detected in hormone-insensitive prostate cancer lines and in tumor tissue from patients with advanced prostate cancer, a disease that is very often resistant to therapeutic intervention (42–44). Inhibition of NF-κB activation has also been linked to the chemopreventive properties of several compounds with activity in cancer, such as selenium, green tea, and silymarin (45–47). Down-regulation of NF-κB activity is therefore considered a very attractive strategy for developing new cancer treatments (34). The components of the IKK complex are of particular interest for drug discovery (39), and peptide inhibitors of NEMO have recently been shown to have anticancer activity (48), in addition to anti-inflammatory properties (49).

We have now shown that AGRO100 is an inhibitor of both constitutive and TNF-α-induced NF-κB signaling in a variety of cancer cell lines derived from prevalent solid tumor types. Moreover, we have defined a possible mechanism of this activity by showing that AGRO100 sequesters NEMO in a complex with nucleolin, thereby preventing activation of IKK and precluding phosphorylation of IκBα and subsequent release of NF-κB (Fig. 6B). Although it has not been ascertained that the inhibition of NF-κB is responsible for the anticancer activity of AGRO100, it seems likely that blocking this prosurvival, antiapoptotic pathway in cancer cells that have constitutive activation would lead to antiproliferative effects. It is apparent from Figs. 1 and 4 that the ability of AGRO100 to inhibit TNF-α-induced NF-κB signaling does not correlate directly with its antiproliferative activity. However, this is unsurprising because TNF-α is absent in the experiments shown in Fig. 1 and the effects of inhibiting constitutive NF-κB activity may depend complexly on numerous factors, including the basal level of NF-κB signaling and the extent of its inhibition by AGRO100. It may be significant that AGRO100 has the least growth-inhibitory effect on Hs27 cells, which have no detectable constitutive activation of NF-κB (confirmed by an electrophoretic mobility shift assay to detect NF-κB in unstimulated nuclear extracts). In any case, as we discuss below, it seems that inhibition of NF-κB signaling is one of several potential anticancer effects induced by AGRO100.

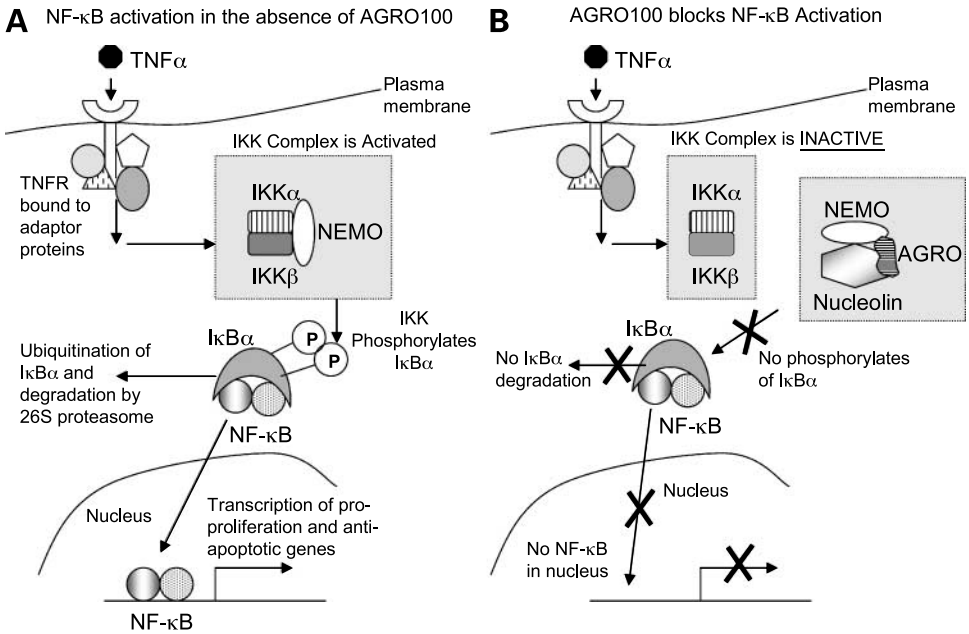


**Figure 6.** NF-κB activation and proposed model for its inhibition in the presence of AGRO100. **A,** on ligation of an appropriate surface receptor, such as the TNF-α receptor (*TNFR*), a signal is transduced to activate the IKK complex, which consists of IKKα, IKKβ, and NEMO. The complex then phosphorylates IκBα, which normally holds NF-κB in an inactive state in the cytoplasm, and causes it to become ultimately degraded by the 26S proteasome. Thus, the nuclear localization signal of NF-κB is unmasked and the transcription factor translocates to the nucleus to activate gene expression. **B,** in the presence of AGRO100, NEMO is sequestered in a complex containing nucleolin and AGRO100. The IKK complex is therefore inactive, and phosphorylation of IκBα cannot occur, which prevents release and activation of NF-κB.

Clearly, more research is needed to fully characterize the mechanism of GROs, such as AGRO100, but the results described herein are consistent with our theory that they work primarily as nucleolin-targeted aptamers. While investigating the role of nucleolin in GRO activity, we have observed that the presence of AGRO100 can induce changes in the protein-protein interactions of nucleolin, which include some enhanced and some reduced interactions.[7] Therefore, our hypothesis about the mechanism of GROs is that their antiproliferative effects result from their binding to nucleolin and modulation of its molecular interactions. We predict that this consequently alters certain activities of this highly multifunctional protein, leading to pleiotropic biological effects. Such effects may include inactivation of NF-κB signaling, inhibition of DNA replication, and induction of cell death, all of which have been reported here or previously (4). We have now shown that AGRO100 inhibits NF-κB activation, most likely by stabilizing a complex containing nucleolin and NEMO. Thus, we have identified NEMO as one of the probable partners of nucleolin whose binding is affected (enhanced in this case) by the presence of AGRO100.

The complex interactions that regulate NF-κB signaling are an area of intense interest and much has been learned about these in recent years. However, the full details of the pathway, especially the mechanisms leading to IKK activation, are not yet fully understood. Although nucleolin has not previously been implicated in NF-κB signaling, our present findings that a nucleolin-binding aptamer inhibits NF-κB activity and that nucleolin is associated with NEMO are suggestive of a role for nucleolin in regulation of the IKK complex. In conclusion, further studies seem to be warranted to define the precise nature of the nucleolin-NEMO interaction and to determine the role of nucleolin in NF-κB signaling.

[7] P.J. Bates, Y. Teng, L.K. Casson, and W.M. Pierce, Jr., unpublished observation.

**Acknowledgments**

We thank Dr. John O. Trent (University of Louisville, Louisville, KY) for providing the diagrams for Fig. 1.

**References**

**1.** Bates PJ, Kahlon JB, Thomas SD, Trent JO, Miller DM. Antiproliferative activity of G-rich oligonucleotides correlates with protein binding. J Biol Chem 1999;274:26369 – 77.

**2.** Dapic V, Bates PJ, Trent JO, Rodger A, Thomas SD, Miller DM. Antiproliferative activity of G-quartet-forming oligonucleotides with backbone and sugar modifications. Biochemistry 2002;41:3676 – 85.

**3.** Dapic V, Abdomerovic V, Marrington R, et al. Biophysical and biological properties of quadruplex oligodeoxyribonucleotides. Nucleic Acids Res 2003;31:2097 – 107.

**4.** Xu X, Hamhouyia F, Thomas SD, et al. Inhibition of DNA replication and induction of S phase cell cycle arrest by G-rich oligonucleotides. J Biol Chem 2001;276:43221 – 30.

**5.** Barnhart KM, Laber DA, Bates PJ, Trent JO, Miller DM. AGRO100: the translation from lab to clinic of a tumor-targeted nucleic acid aptamer. J Clin Oncol (Meet Abstr) 2004;22:3126.

**6.** Laber DA, Sharma VR, Bhupalam L, Taft BS, Hendler FJ, Barnhart KM. Update on the first phase I study of AGRO100 in advanced cancer. J Clin Oncol (Meet Abstr) 2005;23:3064.

**7.** Derenzini M, Sirri V, Trere D, Ochs RL. The quantity of nucleolar proteins nucleolin and protein B23 is related to cell doubling time in human cancer cells. Lab Invest 1995;73:497 – 502.

**8.** Pich A, Chiusa L, Margaria E. Prognostic relevance of AgNORs in tumor pathology. Micron 2000;31:133 – 41.

**9.** Trere D, Derenzini M, Sirri V, et al. Qualitative and quantitative analysis of AgNOR proteins in chemically induced rat liver carcinogenesis. Hepatology 1996;24:1269 – 73.

**10.** Srivastava M, Pollard HB. Molecular dissection of nucleolin's role in growth and cell proliferation: new insights. FASEB J 1999;13:1911 – 22.

**11.** Tuteja R, Tuteja N. Nucleolin: a multifunctional major nucleolar phosphoprotein. Crit Rev Biochem Mol Biol 1998;33:407 – 36.

**12.** Ginisty H, Sicard H, Roger B, Bouvet P. Structure and functions of nucleolin. J Cell Sci 1999;112:761 – 72.

**13.** Borer RA, Lehner CF, Eppenberger HM, Nigg EA. Major nucleolar proteins shuttle between nucleus and cytoplasm. Cell 1989;56:379 – 90.

**14.** Dumler I, Stepanova V, Jerke U, et al. Urokinase-induced mitogenesis is mediated by casein kinase 2 and nucleolin. Curr Biol 1999;9:1468 – 76.

**15.** Hovanessian AG, Puvion-Dutilleul F, Nisole S, et al. The cell-surface-expressed nucleolin is associated with the actin cytoskeleton. Exp Cell Res 2000;261:312 – 28.

**16.** Mi Y, Thomas SD, Xu X, Casson LK, Miller DM, Bates PJ. Apoptosis in leukemia cells is accompanied by alterations in the levels and localization of nucleolin. J Biol Chem 2003;278:8572 – 9.

**17.** Zhou G, Seibenhener ML, Wooten MW. Nucleolin is a protein kinase C-ζ substrate. Connection between cell surface signaling and nucleus in PC12 cells. J Biol Chem 1997;272:31130 – 7.

**18.** Barel M, Le Romancer M, Frade R. Activation of the EBV/C3d receptor (CR2, CD21) on human B lymphocyte surface triggers tyrosine phosphorylation of the 95-kDa nucleolin and its interaction with phosphatidylinositol 3 kinase. J Immunol 2001;166:3167 – 73.

**19.** Larrucea S, Cambronero R, Gonzalez-Rubio C, et al. Internalization of factor J and cellular signalization after factor J-cell interaction. Biochem Biophys Res Commun 1999;266:51 – 7.

**20.** Daniely Y, Borowiec JA. Formation of a complex between nucleolin and replication protein A after cell stress prevents initiation of DNA replication. J Cell Biol 2000;149:799 – 810.

**21.** Wang Y, Guan J, Wang H, Wang Y, Leeper D, Iliakis G. Regulation of DNA replication after heat shock by replication protein A-nucleolin interactions. J Biol Chem 2001;276:20579 – 88.

**22.** Sengupta TK, Bandyopadhyay S, Fernandes DJ, Spicer EK. Identification of nucleolin as an AU-rich element binding protein involved in bcl-2 mRNA stabilization. J Biol Chem 2004;279:10855 – 63.

**23.** Chen CY, Gherzi R, Andersen JS, et al. Nucleolin and YB-1 are required for JNK-mediated interleukin-2 mRNA stabilization during T-cell activation. Genes Dev 2000;14:1236 – 48.

**24.** Zaidi SH, Malter JS. Nucleolin and heterogeneous nuclear ribonucleoprotein C proteins specifically interact with the 3′-untranslated region of amyloid protein precursor mRNA. J Biol Chem 1995;270:17292 – 8.

**25.** Edwards TK, Saleem A, Shaman JA, et al. Role for nucleolin/Nsr1 in the cellular localization of topoisomerase I. J Biol Chem 2000;275:36181 – 8.

**26.** Takagi M, Absalon MJ, McLure KG, Kastan MB. Regulation of p53 translation and induction after DNA damage by ribosomal protein L26 and nucleolin. Cell 2005;123:49 – 63.

**27.** Kim K, Dimitrova DD, Carta KM, Saxena A, Daras M, Borowiec JA. Novel checkpoint response to genotoxic stress mediated by nucleolin-replication protein A complex formation. Mol Cell Biol 2005;25:2463 – 74.

**28.** Khurts S, Masutomi K, Delgermaa L, et al. Nucleolin interacts with telomerase. J Biol Chem 2004;279:51508 – 15.

**29.** Ishikawa F, Matunis MJ, Dreyfuss G, Cech TR. Nuclear proteins that bind the pre-mRNA 3′ splice site sequence r(UUAG/G) and the human telomeric DNA sequence d(TTAGGG)n. Mol Cell Biol 1993;13:4301 – 10.

**30.** Dickinson LA, Kohwi-Shigematsu T. Nucleolin is a matrix attachment region DNA-binding protein that specifically recognizes a region with high base-unpairing potential. Mol Cell Biol 1995;15:456 – 65.

**31.** Dempsey LA, Sun H, Hanakahi LA, Maizels N. G4 DNA binding by LR1 and its subunits, nucleolin and hnRNP D, a role for G-G pairing in immunoglobulin switch recombination. J Biol Chem 1999;274:1066 – 71.

**32.** Hanakahi LA, Sun H, Maizels N. High affinity interactions of nucleolin with G-G-paired rDNA. J Biol Chem 1999;274:15908 – 12.

**33.** Baldwin AS. Control of oncogenesis and cancer therapy resistance by the transcription factor NF-κB. J Clin Invest 2001;107:241 – 6.

**34.** Yamamoto Y, Gaynor RB. Therapeutic potential of inhibition of the NF-κB pathway in the treatment of inflammation and cancer. J Clin Invest 2001;107:135 – 42.

**35.** Karin M, Cao Y, Greten FR, Li ZW. NF-κB in cancer: from innocent bystander to major culprit. Nat Rev Cancer 2002;2:301 – 10.

**36.** Shen W, Waldschmidt M, Zhao X, Ratliff T, Krieg AM. Antitumor mechanisms of oligodeoxynucleotides with CpG and polyG motifs in murine prostate cancer cells: decrease of NF-κB and AP-1 binding activities and induction of apoptosis. Antisense Nucleic Acid Drug Dev 2002;12:155 – 64.

**37.** Benimetskaya L, Berton M, Kolbanovsky A, Benimetsky S, Stein CA. Formation of a G-tetrad and higher order structures correlates with biological activity of the RelA (NF-κB p65) 'antisense' oligodeoxynucleotide. Nucleic Acids Res 1997;25:2648 – 56.

**38.** Hayden MS, Ghosh S. Signaling to NF-κB. Genes Dev 2004;18: 2195 – 224.

**39.** Karin M, Yamamoto Y, Wang QM. The IKK NF-κB system: a treasure trove for drug development. Nat Rev Drug Discov 2004;3:17 – 26.

**40.** Nakanishi C, Toi M. Nuclear factor-κB inhibitors as sensitizers to anticancer drugs. Nat Rev Cancer 2005;5:297 – 309.

**41.** Powell DW, Rane MJ, Joughin BA, et al. Proteomic identification of 14-3-3ζ as a mitogen-activated protein kinase-activated protein kinase 2 substrate: role in dimer formation and ligand binding. Mol Cell Biol 2003; 23:5376 – 87.

**42.** Gasparian AV, Yao YJ, Kowalczyk D, et al. The role of IKK in constitutive activation of NF-κB transcription factor in prostate carcinoma cells. J Cell Sci 2002;115:141 – 51.

**43.** Suh J, Payvandi F, Edelstein LC, et al. Mechanisms of constitutive NF-κB activation in human prostate cancer cells. Prostate 2002;52: 183 – 200.

**44.** Chen CD, Sawyers CL. NF-κB activates prostate-specific antigen expression and is upregulated in androgen-independent prostate cancer. Mol Cell Biol 2002;22:2862 – 70.

**45.** Gasparian AV, Yao YJ, Lu J, et al. Selenium compounds inhibit IκB kinase (IKK) and nuclear factor-κB (NF-κB) in prostate cancer cells. Mol Cancer Ther 2002;1:1079 – 87.

**46.** Yang F, Oz HS, Barve S, de Villiers WJ, McClain CJ, Varilek GW. The green tea polyphenol (−)-epigallocatechin-3-gallate blocks nuclear factor-κB activation by inhibiting IκB kinase activity in the intestinal epithelial cell line IEC-6. Mol Pharmacol 2001;60:528 – 33.

**47.** Dhanalakshmi S, Singh RP, Agarwal C, Agarwal R. Silibinin inhibits constitutive and TNFα-induced activation of NF-κB and sensitizes human prostate carcinoma DU145 cells to TNFα-induced apoptosis. Oncogene 2002;21:1759 – 67.

**48.** Agou F, Courtois G, Chiaravalli J, et al. Inhibition of NF-κB activation by peptides targeting NF-κB essential modulator (NEMO) oligomerization. J Biol Chem 2004;279:54248 – 57.

**49.** May MJ, D'Acquisto F, Madge LA, Glockner J, Pober JS, Ghosh S. Selective inhibition of NF-κB activation by a peptide that blocks the interaction of NEMO with the IκB kinase complex. Science 2000;289: 1550 – 4.

APPENDIX 2: Excerpt from A. C. Girvan Ph.D. Dissertation (University of Louisville, 2006)

# CHAPTER IV

# NUCLEOLIN AND NEMO: POSSIBLE ROLE FOR NUCLEOLIN IN NF-KB SIGNALING

## INTRODUCTION

The NF-κB/Rel family of transcription factors has intensively studied as an important model system for how extracellular stimuli, such as tumor necrosis factor α (TNFα), cause the activation of transcription factors through signal transduction cascades. NF-κB regulates the expression of many genes critical for cellular processes, including inflammation, immune responses, and apoptosis [150]. NF-κB is normally kept inactive in the cytoplasm of unstimulated cells by its inhibitor proteins, IκBα. When an extracellular signal binds to the appropriate cell surface receptor, the signal results in the release of the NF-κB dimer from IκBα, and subsequent translocation to the nucleus to regulate gene transcription [110].

Central to the activation of NF-κB by extracellular stimuli is the IκB kinase (IKK) complex. The IKK complex is composed of two catalytic subunits IKKα and IKKβ, and a regulatory subunit NEMO (NF-κB essential modulator). Signaling pathways lead to the activation of IKK, which then results in the phosphorylation of IκB and its degradation by the ubiquitin-proteosome pathways allowing the release of NF-κB [110]. NEMO is essential in regulating IKK and the activation of NFκ-B; its importance

has been demonstrated in NEMO knockout mice experiments, where there is a complete loss of NF-κB activity in response to stimuli [150]. NEMO has multiple distinct domains which are thought to be used as scaffolding for the binding of IKKα and IKKβ, and possible binding of other unknown proteins as well [110].

Nucleolin is predominantly known as a nucleolar protein that is highly multifunctional. This 110-kD protein has been implicated in several cellular functions like cell growth and proliferation [40-42], ribosome biogenesis [40, 43], DNA replication [44], cytokinesis and nuclear division [45], and apoptosis [46, 47]. Although nucleolin is generally thought of as a nucleolar protein, there has been evidence supporting the role of nucleolin in transporting proteins between the cytoplasm and nucleus [60-62], and several reports demonstrating the mobility of nucleolin in the nucleoplasm, cytoplasm, and cell surface [34, 48-53]. The translocation of nucleolin to the cell surface has been shown in response to stimuli such as heat shock [44, 54], T-cell activation [55], mitosis [56], treatment with cyclin-dependent kinase inhibitor [57], and viral infection [58-60].

We report here that decreased expression of nucleolin by siRNA results in increased NF-κB transcriptional activity. Additionally, upon stimulation with TNFα, nucleolin and NEMO precipitate in the same complex in a time-dependent manner. These results suggest a possible role of nucleolin in the signaling cascade that leads to the transcription of genes regulated by NF-κB.

**MATERIALS AND METHODS**

**Cell culture and treatment**

HeLa cells (cervical cancer cells) in were obtained from American Type Culture Collection (ATCC). Cells were grown to 50% confluence in 6-well plates in a standard incubator in DMEM (Gibco) supplemented with 10% heat-inactivated (65°C for 20 min) fetal bovine serum (Gibco), 100 units/ml penicillin and 100 units/ml streptomycin. TNFα (R & D Systems, Inc.) was added to the culture medium for a final concentration of 10 ng/ml.

**siRNA**

The siRNA duplex sequence is 5'-d(GUUGCAGCAGCCUUCUUGCUU)-3' (antisense) and 5'-d(GCAAGAAGGCUGCUGCAACUU)-3' (sense) (Oligos Etc.). The antisense and sense strands of siRNA were suspended in Diethyl-pyrocarbonate (DEPC)-treated water. All siRNAs were annealed at 90°C for 2 min, then 37°C for 1 hr in Buffer R (100 mM potassium acetate, 30 mM HEPES-KOH pH 7.4, 2 mM magnesium acetate). HeLa cells were transfected with siRNA (100 nM) using Oligofectamine transfection reagent (Invitrogen) in Opti-MEM I reduced serum medium (Invitrogen) according to manufacturer's instructions. Cells were lysed with the addition of M-PER Mammalian protein extraction buffer (Pierce).

**Western blot analysis**

Whole cell lysates were electrophoresed on SDS-polyacrylamide (8%) gels and transferred to PVDF membranes. Membranes were blocked with 5% nonfat dried milk in PBS plus 0.05% Tween20 (PBST) then incubated with primary antibody in PBST (1 μg/ml anti-nucleolin, sc-8031, Santa Cruz or 1 μg/ml anti-NEMO, sc-8032, Santa Cruz).

Following incubation with secondary antibody (0.5 μg/ml anti-mouse HRP-conjugated, Santa Cruz) bands were visualized by chemiluminescence (ECL, Amersham Biosciences).

**Transient transfection and measurement of luciferase activity**

Cells were plated in 24-well plates at a density of 2 x $10^4$ cells per well and were transiently transfected with an NF-κB reporter plasmid and an internal control plasmid (described below) using Superfect reagent (Qiagen), according to the manufacturer's protocol. At 24 h post-transfection, the cells were treated with siRNA as described above. After an incubation of 48 h, TNFα (10 ng/ml) was added to the medium for an additional 6 h and cell lysates were prepared using reporter lysis buffer (Promega). Lysates were added to the substrate reagents supplied in the Dual-Luciferase reporter system (Promega) and luciferase activity was measured using a luminometer (Zylux corporation). The NF-κB reporter plasmid contained tandem repeats of the κB sequence upstream of the minimal simian virus 40 (SV40) promoter and firefly luciferase gene in pLuc-MCS vector (Stratagene) and was a kind gift from Dr. Fajan Yang. As an internal control to account for variations in transfection efficiency, pRLnull (Promega), which expresses *Renilla* luciferase by basal transcription, was used (a gift from Dr. Robert Mitchell). Luciferase activity is expressed as the activity of firefly luciferase divided by *Renilla* luciferase.

**Immunoprecipitation of NEMO**

HeLa cells were plated as described above and treated with TNFα (10 ng/ml) for various from 5 min to 180 min. Cells were lysed with the addition M-PER Mammalian protein extraction buffer (Pierce). The extracts were incubated with 10 μg of anti-NEMO antibody (sc-8330, Santa Cruz) for 2 h at 4°C in RIPA buffer (150 mM NaCl, 10 mM Tris.Hcl pH 7.5, 0.1% SDS, 1% Triton X-100, 1% Deoxycholate, 5 mM EDTA, 1mM PMSF, 2 μg/ml leupeptin). Protein G coated magnetic beads (Magnabind, Pierce) were then added to the samples and incubated for 1 h at 4°C. The beads were captured and unbound sample was removed by washing three times with RIPA buffer. The precipitated proteins were eluted from the beads by the addition of SDS sample loading buffer (4% SDS, 2% glycerol, 5% β-mercaptoethanol, 0.75 M Tris.HCl, pH 8.8) and heating at 65°C for 15 min. Western blot analysis, as described above, was then utilized to detect the presence of NEMO and nucleolin.

## RESULTS

### Decrease of nucleolin expression increases NF-κB transcriptional activity

HeLa cells were transfected with siRNA (100 nM) corresponding to nucleolin or a nonspecific sequence as a control. Following an incubation of 48 h, the cells were stimulated with TNFα (10 ng/ml) for 2 h, then lysed and subjected to western blot analysis to detect levels of nucleolin and β-actin as a loading control. Sufficient knockdown of nucleolin was achieved as seen in Figure 15. To examine NF-κB transcriptional activity, HeLa cells were first transfected with a NF-κB luciferase reporter plasmid and a null renilla plasmid as an internal control. 24 h after transfection, the cells

were treated with siRNA as described above. Following stimulation with TNFα for 6 h, luciferase activity was measured revealing an increase in NF-κB transcriptional activity in response to the knockdown of nucleolin. (Figure 15).

**Asscociation of nucleolin and NEMO increases in the presence of TNFα**

We previously observed co-precipitation of nucleolin and NEMO in the presence of GRO in the S-100 fraction of cell lysates (see Chapter 3). This association suggested nucleolin may be involved in the signaling events leading to NF-κB transcription. To examine this possibility, cells were treated with TNFα from 5 to 180 min. Cells were lysed and subjected to immunopreciptation with NEMO antibody. Western blotting revealed the association of nucleolin and NEMO increases in the presence of TNFα (Figure 16).

**Re-localization of nucleolin in response to TNFα stimulation**

We then investigated the effects of stimulation with TNFα on the levels and localization of nucleolin. Western blot analysis of lysates from HeLa cells (Figure 17) revealed an increase in S-100 nucleolin and a concomitant reduction in nuclear nucleolin, suggesting that there is rapid translocation of nucleolin in response to TNFα.

**Figure 15: Decreased expression of nucleolin results in increased NF-κB transcriptional activity.**

(A) Western blot analysis probing for nucleolin and β-actin from cell lysates transfected with siRNA (100 nM) corresponding to nucleolin or a non-specific sequence then stimulated with TNFα (10 ng/ml); (B) NF-κB transcriptional activity in the presence of siRNA for nucleolin or a non-specific sequence measured by luciferase assay.

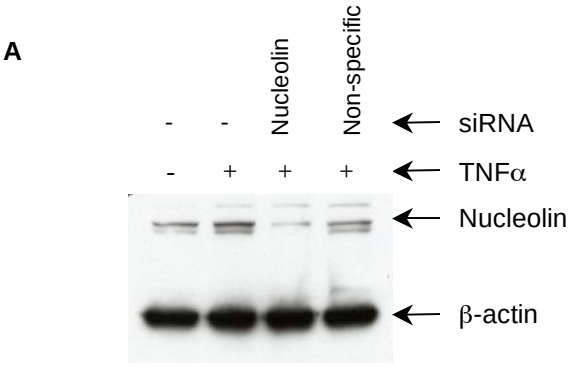
A
Nucleolin
Non-specific
- - siRNA
- + + + TNFα
Nucleolin
β-actin

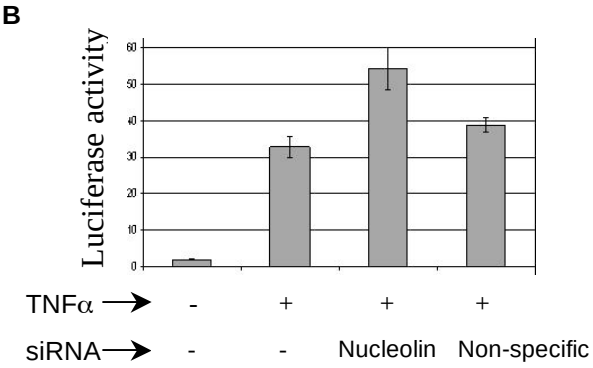
B
Luciferase activity
60
50
40
30
20
10
0
TNFα - + + +
siRNA - - Nucleolin Non-specific

**Figure 16: Association of nucleolin and NEMO increases in the presence of TNFα.**

HeLa cells were treated with TNFα (10 ng/ml), lysed, and subjected to immunopreciptiation with NEMO antibody. Western blot anlaysis revealed the presence of nucleolin and NEMO.

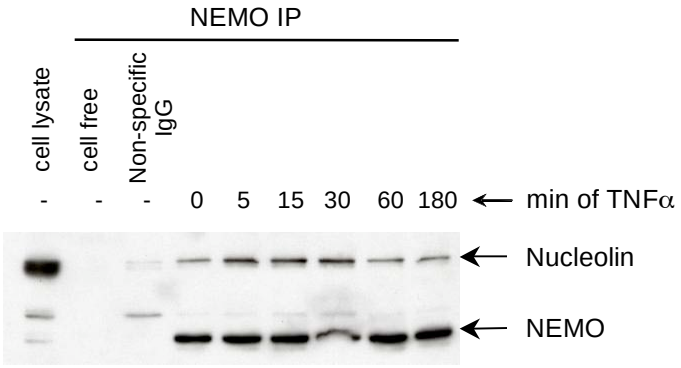
NEMO IP
cell lysate
cell free
Non-specific IgG
- - - 0 5 15 30 60 180
min of TNFα
Nucleolin
NEMO

**Figure 17: Translocation of nucleolin in response to TNFα stimulation.**

Nuclear and S-100 fractions were prepared from HeLa cells that had been stimulated with TNFα (10 ng/ml) for the time indicated. These extracts were subjected to western blot analysis to determine the levels of nucleolin and β-actin, which was used as a control for equal loading.

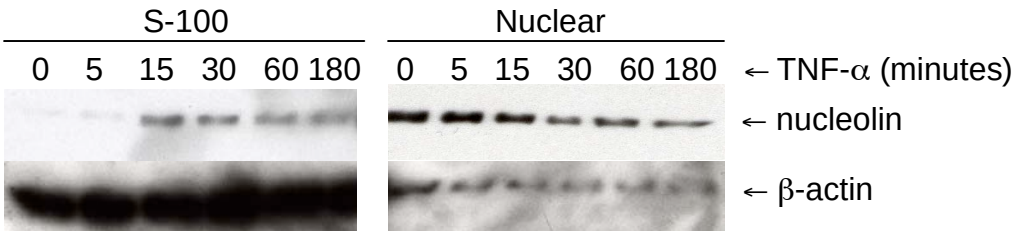
S-100
Nuclear
0 5 15 30 60 180
0 5 15 30 60 180
← TNF-α (minutes)
← nucleolin
← β-actin

## DISCUSSION

There has been a lot of interest in NF-κB signaling recently due to its involvement in several cellular processes. Although research has revealed much information about the events leading to NF-κB transcription, there are still unanswered questions in the signaling cascade, especially in the activation of the IKK complex.

We report here that nucleolin may play a role in the signaling cascade of NF-κB transcription; although there needs to be additional research to validate this hypothesis, we show evidence suggesting that nucleolin may be involved in the signaling cascade. Down-regulation of nucleolin by siRNA results in an increase in NF-κB transcriptional activity (Figure 15). Additionally, the association of nucleolin and NEMO increases in the presence of TNFα in a time-dependent manner (Figure 16), and nucleolin translocates in response to TNFα (Figure 17). This evidence suggests nucleolin may play a role in the activation of IKK.

There has been no previous reports describing the interaction of nucleolin and NEMO in NF-κB signaling; there is other circumstantial evidence supporting a role in this pathway. For example, it has been reported that nucleolin is phosphorylated in response to TNFα [151], and several other stimuli known to activate NF-κB can also induce mobilization of nucleolin [47, 55]. Nucleolin is a protein that shuttles between the nucleus and cytoplasm [50], and NEMO also undergoes nucleocytoplasmic shuttling [150]. Because of the NEMO-nucleolin colocalization in response to TNFα, it is possible

that nucleolin may be involved in its trafficking. In conclusion, further studies are needed to identify the role of nucleolin in NF-κB signaling and the interaction between nucleolin and NEMO.

## REFERENCES


1. Ma, D.D., et al., *Synthetic oligonucleotides as therapeutics: the coming of age.* Biotechnol Annu Rev, 2000. **5**: p. 155-96.
2. Nakata, Y., et al., *Nucleic acid modulation of gene expression: approaches for nucleic acid therapeutics against cancer.* Crit Rev Eukaryot Gene Expr, 2005. **15**(2): p. 163-82.
3. Martinand-Mari, C., B. Lebleu, and I. Robbins, *Oligonucleotide-based strategies to inhibit human hepatitis C virus.* Oligonucleotides, 2003. **13**(6): p. 539-48.
4. Rogers, F.A., J.A. Lloyd, and P.M. Glazer, *Triplex-forming oligonucleotides as potential tools for modulation of gene expression.* Curr Med Chem Anticancer Agents, 2005. **5**(4): p. 319-26.
5. Knauert, M.P. and P.M. Glazer, *Triplex forming oligonucleotides: sequence-specific tools for gene targeting.* Hum Mol Genet, 2001. **10**(20): p. 2243-51.
6. Gewirtz, A.M., D.L. Sokol, and M.Z. Ratajczak, *Nucleic acid therapeutics: state of the art and future prospects.* Blood, 1998. **92**(3): p. 712-36.
7. Mahato, R.I., K. Cheng, and R.V. Guntaka, *Modulation of gene expression by antisense and antigene oligodeoxynucleotides and small interfering RNA.* Expert Opin Drug Deliv, 2005. **2**(1): p. 3-28.
8. Schiavone, N., et al., *Antisense oligonucleotide drug design.* Curr Pharm Des, 2004. **10**(7): p. 769-84.
9. Gleave, M.E. and B.P. Monia, *Antisense therapy for cancer.* Nat Rev Cancer, 2005. **5**(6): p. 468-79.
10. Nimjee, S.M., C.P. Rusconi, and B.A. Sullenger, *Aptamers: an emerging class of therapeutics.* Annu Rev Med, 2005. **56**: p. 555-83.
11. Toulme, J.J., C. Di Primo, and D. Boucard, *Regulating eukaryotic gene expression with aptamers.* FEBS Lett, 2004. **567**(1): p. 55-62.
12. Tombelli, S., M. Minunni, and M. Mascini, *Analytical applications of aptamers.* Biosens Bioelectron, 2005. **20**(12): p. 2424-34.
13. Hermann, T. and D.J. Patel, *Adaptive recognition by nucleic acid aptamers.* Science, 2000. **287**(5454): p. 820-5.
14. Davis, J.T., *G-quartets 40 years later: from 5'-GMP to molecular biology and supramolecular chemistry.* Angew Chem Int Ed Engl, 2004. **43**(6): p. 668-98.
15. Keniry, M.A., *Quadruplex structures in nucleic acids.* Biopolymers, 2000. **56**(3): p. 123-46.
16. Mills, M., et al., *Unusual DNA conformations: implications for telomeres.* Curr Med Chem Anticancer Agents, 2002. **2**(5): p. 627-44.
17. Mergny, J.L., et al., *Natural and pharmacological regulation of telomerase.* Nucleic Acids Res, 2002. **30**(4): p. 839-65.

18. Neidle, S. and G. Parkinson, *Telomere maintenance as a target for anticancer drug discovery.* Nat Rev Drug Discov, 2002. **1**(5): p. 383-93.
19. Seenisamy, J., et al., *The dynamic character of the G-quadruplex element in the c-MYC promoter and modification by TMPyP4.* J Am Chem Soc, 2004. **126**(28): p. 8702-9.
20. De Armond, R., et al., *Evidence for the presence of a guanine quadruplex forming region within a polypurine tract of the hypoxia inducible factor 1alpha promoter.* Biochemistry, 2005. **44**(49): p. 16341-50.
21. Rankin, S., et al., *Putative DNA quadruplex formation within the human c-kit oncogene.* J Am Chem Soc, 2005. **127**(30): p. 10584-9.
22. Fry, M. and L.A. Loeb, *The fragile X syndrome d(CGG)n nucleotide repeats form a stable tetrahelical structure.* Proc Natl Acad Sci U S A, 1994. **91**(11): p. 4950-4.
23. Saha, T. and K. Usdin, *Tetraplex formation by the progressive myoclonus epilepsy type-1 repeat: implications for instability in the repeat expansion diseases.* FEBS Lett, 2001. **491**(3): p. 184-7.
24. Catasti, P., et al., *Structure-function correlations of the insulin-linked polymorphic region.* J Mol Biol, 1996. **264**(3): p. 534-45.
25. Dempsey, L.A., et al., *G4 DNA binding by LR1 and its subunits, nucleolin and hnRNP D, A role for G-G pairing in immunoglobulin switch recombination.* J Biol Chem, 1999. **274**(2): p. 1066-71.
26. Sundquist, W.I. and S. Heaphy, *Evidence for interstrand quadruplex formation in the dimerization of human immunodeficiency virus 1 genomic RNA.* Proc Natl Acad Sci U S A, 1993. **90**(8): p. 3393-7.
27. Pollice, A., et al., *In vitro binding of nucleolin to double-stranded telomeric DNA.* Biochem Biophys Res Commun, 2000. **268**(3): p. 909-15.
28. Hanakahi, L.A., H. Sun, and N. Maizels, *High affinity interactions of nucleolin with G-G-paired rDNA.* J Biol Chem, 1999. **274**(22): p. 15908-12.
29. Duquette, M.L., et al., *AID binds to transcription-induced structures in c-MYC that map to regions associated with translocation and hypermutation.* Oncogene, 2005. **24**(38): p. 5791-8.
30. Sun, H., et al., *The Bloom's syndrome helicase unwinds G4 DNA.* J Biol Chem, 1998. **273**(42): p. 27587-92.
31. Fry, M. and L.A. Loeb, *Human werner syndrome DNA helicase unwinds tetrahelical structures of the fragile X syndrome repeat sequence d(CGG)n.* J Biol Chem, 1999. **274**(18): p. 12797-802.
32. Lin, Y.C., et al., *Binding and partial denaturing of G-quartet DNA by Cdc13p of Saccharomyces cerevisiae.* J Biol Chem, 2001. **276**(50): p. 47671-4.
33. Isalan, M., et al., *Selection of zinc fingers that bind single-stranded telomeric DNA in the G-quadruplex conformation.* Biochemistry, 2001. **40**(3): p. 830-6.
34. Bates, P.J., et al., *Antiproliferative activity of G-rich oligonucleotides correlates with protein binding.* J Biol Chem, 1999. **274**(37): p. 26369-77.
35. Xu, X., et al., *Inhibition of DNA replication and induction of S phase cell cycle arrest by G-rich oligonucleotides.* J Biol Chem, 2001. **276**(46): p. 43221-30.
36. Dapic, V., et al., *Biophysical and biological properties of quadruplex oligodeoxyribonucleotides.* Nucleic Acids Res, 2003. **31**(8): p. 2097-107.

37. Dapic, V., et al., *Antiproliferative activity of G-quartet-forming oligonucleotides with backbone and sugar modifications.* Biochemistry, 2002. **41**(11): p. 3676-85.
38. Laber, D.A., Choudry, M. A., Taft, B. S., Bhupalam, L., Sharma, V. R., Hendler, F. J., Barnhart, K. M., *A phase I study of AGRO100 in advanced cancer.* J Clin Oncol (Meeting Abstracts), 2004 **22**(14S): p. 3112.
39. Laber, D., Bates, P., Trent, J., Barnhart, K., Taft, B., and Miller, D., *Long term clinical response in renal cell carcinoma patients treated with quadraplex forming oligonucleotides.* Clin Cancer Res, 2005. **11**(24 Part 2): p. 9088S.
40. Tuteja, R. and N. Tuteja, *Nucleolin: a multifunctional major nucleolar phosphoprotein.* Crit Rev Biochem Mol Biol, 1998. **33**(6): p. 407-36.
41. Ginisty, H., et al., *Structure and functions of nucleolin.* J Cell Sci, 1999. **112 ( Pt 6)**: p. 761-72.
42. Srivastava, M. and H.B. Pollard, *Molecular dissection of nucleolin's role in growth and cell proliferation: new insights.* Faseb J, 1999. **13**(14): p. 1911-22.
43. Ginisty, H., F. Amalric, and P. Bouvet, *Nucleolin functions in the first step of ribosomal RNA processing.* Embo J, 1998. **17**(5): p. 1476-86.
44. Daniely, Y. and J.A. Borowiec, *Formation of a complex between nucleolin and replication protein A after cell stress prevents initiation of DNA replication.* J Cell Biol, 2000. **149**(4): p. 799-810.
45. Leger-Silvestre, I., et al., *Ultrastructural changes in the Schizosaccharomyces pombe nucleolus following the disruption of the gar2+ gene, which encodes a nucleolar protein structurally related to nucleolin.* Chromosoma, 1997. **105**(7-8): p. 542-52.
46. Brockstedt, E., et al., *Identification of apoptosis-associated proteins in a human Burkitt lymphoma cell line. Cleavage of heterogeneous nuclear ribonucleoprotein A1 by caspase 3.* J Biol Chem, 1998. **273**(43): p. 28057-64.
47. Mi, Y., et al., *Apoptosis in leukemia cells is accompanied by alterations in the levels and localization of nucleolin.* J Biol Chem, 2003. **278**(10): p. 8572-9.
48. Larrucea, S., et al., *Cellular adhesion mediated by factor J, a complement inhibitor. Evidence for nucleolin involvement.* J Biol Chem, 1998. **273**(48): p. 31718-25.
49. Callebaut, C., et al., *Identification of V3 loop-binding proteins as potential receptors implicated in the binding of HIV particles to CD4(+) cells.* J Biol Chem, 1998. **273**(34): p. 21988-97.
50. Borer, R.A., et al., *Major nucleolar proteins shuttle between nucleus and cytoplasm.* Cell, 1989. **56**(3): p. 379-90.
51. Hovanessian, A.G., et al., *The cell-surface-expressed nucleolin is associated with the actin cytoskeleton.* Exp Cell Res, 2000. **261**(2): p. 312-28.
52. Dumler, I., et al., *Urokinase-induced mitogenesis is mediated by casein kinase 2 and nucleolin.* Curr Biol, 1999. **9**(24): p. 1468-76.
53. Sorokina, E.A. and J.G. Kleinman, *Cloning and preliminary characterization of a calcium-binding protein closely related to nucleolin on the apical surface of inner medullary collecting duct cells.* J Biol Chem, 1999. **274**(39): p. 27491-6.
54. Wang, Y., et al., *Regulation of dna replication after heat shock by replication protein a-nucleolin interactions.* J Biol Chem, 2001. **276**(23): p. 20579-88.

55. Gil, D., D. Gutierrez, and B. Alarcon, *Intracellular redistribution of nucleolin upon interaction with the CD3epsilon chain of the T cell receptor complex.* J Biol Chem, 2001. **276**(14): p. 11174-9.
56. Weisenberger, D. and U. Scheer, *A possible mechanism for the inhibition of ribosomal RNA gene transcription during mitosis.* J Cell Biol, 1995. **129**(3): p. 561-75.
57. David-Pfeuty, T., *Potent inhibitors of cyclin-dependent kinase 2 induce nuclear accumulation of wild-type p53 and nucleolar fragmentation in human untransformed and tumor-derived cells.* Oncogene, 1999. **18**(52): p. 7409-22.
58. Matthews, D.A., *Adenovirus protein V induces redistribution of nucleolin and B23 from nucleolus to cytoplasm.* J Virol, 2001. **75**(2): p. 1031-8.
59. Cannavo, G., et al., *Abnormal intracellular kinetics of cell-cycle-dependent proteins in lymphocytes from patients infected with human immunodeficiency virus: a novel biologic link between immune activation, accelerated T-cell turnover, and high levels of apoptosis.* Blood, 2001. **97**(6): p. 1756-64.
60. Waggoner, S. and P. Sarnow, *Viral ribonucleoprotein complex formation and nucleolar-cytoplasmic relocalization of nucleolin in poliovirus-infected cells.* J Virol, 1998. **72**(8): p. 6699-709.
61. Kibbey, M.C., et al., *A 110-kD nuclear shuttling protein, nucleolin, binds to the neurite-promoting IKVAV site of laminin-1.* J Neurosci Res, 1995. **42**(3): p. 314-22.
62. Lee, C.H., et al., *The nucleolin binding activity of hepatitis delta antigen is associated with nucleolus targeting.* J Biol Chem, 1998. **273**(13): p. 7650-6.
63. Pich, A., L. Chiusa, and E. Margaria, *Prognostic relevance of AgNORs in tumor pathology.* Micron, 2000. **31**(2): p. 133-41.
64. Trere, D., et al., *Qualitative and quantitative analysis of AgNOR proteins in chemically induced rat liver carcinogenesis.* Hepatology, 1996. **24**(5): p. 1269-73.
65. Derenzini, M., et al., *The quantity of nucleolar proteins nucleolin and protein B23 is related to cell doubling time in human cancer cells.* Lab Invest, 1995. **73**(4): p. 497-502.
66. Jemal, A., et al., *Cancer statistics, 2005.* CA Cancer J Clin, 2005. **55**(1): p. 10-30.
67. Coppelli, F.M. and J.R. Grandis, *Oligonucleotides as anticancer agents: from the benchside to the clinic and beyond.* Curr Pharm Des, 2005. **11**(22): p. 2825-40.
68. Patton, J.G., et al., *Cloning and characterization of PSF, a novel pre-mRNA splicing factor.* Genes Dev, 1993. **7**(3): p. 393-406.
69. Gozani, O., J.G. Patton, and R. Reed, *A novel set of spliceosome-associated proteins and the essential splicing factor PSF bind stably to pre-mRNA prior to catalytic step II of the splicing reaction.* Embo J, 1994. **13**(14): p. 3356-67.
70. Lutz, C.S., et al., *The snRNP-free U1A (SF-A) complex(es): identification of the largest subunit as PSF, the polypyrimidine-tract binding protein-associated splicing factor.* Rna, 1998. **4**(12): p. 1493-9.
71. Emili, A., et al., *Splicing and transcription-associated proteins PSF and p54nrb/nonO bind to the RNA polymerase II CTD.* Rna, 2002. **8**(9): p. 1102-11.
72. Zhang, Z. and G.G. Carmichael, *The fate of dsRNA in the nucleus: a p54(nrb)-containing complex mediates the nuclear retention of promiscuously A-to-I edited RNAs.* Cell, 2001. **106**(4): p. 465-75.

73. Shav-Tal, Y. and D. Zipori, *PSF and p54(nrb)/NonO--multi-functional nuclear proteins.* FEBS Lett, 2002. **531**(2): p. 109-14.
74. Straub, T., et al., *The RNA-splicing factor PSF/p54 controls DNA-topoisomerase I activity by a direct interaction.* J Biol Chem, 1998. **273**(41): p. 26261-4.
75. Akhmedov, A.T. and B.S. Lopez, *Human 100-kDa homologous DNA-pairing protein is the splicing factor PSF and promotes DNA strand invasion.* Nucleic Acids Res, 2000. **28**(16): p. 3022-30.
76. Bertrand, P., et al., *Human POMp75 is identified as the pro-oncoprotein TLS/FUS: both POMp75 and POMp100 DNA homologous pairing activities are associated to cell proliferation.* Oncogene, 1999. **18**(31): p. 4515-21.
77. Zhang, W.W., et al., *Purification and characterization of a DNA-binding heterodimer of 52 and 100 kDa from HeLa cells.* Biochem J, 1993. **290 ( Pt 1)**: p. 267-72.
78. Dong, B., et al., *Purification and cDNA cloning of HeLa cell p54nrb, a nuclear protein with two RNA recognition motifs and extensive homology to human splicing factor PSF and Drosophila NONA/BJ6.* Nucleic Acids Res, 1993. **21**(17): p. 4085-92.
79. Choi, Y.D. and G. Dreyfuss, *Isolation of the heterogeneous nuclear RNA-ribonucleoprotein complex (hnRNP): a unique supramolecular assembly.* Proc Natl Acad Sci U S A, 1984. **81**(23): p. 7471-5.
80. Carpenter, B., et al., *The roles of heterogeneous nuclear ribonucleoproteins in tumour development and progression.* Biochim Biophys Acta, 2005.
81. Dreyfuss, G., et al., *hnRNP proteins and the biogenesis of mRNA.* Annu Rev Biochem, 1993. **62**: p. 289-321.
82. Iwanaga, K., et al., *Heterogeneous nuclear ribonucleoprotein B1 protein impairs DNA repair mediated through the inhibition of DNA-dependent protein kinase activity.* Biochem Biophys Res Commun, 2005. **333**(3): p. 888-95.
83. Lee, S.Y., et al., *A proteomics approach for the identification of nucleophosmin and heterogeneous nuclear ribonucleoprotein C1/C2 as chromatin-binding proteins in response to DNA double-strand breaks.* Biochem J, 2005. **388**(Pt 1): p. 7-15.
84. Kamma, H., et al., *Interaction of hnRNP A2/B1 isoforms with telomeric ssDNA and the in vitro function.* Biochem Biophys Res Commun, 2001. **280**(3): p. 625-30.
85. Ishikawa, F., et al., *Nuclear proteins that bind the pre-mRNA 3' splice site sequence r(UUAG/G) and the human telomeric DNA sequence d(TTAGGG)n.* Mol Cell Biol, 1993. **13**(7): p. 4301-10.
86. Moran-Jones, K., et al., *hnRNP A2, a potential ssDNA/RNA molecular adapter at the telomere.* Nucleic Acids Res, 2005. **33**(2): p. 486-96.
87. Krecic, A.M. and M.S. Swanson, *hnRNP complexes: composition, structure, and function.* Curr Opin Cell Biol, 1999. **11**(3): p. 363-71.
88. Rooke, N., et al., *Roles for SR proteins and hnRNP A1 in the regulation of c-src exon N1.* Mol Cell Biol, 2003. **23**(6): p. 1874-84.
89. Pinol-Roma, S., *HnRNP proteins and the nuclear export of mRNA.* Semin Cell Dev Biol, 1997. **8**(1): p. 57-63.

90. He, Y., et al., *Roles of heterogeneous nuclear ribonucleoproteins A and B in cell proliferation.* J Cell Sci, 2005. **118**(Pt 14): p. 3173-83.
91. Tockman, M.S., et al., *Prospective detection of preclinical lung cancer: results from two studies of heterogeneous nuclear ribonucleoprotein A2/B1 overexpression.* Clin Cancer Res, 1997. **3**(12 Pt 1): p. 2237-46.
92. Miller, J., A.D. McLachlan, and A. Klug, *Repetitive zinc-binding domains in the protein transcription factor IIIA from Xenopus oocytes.* Embo J, 1985. **4**(6): p. 1609-14.
93. Engelke, D.R., et al., *Specific interaction of a purified transcription factor with an internal control region of 5S RNA genes.* Cell, 1980. **19**(3): p. 717-28.
94. Guddat, U., A.H. Bakken, and T. Pieler, *Protein-mediated nuclear export of RNA: 5S rRNA containing small RNPs in xenopus oocytes.* Cell, 1990. **60**(4): p. 619-28.
95. Polymeropoulos, M.H., et al., *Mutation in the alpha-synuclein gene identified in families with Parkinson's disease.* Science, 1997. **276**(5321): p. 2045-7.
96. Kruger, R., et al., *Ala30Pro mutation in the gene encoding alpha-synuclein in Parkinson's disease.* Nat Genet, 1998. **18**(2): p. 106-8.
97. Zarranz, J.J., et al., *The new mutation, E46K, of alpha-synuclein causes Parkinson and Lewy body dementia.* Ann Neurol, 2004. **55**(2): p. 164-73.
98. Bennett, M.C., *The role of alpha-synuclein in neurodegenerative diseases.* Pharmacol Ther, 2005. **105**(3): p. 311-31.
99. McMahon, H.T., et al., *Complexins: cytosolic proteins that regulate SNAP receptor function.* Cell, 1995. **83**(1): p. 111-9.
100. Reim, K., et al., *Complexins regulate a late step in Ca2+-dependent neurotransmitter release.* Cell, 2001. **104**(1): p. 71-81.
101. Eastwood, S.L. and P.J. Harrison, *Hippocampal synaptic pathology in schizophrenia, bipolar disorder and major depression: a study of complexin mRNAs.* Mol Psychiatry, 2000. **5**(4): p. 425-32.
102. Jung, D., et al., *Mechanism and Control of V(D)J Recombination at the Immunoglobulin Heavy Chain Locus.* Annu Rev Immunol, 2006.
103. Libra, M., et al., *Second primary lymphoma or recurrence: a dilemma solved by VDJ rearrangement analysis.* Leuk Lymphoma, 2004. **45**(8): p. 1539-43.
104. Richter, O.M. and B. Ludwig, *Cytochrome c oxidase--structure, function, and physiology of a redox-driven molecular machine.* Rev Physiol Biochem Pharmacol, 2003. **147**: p. 47-74.
105. Poyton, R.O., et al., *Expression and function of cytochrome c oxidase subunit isologues. Modulators of cellular energy production?* Ann N Y Acad Sci, 1988. **550**: p. 289-307.
106. Aggeler, R. and R.A. Capaldi, *Cross-linking of the gamma subunit of the Escherichia coli ATPase (ECF1) via cysteines introduced by site-directed mutagenesis.* J Biol Chem, 1992. **267**(30): p. 21355-9.
107. Taanman, J.W., *Human cytochrome c oxidase: structure, function, and deficiency.* J Bioenerg Biomembr, 1997. **29**(2): p. 151-63.
108. Taanman, J.W. and S.L. Williams, *Assembly of cytochrome c oxidase: what can we learn from patients with cytochrome c oxidase deficiency?* Biochem Soc Trans, 2001. **29**(Pt 4): p. 446-51.

109. Pahl, H.L., *Activators and target genes of Rel/NF-kappaB transcription factors.* Oncogene, 1999. **18**(49): p. 6853-66.
110. Ghosh, S. and M. Karin, *Missing pieces in the NF-kappaB puzzle.* Cell, 2002. **109 Suppl**: p. S81-96.
111. Luo, J.L., H. Kamata, and M. Karin, *IKK/NF-kappaB signaling: balancing life and death--a new approach to cancer therapy.* J Clin Invest, 2005. **115**(10): p. 2625-32.
112. Assenmacher, N. and K.P. Hopfner, *MRE11/RAD50/NBS1: complex activities.* Chromosoma, 2004. **113**(4): p. 157-66.
113. Brodersen, D.E. and P. Nissen, *The social life of ribosomal proteins.* Febs J, 2005. **272**(9): p. 2098-108.
114. Nissen, P., et al., *The structural basis of ribosome activity in peptide bond synthesis.* Science, 2000. **289**(5481): p. 920-30.
115. Henry, J.L., D.L. Coggin, and C.R. King, *High-level expression of the ribosomal protein L19 in human breast tumors that overexpress erbB-2.* Cancer Res, 1993. **53**(6): p. 1403-8.
116. Terasawa, K., M. Minami, and Y. Minami, *Constantly updated knowledge of Hsp90.* J Biochem (Tokyo), 2005. **137**(4): p. 443-7.
117. Whitesell, L. and S.L. Lindquist, *HSP90 and the chaperoning of cancer.* Nat Rev Cancer, 2005. **5**(10): p. 761-72.
118. Chen, G., P. Cao, and D.V. Goeddel, *TNF-induced recruitment and activation of the IKK complex require Cdc37 and Hsp90.* Mol Cell, 2002. **9**(2): p. 401-10.
119. Miyata, Y. and I. Yahara, *p53-independent association between SV40 large T antigen and the major cytosolic heat shock protein, HSP90.* Oncogene, 2000. **19**(11): p. 1477-84.
120. Koyasu, S., et al., *Two mammalian heat shock proteins, HSP90 and HSP100, are actin-binding proteins.* Proc Natl Acad Sci U S A, 1986. **83**(21): p. 8054-8.
121. Yano, M., et al., *Expression and roles of heat shock proteins in human breast cancer.* Jpn J Cancer Res, 1996. **87**(9): p. 908-15.
122. Islam, M.N. and M.N. Iskander, *Microtubulin binding sites as target for developing anticancer agents.* Mini Rev Med Chem, 2004. **4**(10): p. 1077-104.
123. Pollard, T.D. and J.A. Cooper, *Actin and actin-binding proteins. A critical evaluation of mechanisms and functions.* Annu Rev Biochem, 1986. **55**: p. 987-1035.
124. Nobes, C.D. and A. Hall, *Rho, rac, and cdc42 GTPases regulate the assembly of multimolecular focal complexes associated with actin stress fibers, lamellipodia, and filopodia.* Cell, 1995. **81**(1): p. 53-62.
125. Rao, J. and N. Li, *Microfilament actin remodeling as a potential target for cancer drug development.* Curr Cancer Drug Targets, 2004. **4**(4): p. 345-54.
126. Yanagida, M., et al., *Isolation and proteomic characterization of the major proteins of the nucleolin-binding ribonucleoprotein complexes.* Proteomics, 2001. **1**(11): p. 1390-404.
127. Zaidi, S.H. and J.S. Malter, *Nucleolin and heterogeneous nuclear ribonucleoprotein C proteins specifically interact with the 3'-untranslated region of amyloid protein precursor mRNA.* J Biol Chem, 1995. **270**(29): p. 17292-8.

128. Barel, M., M. Le Romancer, and R. Frade, *Activation of the EBV/C3d receptor (CR2, CD21) on human B lymphocyte surface triggers tyrosine phosphorylation of the 95-kDa nucleolin and its interaction with phosphatidylinositol 3 kinase.* J Immunol, 2001. **166**(5): p. 3167-73.
129. Sengupta, T.K., et al., *Identification of nucleolin as an AU-rich element binding protein involved in bcl-2 mRNA stabilization.* J Biol Chem, 2004. **279**(12): p. 10855-63.
130. Chen, C.Y., et al., *Nucleolin and YB-1 are required for JNK-mediated interleukin-2 mRNA stabilization during T-cell activation.* Genes Dev, 2000. **14**(10): p. 1236-48.
131. Edwards, T.K., et al., *Role for nucleolin/Nsr1 in the cellular localization of topoisomerase I.* J Biol Chem, 2000. **275**(46): p. 36181-8.
132. Kim, K., et al., *Novel checkpoint response to genotoxic stress mediated by nucleolin-replication protein a complex formation.* Mol Cell Biol, 2005. **25**(6): p. 2463-74.
133. Khurts, S., et al., *Nucleolin interacts with telomerase.* J Biol Chem, 2004. **279**(49): p. 51508-15.
134. Dickinson, L.A. and T. Kohwi-Shigematsu, *Nucleolin is a matrix attachment region DNA-binding protein that specifically recognizes a region with high base-unpairing potential.* Mol Cell Biol, 1995. **15**(1): p. 456-65.
135. Baldwin, A.S., *Control of oncogenesis and cancer therapy resistance by the transcription factor NF-kappaB.* J Clin Invest, 2001. **107**(3): p. 241-6.
136. Yamamoto, Y. and R.B. Gaynor, *Therapeutic potential of inhibition of the NF-kappaB pathway in the treatment of inflammation and cancer.* J Clin Invest, 2001. **107**(2): p. 135-42.
137. Shen, W., et al., *Antitumor mechanisms of oligodeoxynucleotides with CpG and polyG motifs in murine prostate cancer cells: decrease of NF-kappaB and AP-1 binding activities and induction of apoptosis.* Antisense Nucleic Acid Drug Dev, 2002. **12**(3): p. 155-64.
138. Hayden, M.S. and S. Ghosh, *Signaling to NF-kappaB.* Genes Dev, 2004. **18**(18): p. 2195-224.
139. Karin, M., Y. Yamamoto, and Q.M. Wang, *The IKK NF-kappa B system: a treasure trove for drug development.* Nat Rev Drug Discov, 2004. **3**(1): p. 17-26.
140. Yang, F., et al., *The green tea polyphenol (-)-epigallocatechin-3-gallate blocks nuclear factor-kappa B activation by inhibiting I kappa B kinase activity in the intestinal epithelial cell line IEC-6.* Mol Pharmacol, 2001. **60**(3): p. 528-33.
141. Gasparian, A.V., et al., *The role of IKK in constitutive activation of NF-kappaB transcription factor in prostate carcinoma cells.* J Cell Sci, 2002. **115**(Pt 1): p. 141-51.
142. Suh, J., et al., *Mechanisms of constitutive NF-kappaB activation in human prostate cancer cells.* Prostate, 2002. **52**(3): p. 183-200.
143. Gasparian, A.V., et al., *Selenium compounds inhibit I kappa B kinase (IKK) and nuclear factor-kappa B (NF-kappa B) in prostate cancer cells.* Mol Cancer Ther, 2002. **1**(12): p. 1079-87.

144. Dhanalakshmi, S., et al., *Silibinin inhibits constitutive and TNFalpha-induced activation of NF-kappaB and sensitizes human prostate carcinoma DU145 cells to TNFalpha-induced apoptosis.* Oncogene, 2002. **21**(11): p. 1759-67.
145. Agou, F., et al., *Inhibition of NF-kappa B activation by peptides targeting NF-kappa B essential modulator (nemo) oligomerization.* J Biol Chem, 2004. **279**(52): p. 54248-57.
146. Allison, D.B., et al., *Microarray data analysis: from disarray to consolidation and consensus.* Nat Rev Genet, 2006. **7**(1): p. 55-65.
147. Fathallah-Shaykh, H.M., *Microarrays: applications and pitfalls.* Arch Neurol, 2005. **62**(11): p. 1669-72.
148. Baak, J.P., et al., *Genomics and proteomics--the way forward.* Ann Oncol, 2005. **16 Suppl 2**: p. ii30-44.
149. Kettani, A., R.A. Kumar, and D.J. Patel, *Solution structure of a DNA quadruplex containing the fragile X syndrome triplet repeat.* J Mol Biol, 1995. **254**(4): p. 638-56.
150. Li, Q. and I.M. Verma, *NF-kappaB regulation in the immune system.* Nat Rev Immunol, 2002. **2**(10): p. 725-34.
151. Guy, G.R., et al., *Okadaic acid mimics multiple changes in early protein phosphorylation and gene expression induced by tumor necrosis factor or interleukin-1.* J Biol Chem, 1992. **267**(3): p. 1846-52.

APPENDIX 3: Teng *et al.* (2007), Manuscript in preparation (draft)

# Proteomic Analysis of the Effects of Novel Anticancer Aptamer, AS1411, on Nucleolin Complexes in Human Prostate Cancer Cells

Yun Teng,[1] Allicia Girvan,[2] Bill Pierce,[3] and Paula J. Bates[1,2]

*Departments of [1] Medicine, [2] Biochemistry and Molecular Biology, [3] Departments of Pharmacology and Toxicology, University of Louisville, Kentucky*

**Grant support:** This work was supported by a grant from the Department of Defense Prostate Cancer Research Program (PC030134).

**Requests for reprints**: Paula J. Bates, James Graham Brown Cancer Center, University of Louisville, 580 South Preston Street, Delia Baxter Building 321, Louisville, KY 40202-1756. Phone: 502 852 2432; Fax: 502 852 2356; Email: paula.bates@louisville.edu

**Keywords:** AS1411, proteomic analysis, nucleolin, protein interaction, non-ribosomal protein

**ABSTRACT**

**AS1411 (formerly AGRO100) is a guanosine-rich phosphodiester oligodeoxynucleotide that is currently being tested in a Phase I clinical trial for the treatment of advanced cancer. This agent has a novel mechanism of action that involves binding to nucleolin, a multifunctional protein that is expressed abnormally by cancer cells. In this study, the nucleolin-binding protein complex was isolated by immunoprecipitation (IP) with anti-FLAG antibody or anti-nucleolin antiboy from human prostate cancer DU145 cells. Forty nonribosomal proteins (PRMT5, PLCγ1, Top1, Myosin9, HSP90, SSRP1, etc) and four ribosomal proteins have been identified by MALDI-TOF-mass spectrometry. To identify the molecular interactions of nucleolin in AS1411-treated and untreated cells, we compared nucleolin-binding proteins from untreated, AS1411-treated and control oligo (CRO)-treated DU145 cells using anti-nucleolin IP . The results clearly showed that PRMT5 binding to nucleolin was decreased in the nucleus of AS1411 treated cells and was increased in the cytoplasm of AS1411 treated cells. Compared to untreated cells, the interaction of nucleolin and PRMT5 in CRO treated cells has no significant change. In comparison to expression in untreated or CRO treated, we also identified that PLCγ1 or Top1 binding to nucleolin was increased in the nucleus and decreased in the cytoplasm from AS1411 treated DU145 cells. In addition, the interaction of NEMO and nucleolin in cytoplasm, interaction of MYH9 and nucleolin either in nucleus or in cytoplasm were all increased in AS1411 treated DU145 cells. We conclude from our studies, a set component of nucleolin binding complexes first identified in human prostate cancer DU145 cells, that suggests nucleolin playing some novel roles in cell biology. Novel anticancer agent AS1411 binding disrupts specific molecular interactions between nucleolin and some of its partners including PRMT5, PLCγ1, Top1, Myosin9, and NEMO. This results in alteration of nucleolin complexes and inhibition of some nucleolin functions which are crucial for malignant cell survival.**

**INTRODUCTION**

Nucleolin is one of the most abundant nucleolar proteins. It has a molecular mass of 110 kDa, and consists of three functional domains. The amino (N)-terminal domain of the molecule contains multiple phosphorylation sites where a casein kinase II phosphorylates serine in interphase and a cdc2 kinase phosphorylates threonines in TPXK motifs during mitosis. The central domain constituted by four RNA-binding domains (RBD) interacts with a small RNA stem-loop structure present in the 5' external transcribed spacer (ETS). B23 is proposed to play a role in pre-rRNA processing in the second internal transcribed spacer (ITS), that leads to the production of 5.8S and 28S rRNA at a late stage of ribosome biogenesis in the nucleolus. The carboxyl (C)-terminal domain (RGG domain) is unusually rich in glycine, arginine, and phenylalanine. Although an RGG domain in heterogeneous nuclear ribonucleoprotein (hnRNP) U has been described initially as an RNA-binding domain, the RGG domain of nucleolin binds RNA nonspecifically and with low affinity, the RGG domain of nucleolin probably is not only involved in interaction with RNA but also in protein-protein interaction.

This multi-domain structure reflects the diverse cellular roles of nucleolin, included ribosome bigogenesis, DNA replication, nucleogenesis, embryogenesis, cytokinesis, apoptosis, protein

transport, cell proliferation, cell cycle progression, and stress response. Nucleolin is highly expressed in proliferating cells (maximum levels in S phase) but undetectable in quiescent cells, and there is a strong positive correlation between nucleolin protein levels and the rate of cell proliferation. This relationship is utilized in oncology through the detection of silver staining nucleolar organizer region proteins (AgNORs), of which nucleolin is a major and constant component. Levels of AgNORs in patients' tumor cells have been shown to correlate with tumor doubling time and reliably predict clinical outcome (high levels indicate poor prognosis) in a variety of cancers. Increasing AgNOR levels are also associated with progression from normal to pre-malignant to malignant states during chemical induced carcinogenesis in rats and during the development of hepatocellular carcinoma in humans. In addition, the nucleolin-containing chrmomosomal region is frequently duplicated or translocated in a broad spectrum of adenocarcinomas, leukemias, and lymphomas. Therefore, high levels of nucleolin are closely associated with malignant disease. In addition, one remarkable characteristic of nucleolin is that it shuttles constantly between the nucleolus and the cytoplasm. It is proposed that NCL acts as a carrier for ribosomal proteins from the cytoplasm to the nucleolus and as an adapter for specific binding of ribosomal proteins to rRNA. Thus, the NCL molecule is believed to set up scaffolding of many proteins participating in rRNA processing and assembly of ribosomal subunits at a number of different stages of ribosome biosynthesis. It is our hypothesis that nucleolin plays a role of cell proliferation that result from transforting proteins to their appropriate targets, and may then also modulate the processing activity of those proteins involving in cell proliferation.

G-rich oligonucleotides (GROs) are a new class of experimental therapeutic agents, which have strong growth inhibitory and pro-apoptotic activity against hormone-insensitive prostate cancer cells in culture and in mice. They are also active in other types of cancer cells, but have minimal effects on non-malignant cells. A truncated version of GRO29A known as AS1411 (formerly AGRO100), has been tested in a Phase I clinical trial of patients with advanced cancer. The results of this trial were recently presented and indicated that AS1411 was well tolerated (no toxicity was observed) and had promising clinical activity. Our understanding of the mechanisms by which AS1411 inhibits cell proliferation is very limited. but it is clear that they work in a novel way that is different from chemotherapy agents or antisense oligonucleotides. Active GROs form stable folded structures called quadruplexes and can bind to specific cellular proteins that recognize their unusual three-dimensional shape (an "aptamer" effect). However, formation of a stable G-quadruplex was not sufficient for activity. In addition, there was a very good correlation between the biological activity of GROs and their abilities to form a specific complex containing a protein that was identified as nucleolin. We also hypothesize that AS1411 binding disrupts specific molecular interactions between nucleolin and a few of its binding partners. This will result in inhibition of some nucleolin functions (those crucial for malignant cell survival), but will leave most functions (those required in normal cells) unaffected.

Here, we describe proteomic analysis of nucleolin-binding complexes isolated by the immunoaffinity method from human prostate cancer DU145 cells. The isolated nucleolin-binding complexes had the characteristics of constitution, function and modification of nucleolin including RNA intergrity, phosphorylation, methylation, cell proliferation and DNA replication. In addition, we also compared the nucleolin-interacting proteins from untreated and AS1411 treated prostate cancer cells and identify the molecular interactions of nucleolin that are altered by AS1411. This suggests that interaction of nucleolin-binding proteins altered

between nucleus and cytoplasm may partly explain molecular mechanism for the antiproliferation and tumor-selectivity of AS1411.

## EXPERIMENTAL PROCEDURES

*Materials*—The oliThe human prostate cancer cell line DU145 was obtained from American Type Culture Collection (ATCC, Manassas, VA). The oligodeoxynucleotides used in the present study were AS1411, an antiproliferative GRO whose sequence is 5'-d(GGTGGTGGTGGTTGTGGTGGTGGTGG)-3', and CRO26, an inactive control oligonucleotide whose sequence is 5'-d(CCTCCTCCTCCTTCTCCTCCTCCTCC)-3'. All oligonucleotides had a phosphodiester backbone and, unless otherwise stated, were purchased in the desalted form from Integrated DNA Technologies Inc. (Coralville, IA). Anti-Flag peptide antibody M2-conjugated agarose beads, anti-Flag peptide antibody M2, Flag peptide, nonionic detergent IGEPAL CA-630 and anti-PRMT5 monoclonal antibody, anti-PLCγ1 polyclonal antibody were from Sigma-Aldrich (Saint Louis, USA). Anti-MYH9, anti-Top I polyclonal antibodies and anti-Eg5 monoclonal antibody were obtained from BTI, TopoGEN, and BD. respectively. MagnaBindTM goat anti-mouse lgG beads was from Pierce. Anti-SSRP1 and anti-HSP90 were from Abcam. Anti-NCL, anti-IKKγ (NEMO), and anti-mouse or anti-rabbit linked to horseradish peroxidase were purchased from Santa Cruz Biotechnology. Trypsin (sequence grade) was from Promega (Madison, WI, USA). ZipTipC18 was from Millipore (Bedford, MA, USA).

*Far-Western Blot Analysis*—DU145 cells were grown to 50% confluence. The cells were treated by AS1411 or CRO at a final concentration of 10μM. After incubation for 2 h at 37℃, cells were washed extensively with PBS and extracted nuclear and S100 with buffer B and buffer C. After 8% SDS-PAGE separation, proteins were transferred to PVDF membranes, and blocked with PBST containing 5% nonfat milk for 1 h, then incubated for 1 h at room temperature in PBST with His-tagged RBD12-RGG at a final concentration of 1 μg/ml. Membranes were washed three times during 15 min in PBST before being subjected to a standard Western blot analysis with His-probe (Santa Cruz, CA, USA).

*Construction of epitope-tagged expression plasmids*—To construct FLAG-tagged nucleolin expression plasmid pFLAG-NCL, a 2394-base pair *Nru*I-*Xho*I fragment (amino acids 7-707) of pBS-nucleolin (IMAGE 591D39, ATCC) was subcloned into the *EcoR*V-*Xho*I fragment of a pCMV2-FLAG vector (Sigma-Aldrich). The reading frame and sequence of the resulting pFLAG-NCL plasmid were confirmed by cycle sequencing. We also have established a high protein expression and purification system for nucleolin RBD12-RGG. The sequence of the expressed protein RBD12-RGG shown in figure 1 contains the two RBD and one RGG domain. PCR was run with pMAL-pNUC as template plasmid using Deep Vent polymerase and the following primer sets, 5'-GGGAATTCCATATGGGCACAGAACCGACTACGG-3' and 5'-CCGCTCGAGTTCAAACTTCGTCTTCTTTCC-3'. The amplified product was digested with *Nde*I and *Xho*I and subcloned upstream of a sequence encoding the C-terminally tagged His epitope in a pET vector (Fig.1). The histidine-tagged RBD12-RGG was expressed in Rosetta DE3 cells induced with IPTG and purified with Talon Cobalt Affinity Column. The purity of the protein fractions was checked using an acrylaminde gel stained with coomassie blue. Mass spectrometric data confirmed the correct fragmentation pattern for the nucleolin protein sequence.

*Transient transfection and expression in DU145 cells*—Human prostate cancer DU145 cells were maintained in DMEM (Gibco, BRL) supplemented with 10% heat-inactivated fetal calf serum. The cells were cultured at 37℃ in an incubator with 5% $CO_2$. Confluent cells (70%) cultured in T75 flasks were transfected with 10μg of the expression plasmid DNA using LipofectAMINE plus reagent (invitrogen, Carlsbad, CA, USA ) according to the manufacturer's instructions. Two days after transfection, cells were harvested and the expression of FLAG-NCL construction was measured with standard western blot analysis using anti-FLAG peptide antibody.

*Immunofluorescence*—After 24 h of transfection, cells were plated in 8-well culture slides (Biocoat, Becton Dickinson, Franklin Lake, NJ, USA) and cultured. After an additional 24 h, the cells were fixed with 4% paraformaldehyde in PBS for 15 minutes. After washing with PBST (0.2% Triton X-100, Sigma), the cells were blocked with 5% goat serum in PBST for 1 hour at room temperature. The cells were incubated with 10 μg/mL of mouse anti- Flag IgG or 5 μg/mL of mouse anti-NCL IgG as the first antibodies overnight at 4℃. After another washing with PBST, the cells were further incubated with fluorescein isothiocyanate (FITC) conjugated anti-mouse IgG as the second antibodies for 1 h at room temperature. Fluorescent images were visualized with a Bionanoscope (Nikon, Tokyo, Japan).

*Preparation of S100 and nuclear and whole cell lysates from DU145 cells*—At the appropriate time after treatment, cells were harvested and washed twice with cold PBS, and nuclear and S-100 extracts were prepared according to the method of Coqueret et al. Briefly, 300μl of ice-cold extraction buffer B (10 mM HEPES, pH 7.9, 1.5 mM $MgCl_2$, 10 mM KCl, 1 mM phenylmethylsulfonyl fluoride, 1μg/ml leupeptin, 1μg/ml aprotinin) was added to the cells. After three cycles of freeze thaw, S-100 extracts were recovered as supernatant following centrifugation at 12,000 ×g for 1 min, and pellets (nuclei) were resuspended in 100 μl of buffer C (20 mM HEPES, pH 7.9, 1.5 mM $MgCl_2$, 420 mM KCl, 0.2 mM EDTA, 25% glycerol, 1 mM phenylmethylsulfonyl fluoride, 1 μg/ml leupeptin, 1 μg/ml aprotinin). Following 30 min of incubation at 4°C, insoluble material was precipitated by centrifugation at 12,000 ×g for 5 min and nuclear extracts were collected as supernatant. Extracts were either used immediately or stored at -80 °C.

To obtain whole cell lysates, cells were mixed with 500 μl of lysing buffer (50 mM Tris HCL, pH 7.4, with 150 mM NaCl, 1mM EDTA, 1% Triton X-100, 0.5% IGEPAL CA630 and Complete protease inhibitor cocktail (Roche)). The cell lysate was incubated for 30 minutes on a shaker at 4℃ and centrifuged at 12,000 ×g for 10 minutes, the supernatant then was obtained for additional experiments. The concentration of extracted proteins was determined using the Coomassie Plus Protein Assay Reagent (Pierce).

*Immunoprecipitaion assay*—For anti-FLAG beads, after 48 h of transfection, the cells were harvested and washed with PBS and were lysed in 500 μl of lysis buffer described above. The cell lysate was obtained by centrifugation at 12,000 ×g for 10 minutes at 4℃, and was incubated with 40 μL of washed anti-FLAG beads for 4 h at 4℃ for immunoprecipitation. The protein-bound agarose beads were washed five times with the lysis buffer and the

proteins were eluted with 20 μL of 50 mM Tris-HCl, 150 mM NaCl containing 150 μg/mL of 3×FLAG peptide.

For MagnaBind™ goat anti-mouse lgG beads (PIERCE), immunoprecipitations were performed by incubating 200 μg of extract with 2 μg of specific antibody in 500 μl of RIPA buffer (PBS, 50 mM Tris-HCl, pH 7.5, 0.5 M NaCl, 0.1 mM EDTA, 1% Nonidet P-40, 0.5% sodium deoxycholate, 0.1% SDS, 1 mM sodium fluoride, 10 mg/ml phenylmethylsulfonyl fluoride, 2 μM aprotinin, 100 mM sodium orthovanadate) for 1 h at 4 °C, followed by addition of goat anti-mouse lgG or goat anti-rabbit lgG beads (250 μl) and overnight incubation at 4 °C on a rotator. Control immunoprecipitations were performed with normal mouse or rabbit IgG in place of primary antibody. The agarose beads were precipitated (Place samples on magnetic stand until separated) and washed four times with RIPA buffer. They were resuspended in 1× sodium dodecyl sulfate (SDS)-loading buffer (100 mM Tris-HCl, pH 6.8, 200 mM dithiothreitol, 4% SDS, 0.2% bromphenol blue, 20% glycerol), boiled for 5 min, and loaded on 8% SDS-polyacrylamide gels. Immunoblot analysis was performed using nucleolin or other antibodies as primary antibody as described above.

*Electrophoresis and staining*—The co-immunoprecipitative complex was incubated in 1×SDS-loading buffer at 95 °C for 5 min, and separated on 10% polyacrylamide-SDS gels. The silver staining was performed as described previously with modifications as follows. The gel slab after electrophoresis was fixed in 50% methanol, 5% acetic acid, for 30 min with rotation. Then the gel was sensitized with 0.02% sodium thiosulfate for 2 min. After washing with distilled water 3×5min, the gel was incubated in 0.1% silver nitrate solution for 30-60 minutes at 4℃.After washing with distilled water 2×1min, the gel was developed in 0.04% formalin, 2% sodium carbonate until the desired intensity of staining was achieved. Development was terminated with 1% acetic acid solution. For Colloidal Coomassie staining, incubate the gel for overnight in the staining solution (40% Colloidal Coomassie Blue and 10% methanol) after fixing it in a solution of 40% methanol, 10% acetic acid for at least 1 hour. Then destain the gel with several changes of 25% methanol until the background is transparent.

*Protein identification by proteomic analysis by MALDI-TOF-MS*—In-gel trypsin digestion was carried out as described with modification as follows. Briefly, protein bands were excised and incubated in 50 mM $NH_4HCO_3$, 50% acetonitrile at room temperature for 15 min. Swell the gel pieces with 20 mM DTT in 0.1 M $NH_4HCO_3$ and incubate for 45 min at 56℃. After removed DTT solution, the gel was incubated in 55 mM iodoacetamide in 0.1 M $NH_4HCO_3$ for 30 min in the dark. Rinse the gel with 50 mM $NH_4HCO_3$. The gel was shrunk in 50 mM $NH_4HCO_3$, 50% acetonitrile again. After drying in speedvac, an aliquot of 25 μg/mL sequencing-grade trysin in 50 mM $NH_4HCO_3$ was added. After 45 min incubation on ice, the supernatant was discarded and replaced with 20 μl of 50 mM $NH_4HCO_3$. Digestion was performed at 37℃ overnight and fragmented peptides were extracted from the gel with 5% formic acid/50% acetonitrile. To improve the ionization efficiency of MALDI-TOF-MS, ZipTipC18 (Millipore, Bedford, MA, USA) was used to purify peptides before MS analysis. The purification was done according to the manufacturer's manual with no modification. The peptides were eluted with 2 μl of 5 mg/ml α–cyano-4-hydroxycinnamic acid in 50% acetonitrile/0.1% trifluoroacetic acid and applied directly onto target and allowed to airdry. Peptide mass fingerprints were obtained by using a Micromass TofSpec-2E MALDI-TOF mass spectrohohotmeter (Micromass/Waters, Milford, MA). The database fitting program

Mascot, available at the World Wide Web site at Matrix Science (http://www.matrixscience.com/search_form_select.html) was used to interpret MS spectra of protein digests.

*Western Blot Analysis*—Samples were incubated in SDS-loading buffer at 95℃ for 5 minutes, and separated on 8% polyacrylamide-SDS gels, followed by electroblotting to polyvinylidene difluoride membranes (Bio- Rad). After blocking nonspecific binding sites for 1 h in 5% nonfat dried milk in PBST (0.05% Tween 20 in PBS), the membrane was incubated for 1 h at room temperature or overnight at 4℃with primary antibody. After three washes in PBST, the membrane was incubated with horseradish peroxidase-conjugated goat anti-mouse antibody for 45 min at room temperature, washed three times in PBST, and detected using enhanced chemiluminescence (ECL kit from Amersham Biosciences).

**RESULTS**

1. *AS1411 altered interaction of NCL with a subset of proteins in nuclear and S100*—We have previously identitied NCL as an important AS1411-binding protein and have shown that it plays an essential role in AS1411 activity. To confirm our hypothesis that AS1411 modulate only a few of the molecular interactions of NCL, direct interaction of NCL with proteins in nuclear and S100 was evaluated using a ligand blotting assay (far western). After separation, proteins treated with AS1411 or CRO were transferred to a PVDF membrane and incubated with purified truncated recombinant NCL, His –tagged RBD1,2-RGG of NCL to examine the ability of nucleolin to bind to nuclear and S100 proteins in the absence or presence of AS1411. In the far-Western experiment, a set band of proteins was found to interact with the deleted proteins in nucleus or in cytoplasm (see Figure 2). We have been able to reproducibly show that specific protein-protein interactions are affected by the presence of AS1411, but the majority of protein binding is unaffected. To confirm our hypotheses that the antiproliferative effects of AS1411 result from their binding to nucleolin and alter the molecular interaction of nucleolin with specific cellular proteins, we performed further experimental approaches.

2. *Isolation and identification of protein in the NCL-binding complexes.*
Since NCL is found abundantly in the nucleolus of growing eukaryotic cells, cellular localization of the Flag-NCL molecule was confirmed in the transfected cells by immunofluorescence microscopy staining of DU145 cells using an anti-Flag antibody. Although the cells used were not synchronized at any specific cell cycle, the Flag-NCL was stained strongly in the nucleolus of most of the transfected cells we use. Compared to immunofluorescence stain with anti-NCL antibody, the localization of FLAG-NCL in the nucleolus of DU145 was similar as endogenous NCL distributed. Neither FLAG-NCl nor NCL protein were detected in cytoplasm in most of the transfected cells. Therefore, we used the transfected cell culture and immunopurification using anti-Flag antibody would allow selective isolation of NCL-binding protein complexes present endogenous NCL binding protein complexes.

Therefore, the immunoprecipitates were prepared from whole cell extracts for further studies. NCl-binging proteins were captured using anti-FLAG beads and, after extensive washing, proteins eluted by 3×FLAG peptides in denaturing buffer. A typical staining pattern of the

immunoprecipitate obtained from whole cell extract on SDS-PAGE gel is shown in Fig. 3, lane 3. We detected 22 protein bands on a silver stained SDS-PAGE gel. In contrast, only a few protein bands were stained in mock immunoprecipitate prepared from control cells that were transfected with the expression vector lacking the NCL gene (Fig. 3 , lane 2). Thus, these results support the specificity of the association between NCL and the isolated complexes. Table 1 shows the proteins identified in the NCL-binding complexes by the method described. The identification by the in-gel digestion-MALDI-TOF analysis described was carried out for an individual protein band principally on silver stained 10% SDS-polyacrylamide gels. A typical SDS-PAGE staining of the NCL-binding complexes in DU145 cells is shown with the protein names identified on the right side in Fig. 3.

Of the nineteen proteins we identified, three ribosomal proteins (S8, L4 and P0) are ribosomal proteins; one protein is for the small subunit, two for the large subunit. Ribosomal protein L4 and P0 have been identified previously in FLAG-NCL-binding complexes that were isolated from 293 cells by using anti-FLAG antibody. On the other hand, 18 human ribosomal proteins (L3, L4, L5, L6, L7, L8, L9, L13a, L18, L18a, L28, L35a, L37a, S3a, S8, S9, S11, and S26) have been assigned to bind directly to hamster NCL, as shown by far-Western blotting analysis. The ribosomal protein S8 is assigned for the first time in human NCL-binding complexes by this study.

Nonribosomal proteins other than the ribosomal proteins we identified are PRMT5, KIF11 (Eg5), HSP90, SSRP1, and many other proteins as shown in Table 1. To rule out the possibility that NCL-binding proteins interacted with NCL complexes only when NCL were overexpressed, we analyzed PRMT5, KIF11, SSRP1 and HSP90 association with endogenous NCL complexes. DU145 cells whole lysates were incubated with anti-mouse lgG beads and mouse anti-NCL monoclonal antibodies, and the eluted proteins were analyzed by western blotting. We confirmed the presence of other nonribosomal proteins (PRMT5, KIF11, HSP90β, SSRP1, and fibrillarin) by Western blotting analysis with the antibodies available in this study (Fig. 5). These proteins could not be detected in the mock precipitate. These results suggest that the other nonribosomal proteins identified are also true components of the NCL-binding complexes. Of these, MYH9, HSP90β, and β-tubulin have been assigned to bind directly to nucleolin on mammalian cells. Other proteins PRMT5, Eg5, myosin 1C and SSRP1 are assigned for the first time in nucleolin-binding complexes by this assay. However, it should be noted that some protein bands could not be identified by the methods we used, though mass spectra of tryptic peptides were obtained by MALDI-TOF analysis. At present, we are not sure whether these protein bands contain other human proteins whose amino acid sequences are not available in the databases, or if they are totally unknown proteins, or if they could not be identified due to some unknown methodological limitations by MALDI-TOF-MS and database searching. Fibrillarin has also been reported to be in the NCL associated protein complexes obtained from HeLa cells. However, we could detect no protein in the NCL-binding complexes from DU145 cells either by MALDI-TOF (Table 1) or Western blotting analysis (Fig. 5).

In addition, to extend discovery of more nucleolin-binding proteins, we performed coIP to directly pull down the endogenous nucleolin-binding proteins with anti-nucleolin antibody and analyzed individual protein bands on silver stained 8% polyacrylamide gels by the in-gel digestion-MALDI-TOF analysis. 26 proteins have been assigned to interact with nucleolin. Of these, MYH9, DNA helicase II, and Top I have been assigned to bind directly to nucleolin on

endothelial, 293, Hela cells respectively. The other nucleolin-binding proteins we identified including IKKγ (NEMO), PLCγ1, cleavage and polyadenylation specific factor 1, RAS protein activator like 2 and squamous cell carcinoma antigen recognized by T cells 1 are assigned for the first time in nucleolin-binding complexes by this assay. Some of nucleolin-binding proteins identified with anti-nucleolin coIP including MYH9, HSP90β, β-actin and β-tubulin has also been isolated with anti-FLAG coIP in transfected cells. These results suggest that the exogenous nucleolin isolated with anti-FLAG coIP is almost consistent with the endogenous nucleolin isolated with anti-nucleolin coIP.

3. *AS1411 alters interaction of nucleolin-binding proteins.*

We have previously reported AS1411 have potent growth inhibitory effects that are unrelated to any expected antisense or antigene activity. The antiproliferative effects of AS1411 are related to its ability to bind to a specific cellular protein nucleolin. To identify the molecular interactions of nucleolin in AS1411-treated and untreated cells, we compared NCL-binding proteins from untreated, AS1411-treated and control-treated DU145 cells using anti-nucleolin co-immunoprecipitation and coomassie staining assay. We focus on a set of proteins which affected by AS1411 treated, but not by inactive control oligonucleotide (CRO) treated (Fig. 6A). These proteins have been further identified as PRMT5, IKKγ, Top I, MYH9 and PLCγ1 by mass spectrometry. To confirm the results of MS, we performed IP with anti-NCL antibody and probed with anti-IKKγ, Top I, MYH9 and PLCγ1 antibodies respectively. As expected, IKKγ, Top I, MYH9 and PLCγ1 can bind to endogenous NCL complex in either nuclear or cytoplasm of DU145. Neither NCL or specific proteins could not be identified in mock immunoprecipitate with normal mouse lgG or cell free. Thus, these results support the specificity of immunoprecipitation. Among these proteins binding to nucleolin, PRMT5 was decreased in the nucleus of AS1411 treated cells and was increased in the cytoplasm of AS1411 treated cells. Top I and PLCγ1 were increased in the nucleus of AS1411 treated cells and were decreased in the cytoplasm from AS1411 treated cells. MYH9 was increased in the either nucleus or cytoplasm of AS1411 treated cells. Both Eg5 and SSRP1 have no significant change in AS1411 treated cells. In addition, compared to untreated cells, the interaction of NCL and specific proteins in CRO treated cells has no significant change.

**DISCUSSION**

We have reported previously that certain guanosine-rich oligodeoxynucleotide AS1411 has antiproliferative activity against a variety of cancer cell lines. There is strong evidence that nucleolin is the primary target of AS1411. In this report we show that more non-ribosomal proteins interacts with endogenous nucleolin or exogenous nucleolin from either human prostate cancer DU145 cells or flag-tagged nucleolin cell lines. We also show that specific nucleolin interactions are affected by the presence of novel anticancer agent AS1411, but the majority of protein binding is unaffected.

We found that the RBD1,2-RGG domain responsible a lot of the interaction of nucleolin by Farwestern blotting that the presence of AS1411 can induce changes in the protein-protein interactions of nucleolin, which include some enhanced and some reduced interactions. In order to identify the protein interacted with nucleolin we tried to analyze the corresponding protein bands on silver stained gel by a method combined with in-gel digestion and mass spectrophotometry. The obtained mass data were fitted by Mascot database search analysis and allowed us to identify 40 proteins. Besides four of the human nucleolin-binding ribosomal proteins (S8, L4, P0, and L19), we identified 36 more non-ribosomal proteins in nucleolin-binding complexes. Depite it is not clear yet how these nucleolin-binding proteins anre involved in biological functions of nucleolin. However, we found a subset of the components of the cytokeleton, β-tubulin, β-actin, myosin1C, and myosin9, that have been known to interact directly with nucleolin in mammalian cells. Among these cytoskeleton proteins, the interaction of MYH9 and nucleolin was increased in both nucleus and cytoplasm from AS1411 treated cells. In control, this alteration of interaction was not observed between CRO treated cells and untreated cells. In addition, the interaction of other cytoskeleton proteins with nucleolin has not been altered in AS1411 treated cells.

Nonmuscle myosin heavy chain 9 (MYH9), an actin-based motor protein, is one isoform of the class II myosin family, which mediates a variety of cellular processes including protrusion, migration, and modulation of cell locomotion. MYH9 was reported to be a linker between cell-surface nucleolin and actin cytoskeleton and mediates its function in angiogenic. MYH9 provides an anchorage to cell-surface nucleolin that come from the nucleolin originally located in the nucleus. Recent studies showed that MYH9 plays an important role in modulating T-cell motility and tissue organization during embryo development. The shuttle of nucleolin between nucleus and cell surface depends on anchoring to MYH9, which appears essential for the angiogenic function of cell-surface nucleolin. A specific inhibitor of nonmuscle myosin II, blebbistatin has been identified to inhibite contraction of the cleavage turrow without disrupting mitosis or contractile ring assembly. Previous small-molecule work using microtubule or actin depolymerizers (nocodazole or latrunculin) has demonstrated the importance of microtubules for both positioning and ingression of the cytokinesis furrow, and of actin for the structure of the furrow. Depolymerizing microtubules by nocodazole or latrunculin caused delocalization of myosin II.

Besides cytoskeleton proteins, in this report, we identified Top1 and DNA helicase II, related DNA replication in the nucleolin-binding complexes. Except DNA helicase II, the interaction of Top1 and nucleolin has been altered in AS1411 treated cells. Human Top1 is a nuclear protein involved in the regulation of DNA structure and is the target of an important new class of antineoplastic drugs, camptothecins (CPT). Several lines of evidence indicated that both

nucleolin and Top1 are involved in rRNA synthesis and processing. The presence of N-terminus of nucleolin is necessary and sufficient for Top1 binding. *Saccharomyces cerevisiae* nucleolin ortholgy NSR1 is involved in the cellular locatization of yeast Top1 and that loss of NSR1 alters cellular sensitivity to topoisomerase-targeting drugs but not to DNA damaging agents in general. Top1 may also be important in rDNA transcription, rDNA genomic stability, rDNA silencing as well as in nucleolar rRNA processing: mammalian cells treated with CPT exhibit defects in rRNA processing and decreased 60S ribosomal subunits. A direct role of nucleolin in DNA replication has been suggested before, as specific inhibition of this process by G-rich oligonucleotides correlates positively with their ability to bind nucleolin. As neither nucleolin nor Top I on their own can stabilize two T-antigen hexamers during DNA unwinding, which is that both nucleolin and Top I are present in the helicase complexes. Thus, nucleolin may act as a clamp to assist the proper orientation of T-antigen hexamers and Top I. As Top I interacts with the T antigen and nucleolin through its N terminus, its catalytically active C-terminal domain should have unrestricted access to the DNA in front of the replication fork. In this study, we show that the interaction of Top I and nucleolin was increased in the nucleus and decreased in the cytoplasm of AS1411 treated cells. Although it has not been ascertained that the alteration of this interaction between nucleolin and Top1 is responsible for the anticancer activity of AS1411, it almost explains that treatment of cells with antiprolifeartive AS1411 causes an arrest of cell cycle progression and an inhibition of DNA replication, which have been reported previously. DNA helicase II is a ubiquitous DEXH nucleic acid helicase of higher eukaryotes that has been found in different species from *Drosphila* to men. It contains two double-stranded RNA (dsRNA) binding domains at the N terminus, an expanded helicase core in the middle, and an RGG-box at the C terminus. It has been characterized as a nucleic acid helicase that unwinds both double-stranded DNA (dsDNA) and dsRNA. Although the interaction of DNA helicase II and nucleolin has not changed, it also concern to play a role together with DNA topoisomerases in maintaining proper DNA topology, which is essential for genome stability. In addition, it is interesting to note that nucleolin itself has been reported to have helicase activity and is also known as DNA helicase IV.

Phospholipase C, gamma 1 (PLCγ1) is another novel interactor for nucleolin first reported in this study. A phospholipase is an enzyme that converts phospholipids into fatty acids and other lipophilic substances. There are four major classes, termed A, B, C and D. Phospholipases A2 (PLA2s) are a large family of enzymes that specifically deacylate fatty acids from the 2nd carbon atom (sn2, thus PLA2) of the triglyceride backbone of phospholipids, producing a free fatty acid and a lyso-phospholipid. Phospholipase C is a key enzyme in phosphatidylinositol (PIP2) metabolism and lipid signaling pathways. It is activated by either Gαq protein or Gβγ subunits or by transmembrane receptors with intrinsic or associated tyrosine kinase activity. The Phospholipase C family consists of 13 isozymes split between six subfamilies, PLC-δ, -β, -γ, -ε, -ζ, and the recently discovered -η isoform. PLCγ is activated by receptor tyrosine kinases and play a role in directed cell migration and wound-healing, as well as in neurite outgrowth, membrane ruffling, macropinocytosis and possibly mitogenesis. The substrate and products of PLC-γ1 are critically important in cytoskeletal reorganization, cell adhesion and migration. Once activated, PLC-γ1 hydrolyses $PtdIns(4,5)P_2$ to produce the second messengers inositol-1,4,5-trisphosphate ($InsP_3$) and diacylglycerol (DAG). After polyvalent antigen stimulation, PLCγ1 translocates to the plasma membrane from primarily cytosolic. PLCγ1, when activated by tyrosine phosphorylation, increases the growth and invasiveness of various cancer cell types. Our results provide the first molecular basis of phospholipase signal transduction pathway for nucleolin that is

believed participating in rRNA processing and assembly of ribosome. We detected PLCγ1 from isolated nucleolin complex either in nucleus or in cytoplasm. We also identified the interaction of nucleolin and PLCγ1 was altered. Few of studies demonstrated the role of nucleolin in signal transduction pathway involving tyrosine kinase, lipophilic. So the role of nucleolin in regulation of PLCγ1 activity is unknown.

We have identified here that nucleolin interacts directly with PRMT5 in human prostate cancer DU145 cells. The type II protein arginine methyltransferase PRMT5 binding to nucleolin was decreased in the nucleus of AS1411 treated DU145 cells, and increased in the cytoplasm of AS1411 treated cells, but was not affected by inactive control oligonucleotide CRO. Although PRMT5 is novel interactor for nucleolin, nucleolin has been previously demonstrated to interact with another member of PRMTs family, PRMT1. Currently, eight mammalian protein arginine methyltransferases (PRMTs) and five different forms of methylated Arg: Mma, aDma, sDma and recently δMma and Tma have been identified. The PRMTs responsible for protein arginine methylation have been classified in two major classes; type I enzymes (PRMT1, PRMT3, PRMT4, and PRMT6) promote the formation of asymmetrical ω-$N^G$, $N^G$-dimethylated arginines (aDMA), and type II enzymes (PRMT5 and PRMT7) catalyze the formation of symmetrical ω-$N^G$, $N'^G$-dimethylated arginines (sDMA). ω-$N^G$-onomethylarginine is thought to be an intermediate formed by both enzyme types. The PRMTs are ubiquitously expressed enzymes, and they may achieve a degree of tissue specificity by alternative splicing. Previous work has shown that antisense PRMT5 cells grew slower and FLAG-tagged PRMT5 cells grew faster than wide type cells, indicating that PRMT5 is required for normal cell growth and proliferation. We have shown here that PRMT5 was decreased in nucleus and increased in cytoplasm in dose-dependent and time-course in AS1411 treated cells. So PRMT5 decreased in nucleus may partially be explained AS1411 with anitproliferative activity against cancer cells.

Recently, we identified that AS1411 also associates with the NEMO (NFκB essential modulator, also known as IKKγ, FIP3 and IKKAP1), which is a regulatory subunit of the IκB kinase (IKK) complex. Moreover, we have defined the probable mechanism of this activity by showing that AS1411 sequesters NEMO in a complex with nucleolin, thereby preventing activation of IKK and precluding phosphorylation of IκBα and subsequent release of NF-κB. The interaction has been identified here, to increase in cytoplasm from AS1411 treated cells comparing untreated or CRO treated cells. This result consistents with our precious studies. Inhibition of NF-κB activation has also been linked to the chemopreventive properties of several compounds with activity in cancer, such as selenium, green tea, and silymarin. Down-regulation of NF-κB activity is therefore considered a very attractive strategy for developing new cancer treatments.

Microtubule motors bind to and move unidirectionally on microtubules, and they have been proposed to generate the force required for spindle assembly and maintenance, attachment of the chromosomes to the spindle, and movement of chromosomes toward opposite poles. The microtubule motor proteins, which are members of the kinesin, dynein, or myosin families, can account for many of the movements of the spindle and chromosomes in dividing cells. All antimitotic tubulin agents interfere with the assembly and/or disassembly of microtubules and produce a characteristic mitotic arrest phenotype. Human Eg5 (also known as KIF11), a member of the kinesin superfamily, plays a key role in mitosis, as it is required for the assembly of a bipolar spindle. Nucleolin is a nucleolar protein that is specifically

phosphorylated in cells entering mitosis, and compounds that cause mitotic arrest showed the phenotype of increased amounts of phosphonucleolin. In a study used nucleolin phosphorylation as a readout of mitosis, the motility of mitotic kinesin Eg5 was proposed to be specifically inhibited by 1,4-dihydropyrimidine-based compound monastrol with phosphonucleolin increasing. In this study, we identified Eg5 from isolated endogenous nucleolin-complexes. However, we didn't find significant alteration of interaction of Eg5 and nucleolin either in nucleous or in cytoplasm from treated cells comparing untreated cells. Although the interactions between nucleolin and many cytoskeleton motor proteins have been identified, few of them has been altered from AS1411 treated cells. We suggest AS1411 has a different mechanism with monastrol in proliferation inhibition.

In conclusion, with immunoprecipitation and MALDI-MS, a total of 40 nucleolin-binding proteins, including 36 nonribosomal proteins have been identified. These proteins contain five of interaction altered by AS1411, involving cytoskeleton, protein methylation, DNA replication, and NF-κB passway. The large-scle proteomic analysis used here may contribute to understanding of the anticancer agents AS1411 mechanism. This may ultimately lead to the development of therapies that are even more active and specific than AS1411.

**Figures legend**

Figure 1. **Sequence of RBD12-RGG. RBD are shown in bold with the RGG domain underlined. The His tag was added to the C-terminus for purification**.

Figure 2. **Farwestern blots probed for NCL binding to nuclear or cytoplasm proteins in the presence of AS1411 or CRO.** Extracts from AS1411 or CRO treated DU145 cells were separated by 8% SDS-PAGE. Proteins transferred on a PVDF membrane were incubated with His-tagged RBD1, 2-RGG at a final concentration of 1μg/ml. After extensive washing, nucleolin was detected using anti-NCL monoclonal antibodies and revealed using ECL.

Figure 3. **Localization of FLAG-NCL and NCL in the transfected DU145 cells**. The sequence for FLAG was fused in frame to the N terminus of NCL. DU145 cells cultured in a slide were transfected with the FLAG or FLAG-NCL expression plasmid. The cells were photographed at 800-fold magnification under a microscope. Immunocytostaining was done for FLAG-NCL (right) by anti-FLAG antibody or endogenous NCL (left) by anti-NCL antibody.

Figure 4. **SDS-PAGE staining pattern of the proteins coprecipitated with Flag-NCL or NCL**. (A) Eluate with Flag peptide was subjected to 8% SDS-PAGE gel. The gel was silver-stained. The proteins identified by MALDI-TOF were indicated at the right side of the gel. Names in gray indicate the proteins identified in the control. Lane 1, molecular weight markers; –, mock; NCL, NCL-binding complexes. (B) Isolated with anti-nucleolin antibodies was subjected to 8% SDS-PAGE gel. The gel was stained with Colloidal Coomassie. The bands of proteins were identified by MALDI-TOF-MS.

Figure 5. **NCL-binding protein identification by Western blotting analysis**. Coprecipitated proteins with Flag-NCL were separated on 8% SDS-PAGE gel and blotted onto PVDF membrane. Proteins were detected with the five antibodies indicated. PRMT5, KIF11, HSP90, SSRP1, and fibrillarin: lgG, immunoprecipitated with normal mouse lgG; NCL, immunoprecipitated with mouse anti-NCL antibody; cell free, immunoprecipitated without cell.

Figure 6. **AS1411 altered the interaction of NCL-binding complex in DU145 cells**. NCL was immunoprecipitated from DU145 cells of untreated or treated with AS1411 or CRO. The immunoprecipitated was probed for PRMT5, PLCγ1, Eg5, SSRP1, NEMO, Top1, and MYH9, separately, followed by stripping and re-probing for NCL (bottom).

Table 1. **Proteins that are identified in the nucleolin-binding complexes in DU145 cells by the combination of in-gel digestion, MALDI-TOF and database searching.**

Fig. 1


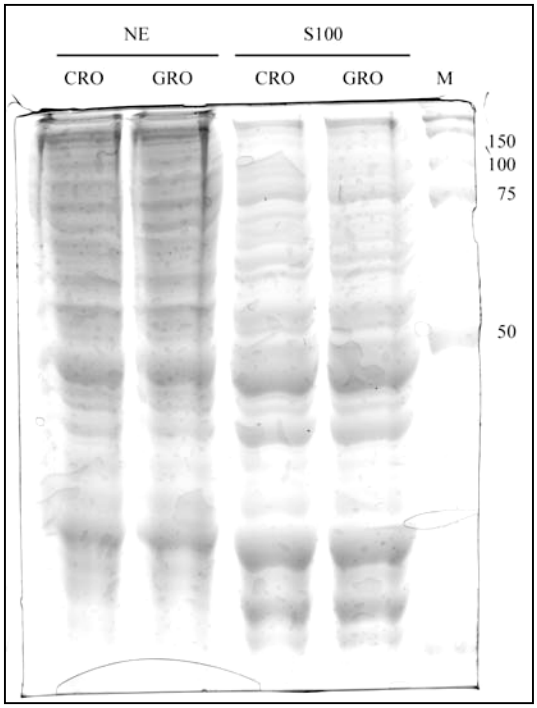


Fig. 2

Fig. 3

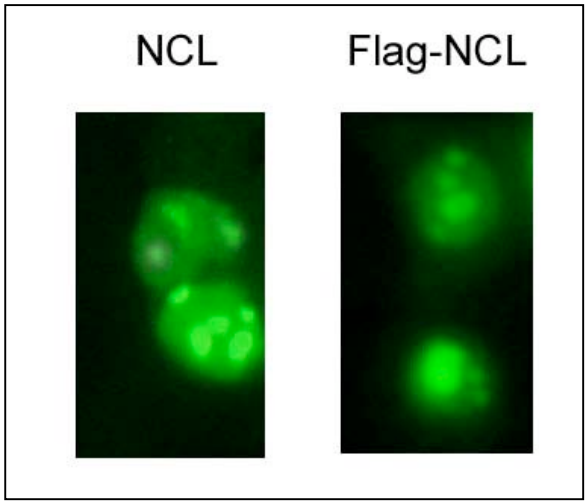

Fig. 4A

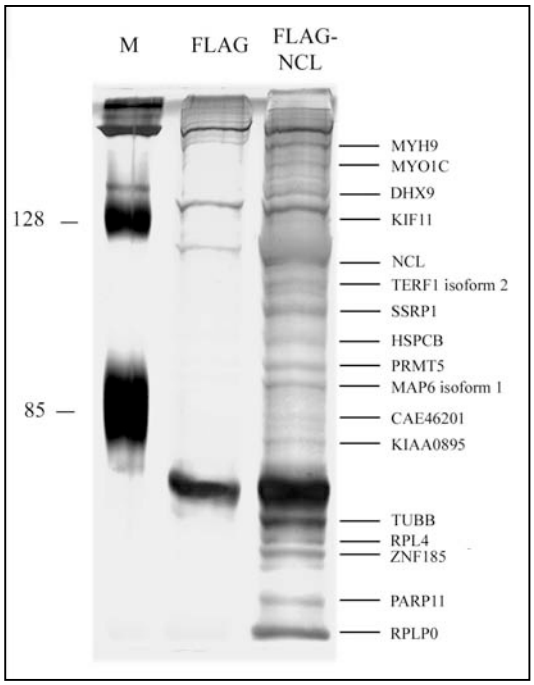
M
FLAG
FLAG-NCL
128
85
MYH9
MYO1C
DHX9
KIF11
NCL
TERF1 isoform 2
SSRP1
HSPCB
PRMT5
MAP6 isoform 1
CAE46201
KIAA0895
TUBB
RPL4
ZNF185
PARP11
RPLP0

Fig. 4B

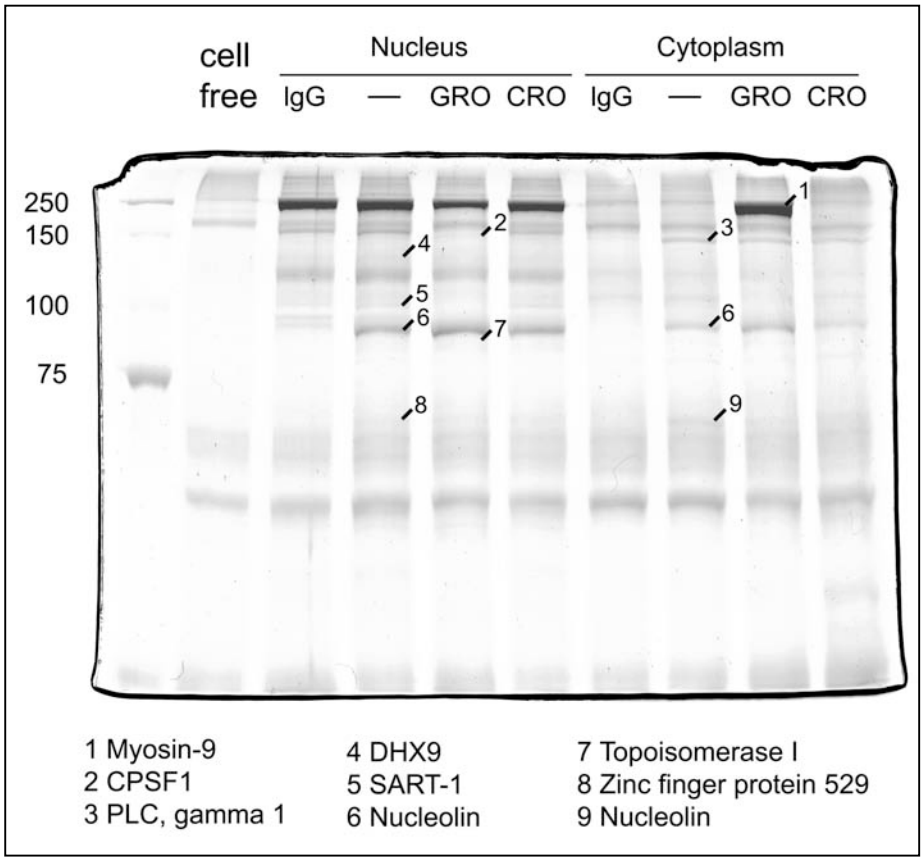
cell free
Nucleus
Cytoplasm
IgG
—
GRO
CRO
IgG
—
GRO
CRO
250
150
100
75
1
2
3
4
5
6
7
8
9
1 Myosin-9
2 CPSF1
3 PLC, gamma 1
4 DHX9
5 SART-1
6 Nucleolin
7 Topoisomerase I
8 Zinc finger protein 529
9 Nucleolin

Fig. 5

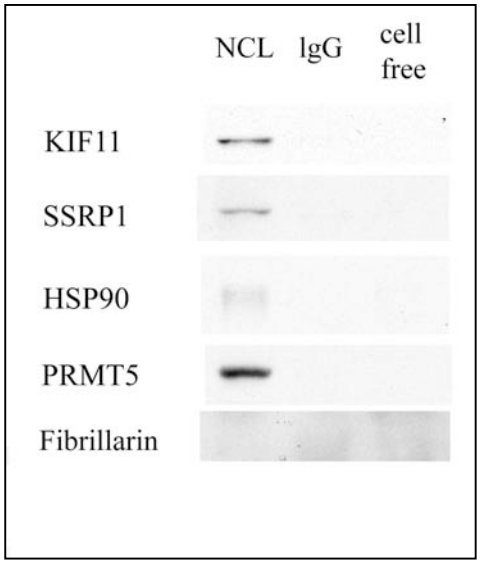

Fig. 6

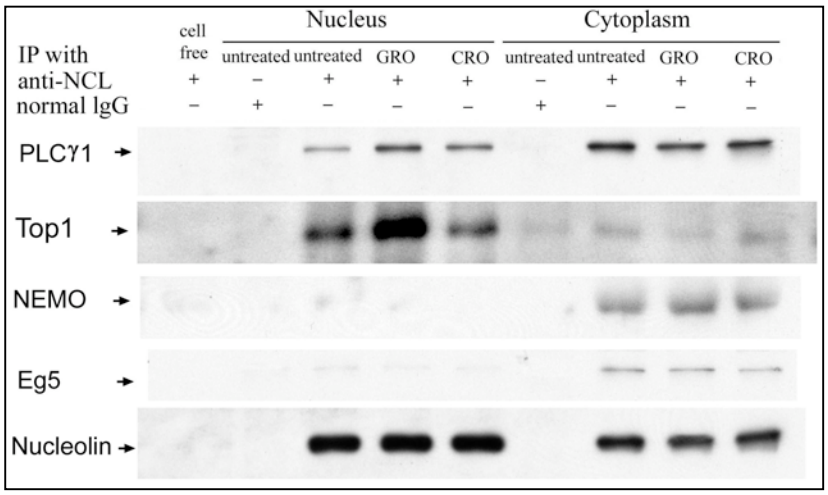
cell free
Nucleus
Cytoplasm
IP with
anti-NCL
normal lgG
untreated untreated GRO CRO untreated untreated GRO CRO
+ – + + + – + + +
– + – – – + – – –
PLCγ1
Top1
NEMO
Eg5
Nucleolin

A

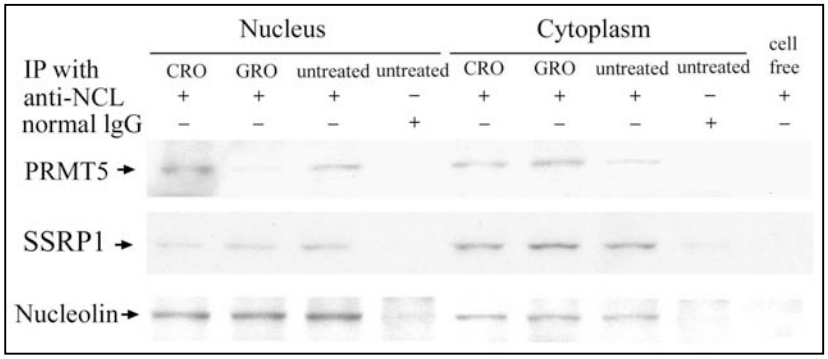
Nucleus
Cytoplasm
cell free
IP with
anti-NCL
normal lgG
CRO GRO untreated untreated CRO GRO untreated untreated
+ + + – + + + – +
– – – + – – – + –
PRMT5
SSRP1
Nucleolin

B

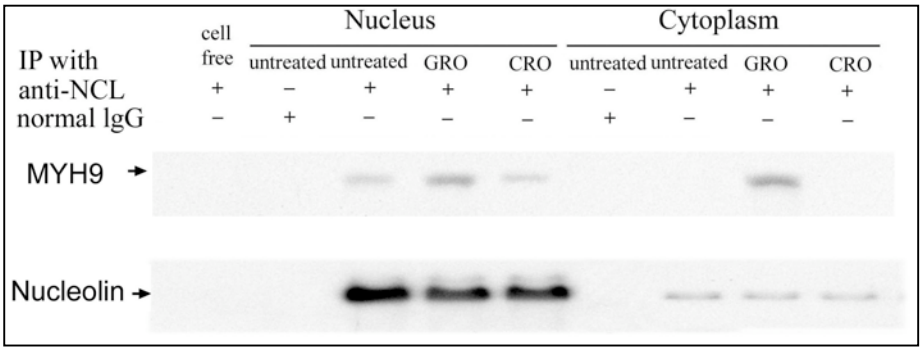
cell free
Nucleus
Cytoplasm
IP with
anti-NCL
normal lgG
untreated untreated GRO CRO untreated untreated GRO CRO
+ – + + + – + + +
– + – – – + – – –
MYH9
Nucleolin

C

Table 1

| Protein name | Accession (GI) | Mass (Mr) | pI | Matched (No) | Coverage (%) |
|---|---|---|---|---|---|
| **Ribosomal subunit proteins** | | | | | |
| ribosomal protein S8 | 55961080 | 22094 | 10.37 | 8 | 45% |
| ribosomal protein L4 | 60656419 | 47953 | 11.07 | 9 | 22% |
| ribosomal protein, large, P0 | 16933546 | 34423 | 5.71 | 7 | 30% |
| **Nonribosomal subunit proteins** | | | | | |
| kinesin family member 11 | 55664217 | 120111 | 5.47 | 21 | 29% |
| TPA: HIN1-like cysteine protease | 33186830 | 50162 | 6.31 | 7 | 18% |
| DEAH (Asp-Glu-Ala-His) box polypeptide 9 | 56206329 | 142181 | 6.41 | 11 | 12% |
| KIAA0895 protein | 57863780 | 54471 | 9.52 | 7 | 28% |
| Zinc finger protein 185 (LIM-domain) | 14286186 | 49955 | 5.26 | 8 | 24% |
| structure specific recognition protein 1 | 4507241 | 81367 | 6.45 | 14 | 25% |
| hypothetical protein | 34366427 | 29348 | 5.99 | 5 | 32% |
| Nucleolin | 55956788 | 76224 | 4.59 | 10 | 19% |
| myosin IC | 28279972 | 118874 | 9.48 | 18 | 28% |
| heat shock 90kDa protein 1, beta | 34304590 | 83212 | 4.97 | 15 | 26% |
| microtubule-associated protein 6 isoform 1 | 48375173 | 86680 | 9.2 | 7 | 9% |
| ACTB protein, actin, beta | 15277503 | 40536 | 5.55 | 9 | 48% |
| protein arginine N-methyltransferase 5 | 2323410 | 73424 | 5.88 | 14 | 35% |
| tubulin, beta polypeptide | 57209813 | 48135 | 4.7 | 7 | 27% |
| telomeric repeat binding factor 1 isoform 2 | 4507437 | 48764 | 6.32 | 6 | 20% |
| phospholipase C, gamma 1 | 82583660 | 149865 | 5.73 | 23 | 16% |
| Human Dna Topoisomerase I | 23200355 | 67062 | 9.30 | 9 | 17% |
| Myosin-9 (Myosin heavy chain, nonmuscle IIa) | 12667788 | 227515 | 5.5 | 42 | 25% |
| Cleavage and polyadenylation specific factor 1 | 16878041 | 162036 | 5.99 | 21 | 16% |
| Nuclear DNA helicase II | 71153504 | 142103 | 6.35 | 7 | 7% |
| RAS protein activator like 2 | 25121936 | 144111 | 7.87 | 10 | 8% |
| Squamous cell carcinoma antigen recognized by T cells 1 | 12654461 | 90371 | 5.89 | 10 | 21% |
| Zinc finger protein 529 | 24308255 | 55313 | 9.05 | 8 | 17% |

**APPENDIX 4: Teng *et al.* (2007), Manuscript submitted to Cancer Research**

# Protein Arginine Methyltransferase 5 (PRMT5) Associates with Nucleolin and is Altered in Prostate Cancer Cells Treated with Nucleolin-targeted Aptamer, AS1411

Yun Teng,[1] Allicia C. Girvan,[2] Lavona K. Casson,[1] Shelia D. Thomas,[1] Mingwei Qian,[1] William M. Pierce, Jr[3], Paula J. Bates[1,2]

*Departments of [1]Medicine, [2]Biochemistry and Molecular Biology, [3]Pharmacology and Toxicology, James Graham Brown Cancer Center, University of Louisville, Louisville, Kentucky*

**Running Title:** AS1411 Alters Distribution of PRMT5-Nucleolin Complex

**Key Words:** AS1411, aptamer, nucleolin, protein arginine methyltransferase 5 (PRMT5), symmetric dimethylated arginine (sDMA)

**Grant Support:** This work was supported by a grant to PJB from the Department of Defense Prostate Cancer Research Program (W81XWH-04-1-0183).

**Requests for Reprints**: Paula J. Bates, University of Louisville, 580 South Preston Street, Delia Baxter Building 321, Louisville, KY 40202-1756. Phone: 502 852 2432; Fax: 502 852 2356; Email: paula.bates@louisville.edu

## ABSTRACT

AS1411 is a quadruplex-forming oligonucleotide aptamer that targets nucleolin. It is currently being tested in clinical trials as a treatment for various cancers. We have proposed that AS1411 works by altering the molecular interactions of nucleolin, leading to changes in the activity of nucleolin and its associated proteins. Here, we report that protein arginine methyltransferase 5 (PRMT5) is a nucleolin-associated protein whose localization and activity are altered in AS1411-treated cancer cells. PRMT5 is a type II arginine methyltransferase that catalyzes the formation of symmetric dimethylarginine (sDMA). We found that levels of PRMT5 were decreased in the nucleus of AS1411-treated DU145 human prostate cancer cells, but increased in the cytoplasm. These changes were dependent on nucleolin because they were not observed in cells treated with nucleolin-specific siRNA. Treatment with AS1411 also resulted in altered levels of PRMT5 activity (assessed by sDMA levels) in accord with changes in its localization. In addition, our data indicate that nucleolin itself is a substrate for PRMT5 and that the subcellular distribution of sDMA-modified nucleolin was altered in AS1411-treated cells. We also examined expression of selected PRMT5 target genes in AS1411-treated cells because histone arginine methylation by PRMT5 is associated with transcriptional repression. For some genes, including *cyclin E2* and tumor suppressor *ST7*, a significant upregulation was noted, which corresponded with a decrease in the amount of PRMT5 bound to the gene promoter. We conclude that nucleolin is a novel binding partner and substrate for PRMT5, and that AS1411 causes relocalization of the nucleolin-PRMT5 complex from the nucleus to the cytoplasm. Consequently, the nuclear activity of PRMT5 is decreased, leading to de-repression of some PRMT5 target genes, which may contribute to the biological effects of AS1411.

## INTRODUCTION

Oligonucleotide aptamers are short sequences of DNA or RNA (or modified versions thereof) that can bind to specific proteins via recognition of their three-dimensional structure. Thus, they are mechanistically similar to therapeutic monoclonal antibodies, but may have certain advantages over antibodies, such as stability, ease of manufacture and non-immunogenicity (1). Aptameric oligonucleotides frequently contain secondary structure motifs, such as hairpins or G-quartets, and are usually discovered by *in vitro* evolution techniques (1), although some have been discovered by chance (2, 3).

We have previously reported on phosphodiester G-rich oligonucleotides, termed GROs, which function as nucleolin-binding aptamers (3-7). These have strong growth inhibitory activity against various types of cancer cells, but have minimal effects on non-malignant cells (4, 7). Active GROs can form stable G-quadruplex structures that are resistant to degradation by heat or exonucleases (5, 6). One of the GROs, now known as AS1411 (formerly AGRO100 or GRO26B-OH), is the first aptamer to be tested in clinical trials as a cancer therapeutic. The results of Phase I clinical trials in patients with advanced cancer were presented recently and indicate that AS1411 was well tolerated with no reports of any serious adverse events (8, 9). Furthermore, there was evidence of promising clinical activity, including objective responses in patients with metastatic renal cell carcinoma (8, 9).

Nucleolin (the molecular target of AS1411) is a remarkably multifunctional protein that can be present in the nucleoli, nucleoplasm, cytoplasm and plasma membrane of cells (reviewed in 10-12). Levels of nucleolin are known to correlate with the rate of cellular proliferation, being elevated in rapidly dividing cells, such as malignant cells, but barely detectable in quiescent cells (13, 14). Some of the most studied aspects of nucleolin biology are its roles in ribosome biogenesis, which include the control of rDNA transcription, pre-ribosome packaging, and organization of nucleolar chromatin. Another major role is as a shuttle protein that transports viral and cellular proteins between the cytoplasm and nucleus/nucleolus of the cell. Nucleolin has also been implicated, directly or indirectly, in many other functions including apoptosis, nuclear matrix structure, DNA replication, mRNA stability, transcriptional regulation, signal transduction, telomere maintenance, cytokinesis, as a nucleic acid helicase and as a G-quadruplex binding protein (see 3, 4, 7, 10-12, 15 and references therein). In addition, there are numerous reports describing the presence of nucleolin on the cell surface and its function as a receptor for a variety of ligands (16-22). The significance of nucleolin in cancer biology is becoming increasingly apparent and several recent studies have indicated a direct role in malignant transformation. For example, nucleolin was found to transform rat embryo fibroblasts (23), reduce levels of p53 tumor suppressor protein in breast cancer cells (23), stabilize the anti-apoptotic bcl-2 mRNA in leukemia cells (24), activate HPV18 transcription in cervical cancer (25), and promote migration in endothelial cells (22). Nucleolin has also been linked to the development of chemoresistance in breast cancer (26).

Although the primary target of AS1411 has been identified, the precise mechanism of its antiproliferative activity is not yet fully understood. Like many other nucleolin-binding ligands, AS1411 binds to cell surface nucleolin and is internalized by cancer cells (P. Bates, unpublished observations). We propose that, once inside the cell, binding of AS1411 modulates the interactions between nucleolin and its binding partners, leading to pleiotropic biological effects. Our current research aims to identify proteins whose interactions with nucleolin are altered in AS1411-treated prostate cancer cells and to investigate the biological consequences of these changes. In this report, we describe our identification of protein arginine methyltransferase 5 (PRMT5) as a novel binding partner for nucleolin and the effects of AS1411 on the subcellular localization and activity of PRMT5.

## MATERIALS AND METHODS

**Materials**. The human prostate cancer cell line DU145 was obtained from American Type Culture Collection (ATCC, Manassas, VA). The oligodeoxynucleotides used in the present study were AS1411, 5'-d(GGTGGTGGTGGTTGTGGTGGTGGTGG)-3', and an inactive control oligonucleotide, CRO, 5'-d(CCTCCTCCTCCTTCTCCTCCTCCTCC)-3'. All oligonucleotides had a phosphodiester backbone and were purchased in the desalted form from Integrated DNA Technologies (IDT, Coralville, IA). Anti-FLAG peptide antibody (M2), M2-conjugated agarose beads, FLAG peptide, nonionic detergent IGEPAL CA-630, anti-ß-actin and anti-PRMT5 monoclonal antibodies were from Sigma-Aldrich (Saint Louis, MO). Anti-aDMA (ASYM24) and anti-sDMA (SYM10) polyclonal antibodies were obtained from Upstate Biotechnology (Lake Placid, NY). MagnaBind goat anti-mouse lgG beads and anti-rabbit lgG beads were from Pierce (Rockford, IL). Anti-nucleolin monoclonal antibody (MS-3) and anti-mouse or anti-rabbit antibodies linked to horseradish peroxidase were purchased from Santa Cruz Biotechnology (Santa Cruz, CA). QuantiTect Reverse Transcription Kit was from Qiagen (Valencia, CA). Amylose-linked Magnetic Beads were from New England Biolabs (Beverly, MA).

**Plasmid construction.** To construct FLAG-tagged nucleolin expression plasmid (pFLAG-nucleolin), a 2394-base pair *Nru*I-*Xho*I fragment (encoding amino acids 7-707) of pBS-nucleolin (IMAGE 591D39, ATCC) was subcloned into the *EcoR*V-*Xho*I fragment of a pCMV2-FLAG vector (Sigma-Aldrich). The reading frame and sequence of the resulting pFLAG-nucleolin plasmid were confirmed by automated sequencing.

**Cell culture, transient transfection and treatment with oligonucleotides.** Human DU145 cells were maintained in DMEM (Gibco-BRL/Invitrogen, Grand Island, NY) supplemented with 10% heat-inactivated fetal calf serum and 100 units/ml of penicillin and streptomycin. The cells were cultured at 37℃ in an incubator with 5% $CO_2$. For transient transfection, cells cultured in T75 flasks (approximately 70% confluent) were transfected with 10 μg of pFLAG-nucleolin using LipofectAMINE Plus reagent (Invitrogen, Carlsbad, CA) according to the manufacturer's instructions. For treatment with oligonucleotides, a stock solution (typically 1000 μM) of the relevant sequence in water was added directly to the cell culture medium to give the desired final concentration. Except where otherwise indicated, the final concentration of oligonucleotide was 10 μM and cells were treated for 24 h before preparation of cell extracts.

**Immunofluorescence**. After 24 h of transfection with pFLAG-nucleolin or empty vector (pFLAG), cells were plated in 8-well culture slides (Biocoat, Becton Dickinson, Franklin Lake, NJ, USA). After an additional 24 h at 37℃, the cells were fixed with 4% paraformaldehyde in PBS (phosphate buffered saline) for 15 minutes. After washing with PBSTX (PBS with 0.2% Triton X-100), the cells were blocked with 5% goat serum in PBSTX for 1 hour at room temperature. The cells were incubated with primary antibody (10 μg/mL of anti-FLAG or 5 μg/mL of anti-nucleolin) overnight at 4℃. The cells were washed and incubated with fluorescein isothiocyanate (FITC)-conjugated anti-mouse secondary antibody for 1 h at room temperature. Fluorescent images were visualized with a Bionanoscope (Nikon, Tokyo, Japan).

**Preparation of protein extracts from DU145 cells**. At the appropriate time after treatment, cells were washed twice with cold PBS, and nuclear and cytoplasmic extracts were prepared according to the following method: Cells were incubated with 300 μl of ice-cold extraction buffer B (10 mM HEPES, pH 7.9, 1.5 mM $MgCl_2$, 10 mM KCl, 1 mM phenylmethylsulfonyl fluoride, 1 μg/ml leupeptin, 1 μg/ml aprotinin) and then lysed by three cycles of freeze-thaw. Samples were centrifuged at 12,000 ×g for 1 min and cytoplasmic

extracts were recovered as supernatant. The resultant pellets (nuclei) were resuspended in 100 μl of buffer C (20 mM HEPES, pH 7.9, 1.5 mM $MgCl_2$, 420 mM KCl, 0.2 mM EDTA, 25% glycerol, 1 mM phenylmethylsulfonyl fluoride, 1 μg/ml leupeptin, 1 μg/ml aprotinin). Following 30 min of incubation at 4°C, samples were centrifuged at 12,000 ×g for 5 min and nuclear extracts were collected as supernatant. Extracts were either used immediately or stored at -80 °C. To obtain whole cell lysates, cells were mixed with 500 μl of lysis buffer (50 mM Tris HCl, pH 7.4, with 150 mM NaCl, 1mM EDTA, 1% Triton X-100, 0.5% IGEPAL CA630) and complete protease inhibitor cocktail (Roche Diagnostics, Mannheim, Germany). The cell lysate was incubated for 30 minutes on a shaker at 4℃ and centrifuged at 12,000 ×g for 10 min, the supernatant then was obtained for additional experiments. The concentration of extracted proteins was determined using the Coomassie Plus Protein Assay Reagent (Pierce).

**Immunoprecipitation assays**. For capture of FLAG-tagged protein, extracts from transiently transfected cells were incubated with 40 μl of washed anti-FLAG beads for 4 h at 4℃ and precipitated by centrifugation. The protein-bound agarose beads were washed five times with the lysis buffer and the proteins were eluted with 20 μl of 50 mM Tris-HCl, 150 mM NaCl containing 150 μg/mL of 3×FLAG peptide. For immunoprecipitations of endogenous proteins, 200 μg of extract from non-transfected DU145 cells were incubated with 2 μg of specific antibody in 500 μl of RIPA buffer (PBS, 50 mM Tris-HCl, pH 7.5, 0.5 M NaCl, 0.1 mM EDTA, 1% Nonidet P-40, 0.5% sodium deoxycholate, 0.1% SDS, 1 mM sodium fluoride, 10 mg/ml phenylmethylsulfonyl fluoride, 2 μM aprotinin, 100 mM sodium orthovanadate) for 1 h at 4 °C. This was followed by addition of MagnaBind goat anti-mouse lgG or goat anti-rabbit lgG beads (250 μl) and overnight incubation at 4 °C on a rotator. The beads were captured using a magnetic stand and washed four times with RIPA buffer. To recover precipitated proteins, beads were resuspended in 1× sodium dodecyl sulfate (SDS)-loading buffer (100 mM Tris-HCl, pH 6.8, 200 mM dithiothreitol, 4% SDS, 0.2% bromphenol blue, 20% glycerol), boiled for 5 min, then captured and the supernatant containing eluted proteins was removed. Control immunoprecipitations were performed in parallel using normal mouse or rabbit IgG in place of primary antibody. Samples were loaded on 8% SDS-polyacrylamide gels and western analysis was performed using nucleolin or PRMT5 or other antibodies as primary antibody as described below.

**Electrophoresis and silver staining**. Immunoprecipitated protein samples were incubated in 1×SDS-loading buffer at 95 °C for 5 min, and separated on 10% polyacrylamide-SDS gels. The silver staining was performed as follows: The gel slab after electrophoresis was fixed in 50% methanol, 5% acetic acid, for 30 min with rotation. Then the gel was sensitized with 0.02% sodium thiosulfate for 2 min. After washing 3 times with distilled water for 5min per wash, the gel was incubated in 0.1% silver nitrate solution for 30-60 minutes at 4℃.After washing twice for 1 min per wash with distilled water, the gel was developed in 0.04% formalin, 2% sodium carbonate until the desired intensity of staining was achieved. Development was terminated with 1% acetic acid solution.

**Protein identification by proteomic analysis by MALDI-TOF-MS**. In-gel trypsin digestion was carried out as described (27) with modification as follows: Protein bands were excised and incubated in 50 mM $NH_4HCO_3$/50% acetonitrile at room temperature for 15 min. The gel pieces were allowed to swell by incubating with 20 mM DTT in 0.1 M $NH_4HCO_3$ for 45 min at 56℃. After removing this DTT solution, the gel was incubated in 55 mM iodoacetamide in 0.1 M $NH_4HCO_3$ for 30 min in the dark. The gel was rinsed with 50 mM $NH_4HCO_3$ and incubated in 50 mM $NH_4HCO_3$/50% acetonitrile to shrink. After drying in a

speedvac, an aliquot of 25 μg/mL sequencing-grade trypsin in 50 mM $NH_4HCO_3$ was added. After 45 min incubation on ice, the supernatant was discarded and replaced with 20 μl of 50 mM $NH_4HCO_3$. Digestion was performed at 37℃ overnight and fragmented peptides were extracted from the gel with 5% formic acid/50% acetonitrile. To improve the ionization efficiency of MALDI-TOF-MS, ZipTipC18 (Millipore, Bedford, MA, USA) was used to purify peptides before MS analysis, according to the manufacturer's manual. The peptides were eluted with 2 μl of 5 mg/ml α–cyano-4-hydroxycinnamic acid in 50% acetonitrile/0.1% trifluoroacetic acid and applied directly onto the target and allowed to air dry. Peptide mass fingerprints were obtained using a Voyager DE-STR MALDI-TOF mass spectrophotometer (PE Biosystems). The Mascot program (Matrix Science, http://www.matrixscience.com/search_form_select.html) was used to interpret MS spectra of protein digests.

**Capture of complexes using purified recombinant maltose binding protein (MBP)-nucleolin fusion proteins.** Plasmids for the expression of MBP fused to nucleolin fragments were a gift from Dr. Nancy Maizels (University of Washington, Seattle, WA). Recombinant proteins were produced by overexpression in *E. coli* and purified as described previously (28). Purified MBP-tagged nucleolin fragments (50 pmol) were incubated with 10 μg of total cell lysate and 100 μl of amylose-linked magnetic beads in 500 μl of column buffer (20 mM Tris-HCl, pH 7.4, 0.2 M NaCl, 1 mM EDTA, 10 mg/ml phenylmethylsulfonyl fluoride) for 1 h at 4 °C. The beads were precipitated and washed three times with column buffer and bound proteins were eluted with 50 μl of SDS loading buffer. Eluted proteins were analyzed for the presence of PRMT5, sDMA and MBP.

**siRNA Transfection.** One day prior to transfection, DU145 cells were plated in 6-well plates at a density of $2.0\times10^5$ cells per well in 1.5 ml of DMEM without antibiotics. For each transfection, 200 pmol of nucleolin Stealth RNAi Select (Cat# NCL-HSS106985, Invitrogen, Carlsbad, CA) or control Stealth RNAi Negative Control (Cat# 12935-200, Invitrogen, Carlsbad, CA) was diluted in 200 μl of Opti-MEM (Invitrogen, Carlsbad, CA). In a separate tube, 10 μl of Lipofectamine 2000 (Invitrogen, Carlsbad, CA) was diluted in 200 μl Opti-MEM and incubated for 5 minutes at room temperature. The diluted oligomer and diluted Lipofectamine 2000 were mixed gently and incubated for 20 minutes at room temperature. The oligmer-Lipofectamin 2000 complexes were then added to the each well containing cells and medium. Cells were incubated at 37℃ in the presence of the transfection solution for 24 h, washed with DMEM containing 10% FCS and processed for western blotting at 72 h post-transfection.

**Western Blot Analysis**. Samples were incubated in SDS-loading buffer at 95℃ for 5 minutes, and separated on 8% polyacrylamide-SDS gels, followed by electroblotting to polyvinylidene difluoride membranes (Bio-Rad, Hercules, CA). After blocking nonspecific binding sites for 1 h in 5% nonfat dried milk in PBST (0.05% Tween 20 in PBS), the membrane was incubated for 1 h at room temperature or overnight at 4℃ with primary antibody. After three washes in PBST, the membrane was incubated with horseradish peroxidase-conjugated goat anti-mouse antibody for 45 minutes at room temperature, washed three times in PBST, and detected using enhanced chemiluminescence (ECL kit from Amersham Biosciences, Piscataway, NJ).

**Real-time Quantitative Reverse Transcription PCR (qRT-PCR)**, **Chromatin Immunoprecipitation (ChIP) Assay and Cell Cycle Analysis**. Total RNA was prepared from untreated and treated DU145 cells using Trizol reagent (Invitrogen, Inc.) according to the manufacturer's instructions. The yield and quality of RNA was evaluated by measuring its

absorbance at A260/A280 using a NanoDrop spectrophotometer (NanoDrop Technologies, Wilmington, DE). The cDNA was prepared with the QuantiTect Reverse Transcription Kit (Qiagen, Valencia, CA). According to the manufacturer's manual, a total of 1 μg of each sample was included in a 20 μl reaction containing 2 μl of 7×gDNA Wipeout Buffer, 4 μl of 5×Quantiscript RT Buffer, 1 μl of RT Primer Mix, and 1 μl of Quantiscript Reverse Transcriptase. One μl of this mixture was used as template for PCR amplification. Thirty-five PCR cycles were performed as follows: 15 s denaturation at 94℃; 15 s annealing at 60℃; and 30 s extension at 72℃. Thermal cycling was performed on a DNA Engine Opitcon System (MJ Research, Waltham, MA). Each sample was run in triplicate based on which average copy numbers were calculated. Copy numbers were normalized to β-actin control amplification. Specific primer pairs were used to amplify the following genes: NM23 (+30 to +250, BC000293), ST7 (+548 to +653, BC030954), Cyclin E2 (+135 to +243, BC020729) and β-actin (+140 to +585). ChIP assays were performed using the EpiQuick ChIP kit (Epigentek Inc., NY) according to the manufacturer's instructions. The promoter sequences amplified have been previously described and were: ST7, -205 to +199 (29); and cyclin E2, -312 to +129 (30). The PCR products were separated on 1% agarose gels and stained with ethidium bromide for visualization. Analysis of cell cycle distriction was carried out by flow cytometric analysis of propidium iodide-stained cells, exactly as previously described (4).

**Denistometry and Statistical Analysis.** In some experiments, densitometry was employed to measure band intensities by scanning autoradiographic films and using UN-SCAN-IT gel software (Silk Scientific Corporation, UT, USA). Band intensities were normalized as indicated in figure legends and the results were expressed as mean and standard error from at least three separate experiments, where indicated. The statistical comparisons between AS1411-treated and control groups were carried out using student's t-test, and differences are indicated as * ($p<0.05$) or ** ($p<0.01$).

## RESULTS

**Identification of PRMT5 as a nucleolin-associated protein.** We used the pFLAG-nucleolin construct to express FLAG-tagged nucleolin in DU145 prostate cancer cells and confirmed that the epitope-tagged protein had similar distribution to endogenous nucleolin (see Figure 1A). To isolate nucleolin-associated proteins, we transiently transfected DU145 cells with pFLAG-nucleolin for 72 h, then prepared protein extracts and carried out immunoprecipitation using anti-FLAG antibody. The captured proteins were separated by electrophoresis and visualized by silver staining, followed by tryptic digestion and MALDI-TOF mass spectrometry analysis. Using this technique, we were able to identify several bands representing candidate nucleolin-interacting proteins (manuscript in preparation, Y. Teng, W. M. Pierce Jr and P. J. Bates). Among these proteins, we focused on validating one particular band whose interaction with nucleolin was altered by AS1411. As shown in Figure 1B (indicated by arrow), this protein was specifically co-precipitated by FLAG-nucleolin and was decreased in immunoprecipitated nuclear extracts from cells treated with AS1411 but unchanged in extracts from cells treated with a control oligonucleotide (CRO). This protein was subsequently identified as protein arginine methyltransterase 5 (PRMT5) by mass peptide fingerprinting of trypsin digests using MALDI-TOF mass spectrometry (Figure 1C).

**Endogenous nucleolin interacts with PRMT5 and AS1411 alters the localization of nucleolin-associated PRMT5.** To evaluate the natural interaction of endogenous nucleolin and PRMT5 in DU145 cells, we performed immunoprecipitation using anti-nucleolin antibody and probed with anti-PRMT5 antibody. PRMT5 complexes have been reported in both the nuclear and cytoplasmic compartments of the cell (31) and, in this case, PRMT5 was

co-precipitated with endogenous nucleolin using either nuclear or cytoplasmic extracts from wild type DU145 cells (Figure 1D). The results also clearly showed that nucleolin-associated PRMT5 was decreased in the nucleus of AS1411-treated cells and was increased in the cytoplasm of AS1411-treated cells, compared to untreated cells. The control oligonucleotide (CRO) had no effect on the localization of nucleolin-associated PRMT5 and there was no apparent change in the levels of nucleolin in extracts from AS1411-treated cells. Neither nucleolin nor PRMT5 could be identified in mock immunoprecipitates using normal mouse lgG or in nucleolin immunoprecipitates without added protein extracts, thus confirming the specificity of the interaction. These finding were highly reproducible and statistically significant (Figure 1D, bottom panel).

**AS1411 induces nuclear-to-cytoplasmic redistribution of PRMT5 via a nucleolin-mediated mechanism.** To further investigate this phenomenon, we analyzed levels of PRMT5 in nuclear and cytoplasmic extracts from AS1411-treated cells by western blotting. Figure 2A shows that there is a time-dependent decrease in levels of nuclear PRMT5, which is matched closely by a concomitant increase in levels of cytoplasmic PRMT5. The redistribution of PRMT5 was apparent by 4 h after addition of AS1411 and was maximal at 24 h. There was very little change is PRMT5 distribution in cells incubated with the control oligonucleotide, CRO. Using similar techniques, we determined that the redistribution of PRMT5 also depends on the dose of AS1411 (see Figure 2B). The degree of PRMT5 relocalization seen in these western blots analyzing total PRMT5 was comparable to that seen in the previous experiments, which examined nucleolin-associated PRMT5 (compare Figure 1D with the 24 h timepoint in Figure 2A), suggesting that it is the nucleolin-associated PRMT5 that is altered by AS1411. To test our hypothesis that the AS1411-induced relocalization of PRMT5 is mediated by nucleolin, we next examined cells that had been transfected with a siRNA that specifically depletes nucleolin (Figure 2C). In these cells, the AS1411-induced changes in PRMT5 were almost completely abrogated, whereas the effect of AS1411 on PRMT5 persisted in cells treated with a control siRNA.

**AS1411 changes the distribution of symmetrical dimethylarginine (sDMA)—a modification that is catalyzed by PRMT5.** Protein arginine methyltransferases are classified as type II enzymes, which catalyze the symmetric dimethylation of target arginines, or type I arginine methyltransferases, which catalyze asymmetric dimethylation (31-36). PRMT5 is thought to be the major type II enzyme that is responsible for sDMA modifications in most cell types. Therefore, to investigate the effect of AS1411 on the activity of PRMT5, we analyzed levels of sDMA in extracts from AS1411-treated and control-treated DU145 cells by western blotting using an antibody (named SYM10) that specifically recognizes sDMA (36). As a control for specificity, we also used an antibody named ASYM24, which recognizes asymmetric dimethylated arginines (aDMA)-containing proteins (36). Extracts from the nucleus and cytoplasm of AS1411-treated, control-treated and untreated DU145 cells were analyzed by western blotting using either SYM10 or ASYM24 and the recognition patterns of the two antibodies were found to be quite distinct, confirming their specificity (see Figure 3A). Moreover, the results shown in Figure 3A indicate that treatment with AS1411 results in a specific decrease in the intensity of bands recognized by SYM10 in the nuclear extracts, with a corresponding increase in the intensity of SYM10-immunoreactive bands in the cytoplasmic extracts. In contrast, there were no changes in the bands detected by ASYM24 in extracts from AS1411-treated cells. Since the sDMA modifications recognized by SYM10 are presumably an indicator of PRMT5 activity, these data are consistent with the observed nuclear-to-cytoplasmic redistribution of the enzyme.

**The nucleolin complex contains sDMA modifications and is a likely substrate for PRMT5.** Because nucleolin is associated with PRMT5 and contains an arginine-rich region

(the "RGG domain") that is a common target for PRMTs (31-36), we wondered if nucleolin itself could be a substrate for PRMT5. To test this idea, we immunoprecipitated with the SYM10 antibody and then western blotted using anti-nucleolin antibody. As indicated in Figure 3B, the anti-sDMA antibody was able to specifically precipitate nucleolin. Furthermore, there was a nuclear-to-cytoplasmic shift in levels of sDMA-precipitated nucleolin in AS1411-treated cells, similar to that seen for PRMT5. This was in contrast to the levels of total nucleolin, for which there was no obvious change (see the nucleolin blot in Figure 1D), suggesting that sDMA-modified nucleolin may represent only a small proportion of the total nucleolin pool. Therefore, we postulated that only a small fraction of the total nucleolin is associated with PRMT5, whereas most of the PRMT5 exists in a complex with nucleolin. This would explain why a large proportion of the total PRMT5 is translocated in AS1411-treated cells by 24 h (Figure 2A), whereas levels of total nucleolin are virtually unchanged by AS1411 (Figure 1D). To test this theory, we estimated the fraction of total nucleolin that was associated with PRMT5, and *vice versa*, by analyzing the amount of protein immunoprecipitated compared to the total protein, also taking into account the efficiency of the immunoprecipitation. Our results (Figure 3C) indicate that a large proportion (> 78%) of the total PRMT5 co-precipitates with nucleolin. We were not able to directly assess PRMT5-associated nucleolin in a similar way because the PRMT5 antibody was not efficient for immunoprecipitation. However, by immunoprecipitating with sDMA antibody, we confirmed that only a small fraction (< 6%) of nucleolin was sDMA-modified, which presumably reflects the amount of nucleolin that is bound to PRMT5 (Figure 3D).

**Association with PRMT5 is mediated by the RGG domain of nucleolin.** To further investigate which domain of nucleolin is responsible for the interaction with PRMT5, binding assays were performed using several recombinant nucleolin polypeptides (see Figure 4A). These recombinant proteins contained the first two RNA binding domains (RBD1,2) and/or the arginine-glycine repeat (RGG) domain fused at their N-terminal ends to a maltose binding protein (MBP) tag. Only these domains were investigated because the N-terminal domain of nucleolin cannot be expressed in *E. coli* and the RBD3,4 domain is subject to partial proteolysis (P. Bates, unpublished observation), probably by autodegradation (10). After *in vitro* incubation of purified MBP-fusion proteins with DU145 cell lysates, bound proteins were recovered using maltose affinity gel beads. As shown in Figure 4B, no PRMT5 was recovered in the precipitate when the recombinant protein contained the MBP tag alone or MBP-tagged RNA binding domains (RBD1,2). In contrast, when MBP was fused to either RGG or RBD1,2-RGG, PRMT5 was precipitated. These results indicate that the RGG C-terminal domain of nucleolin is the minimal domain required for interaction of nucleolin with PRMT5 and that RBD1,2 can promote the RGG-PRMT5 interaction. When the same samples were western blotted using the SYM10 antibody, there was also strong staining of a band corresponding to the MBP-RBD1,2-RGG fragment, confirming our previous postulate that nucleolin is a substrate for sDMA modification by PRMT5.

**AS1411 causes upregulation of some PRMT5 target genes, including tumor suppressor ST7 and cyclin E2.** Previous work has shown that recruitment of PRMT5 to the promoter regions of tumor suppressor genes, *ST7* and *NM23*, leads to transcriptional repression of these genes due to sDMA modification at R8 of histone H3 (29). These two genes, and the *cyclin E2* gene, were upregulated in cells when antisense RNA was used to reduce levels of PRMT5 (29). Based on our observations that levels of PRMT5 are reduced in the nuclei of AS1411-treated cells and since PRMT5 acts as a transcriptional repressor, we predicted that PRMT5 target genes would be upregulated in AS1411-treated cells. To test this theory, we analyzed expression levels of selected PRMT5 target genes by real time RT-PCR using RNA from untreated, AS1411-treated or control-treated DU145 cells. As illustrated in

Figure 5A, AS1411-treated DU145 cells exhibited a 3.9-fold and 2.2-fold higher expression of *cyclin E2* and *ST7* mRNA, respectively, compared to untreated cells. These values are comparable to the changes observed in the previous study where antisense RNA was used to deplete PRMT5 in NIH-3T3 cells (29). However, in contrast to the previous study, expression of the *NM23* gene was not significantly changed in AS1411-treated DU45 cells, suggesting that regulation by PRMT5 may be cell type dependent. To confirm that the observed changes in *ST7* and *cyclin E2* expression were due to decreased binding of PRMT5 to the promoter regions of those genes, we next performed chromatin immunoprecipitation (ChIP) experiments. These showed that the levels of PRMT5 associated with the *cyclin E2* and *ST7* promoters were significantly decreased in cells treated with AS1411 (see Figure 5B), whereas the control oligonucleotide (CRO) had no effect on PRMT5 (Figure 5B) and AS1411 did not affect the positive control ChIP (data not shown). Because cyclin E2 is a cell cycle regulator that accelerates G1/S, we also examined if there was a perturbation of the cell cycle in AS1411-treated cells. We found that there was a small but significant increase in the proportion of cells that were in S phase and a reduction in G2/M (Figure 5C).

**DISCUSSION**

Protein arginine methylation (R-methylation) is a post-translational modification that results in the addition of one or two methyl groups to the guanidino nitrogen atoms of arginine. There are at least nine human PRMTs responsible for arginine methylation and they have been classified in two major classes; type I enzymes promote the formation of asymmetric ω-$N^G$, $N^G$-dimethylated arginines (aDMA), and type II enzymes catalyze the formation of symmetric ω-$N^G$, $N'^G$-dimethylated arginines (sDMA), whereas ω-$N^G$-monomethylarginine (MMA) is thought to be an intermediate formed by both types (31-36). Consensus sequences for various PRMTs have not been defined, although most R-methylated proteins identified to date are modified at glycine/arginine-rich repeats. The biological function of arginine methylation is also not yet fully understood, but there is credible evidence for roles in transcriptional regulation, RNA processing, signal transduction, DNA repair and subcellular protein transport. These roles have been detailed recently in several excellent reviews about arginine methylation (31-36).

In this study, we have identified a specific interaction between nucleolin and the major type II arginine methyltransferase, PRMT5. This appears to be a novel finding because, although an earlier proteomics analysis identified PRMT5 (also known as JBP1 and SKB1) as a protein that co-precipitated with nucleolin, the PRMT5-nucleolin interaction was previously dismissed as non-specific (37). In contrast, our current work clearly demonstrates that the PRMT5-nucleolin interaction is specific and occurs in cultured DU145 prostate cancer cells. Our data also indicate that PRMT5-associated nucleolin contains sDMA, which strongly suggests that nucleolin is a substrate for modification by PRMT5. Interestingly, the RGG domain of nucleolin has been previously shown to be a substrate for asymmetric dimethylation by the type I enzyme, PRMT1 (38). However, it is not unprecedented for a protein to be a target for both types of PRMTs and there is mounting evidence that there can be competition between type I and type II enzymes for the same arginines, with aDMA or sDMA modifications having opposing effects (reviewed in 31). An example is the R3 residue of histone H4, which can be modified by PRMT1 (usually leading to transcriptional activation) or by PRMT5 (resulting in transcriptional repression). Another protein that can contain both aDMA and sDMA modifications is the sliceosomal protein, SmB, and, in this case, the type of arginine methylation was related to the nuclear or cytoplasmic localization of the protein. In terms of cell biology, the significance of nucleolin methylation is not yet known. Its role in

nucleolar localization and nucleic acid binding has been studied, but methylation of the RGG domain was found to be non-essential for these functions (39, 40). It may be relevant that there is substantial overlap between the biological functions of nucleolin and PRMT5; for instance, both have been implicated in transcriptional regulation, chromatin remodeling, spermatocyte maturation, RNA processing, complex formation with SMN1, and mediating nuclear/cytoplasmic localization (10-12, 31-36, 41-47). It is also tempting to speculate that the apparently inconsistent roles (sometimes activating, sometimes repressing) of nucleolin in transcriptional regulation (reviewed in 10-12) could be explained in terms of whether it is associated with (or, perhaps, methylated by) PRMT1 or PRMT5. In short, further research will be required to fully elucidate the relationships involved, but the results presented herein clearly point to an intriguing link between nucleolin biology and arginine methylation, especially with regard to transcriptional regulation and nuclear-cytoplasmic shuttling.

Another major result of this study is the discovery that the nucleolin-targeted aptamer, AS1411, can alter the cellular localization and activity of PRMT5. This has a number of important implications for the mechanism of this novel anticancer agent. The role of PRMT5 in cancer biology has not been widely studied, but there is some evidence that increased PRMT5 levels (particularly, nuclear PRMT5) are associated with malignant transformation. A recent report identified PRMT5 (alternatively called SKB1) as a gene that was specifically overexpressed, at both the mRNA and protein levels, in gastric cancers compared to normal gastric tissues (48). Immunohistochemistry studies comparing normal gastric tissue with moderately and poorly differentiated carcinomas found that, not only was there an increase in the overall levels of PRMT5, but that there was a shift from cytoplasmic to nuclear staining as the degree of malignancy increased (48). Other evidence for the significance of PRMT5 in cancer comes from Pal *et al.* (29). These authors have shown that stable expression of FLAG-tagged PRMT5 can transform NIH-3T3 cells, such that they proliferated faster than wild type cells and could grow in an anchorage-independent manner. Conversely, cells that were stably transfected with antisense PRMT5 cells grew considerably slower than wild type cells. To investigate the mechanism of this effect, these researchers carried out microarray studies to compare gene expression in cells expressing antisense PRMT5 (which had PRMT5 mRNA levels reduced by >90%) with wild type cells. Two tumor suppressors, *ST7* and *NM23*, were found to be upregulated in the antisense cell line and were subsequently identified as direct targets of PRMT5-mediated transcriptional repression. The cell cycle regulator, *cyclin E2*, was also induced in the antisense PRMT5 cells, although it was not determined if this was a direct effect. We have shown here that treatment of DU145 prostate cancer cells with AS1411 reduces the levels of PRMT5 in the nucleus, thereby causing an increase in *ST7* and *cyclin E2* expression due to a decrease in the amount of PRMT5 that is associated with their promoter regions. These results are consistent with another recent report describing how a nuclear-to-cytoplasmic shift of a PRMT5 repressor complex resulted in upregulation of target gene expression (49). We predict that AS1411-induced de-repression of *ST7* and *cyclin E2* genes, and possibly other PRMT5 target genes that have not been identified here, may contribute to the biological activity of AS1411. The human *ST7* gene was first recognized as a candidate tumor suppressor based on its chromosomal location (7q31.1) at a site of frequent LOH (loss of heterozygosity) and its reduced expression in some types of cancer (50). Multiple studies failed to find tumor-associated mutations in the *ST7* gene (reviewed in 50), suggesting that inactivation is due to epigenetic silencing at the level of chromatin organization, probably mediated by PRMT5 (29, 51). More importantly, the role of ST7 as a tumor suppressor has been demonstrated at the functional level. Studies have shown that ectopic expression of the *ST7* gene in human breast or prostate cancer cells resulted in reduced anchorage-independent growth and suppression of tumorigenicity in immunodeficient mice (50). Thus, AS1411-

induced upregulation of *ST7* could evidently contribute to its anticancer activity. The possible role of *cyclin E2* upregulation in the mechanism of AS1411 is less obvious because this gene is a cell cycle regulator that controls the G1-S transition and is generally considered to be growth-promoting. Nonetheless, it is worth noting that the antisense PRMT5 cells grew slower than wild type cells, even while *cyclin E2* levels were enhanced (29). Also, cancer cells treated with AS1411 are accumulated in S phase (Figure 5C), consistent with previous reports that GRO29A (a longer version of AS1411) induces cell cycle arrest in S phase (4).

Our results have additional broader implications in terms of the mechanism of AS1411 activity. Previous work has indicated that GROs bind directly and specifically to nucleolin protein (3), and that antiproliferative activity across a series of GROs is correlated with their nucleolin binding affinity (3, 5, 6). These data support our assertion that GROs, including AS1411, work as nucleolin-targeted aptamers. On the other hand, no obvious changes in the levels or localization of nucleolin are observed in cancer cells treated with AS1411 or other active GROs. Therefore, we hypothesized that AS1411 modulates the activity of nucleolin by altering its posttranslational modifications and/or affecting its interactions with other proteins. Our previous research (7) has identified NEMO/IKKγ, which is a critical factor in NF-κB activation, as a protein that co-precipitated with AS1411 and nucleolin. In that study, we found that the presence of AS1411 increased the association of NEMO with nucleolin in the cytoplasm, resulting in abrogation of NF-κB signaling (7). In this paper, we have described how AS1411 affects both a post-translational modification (symmetric arginine dimethylation) of nucleolin and the localization of a specific nucleolin complex (with PRMT5). Interestingly, these changes were linked to nuclear-to-cytoplasmic redistribution of the nucleolin-PRMT5 complex, suggesting that the shuttling function of nucleolin may be affected by AS1411. Moreover, only a small proportion of cellular nucleolin, consisting of the sDMA-modified protein, was affected by AS1411, which explains why there is no obvious change in total nucleolin levels in cells treated with AS1411. Taken together, our results support the hypothesis that aptamer-induced perturbations of nucleolin (or a subset of nucleolin complexes) are responsible for the biological effects of AS1411. Therefore, in addition to being a promising therapeutic agent, AS1411 may be a useful tool for investigating the regulation and functions of this extraordinary protein. This may ultimately lead to important insights into tumor biology, since there is mounting evidence that overexpression of nucleolin can contribute to cancer development and progression (11).

## ACKOWLEDGEMENT

We thank Dr. Nancy Maizels (University of Washington, Seattle, WA) for the generous gift of plasmids for expression of MBP-nucleolin polypeptides.

## REFERENCES

1. Pestourie C, Tavitian B, Duconge F. Aptamers against extracellular targets for in vivo applications. Biochimie 2005;87:921-30.
2. Cogoi S, Ballico M, Bonora GM, Xodo LE. Antiproliferative activity of a triplex-forming oligonucleotide recognizing a Ki-ras polypurine/polypyrimidine motif correlates with protein binding. Cancer Gene Ther 2004;11:465-76.
3. Bates PJ, Kahlon JB, Thomas SD, Trent JO, Miller DM. Antiproliferative activity of G-rich oligonucleotides correlates with protein binding. J Biol Chem 1999;274:26369-77.
4. Xu X, Hamhouyia F, Thomas SD, et al. Inhibition of DNA replication and induction of S phase cell cycle arrest by G-rich oligonucleotides. J Biol Chem 2001;276:43221-30.
5. Dapic V, Bates PJ, Trent JO, Rodger A, Thomas SD, Miller DM. Antiproliferative

activity of G-quartet-forming oligonucleotides with backbone and sugar modifications. Biochemistry 2002;41:3676-85.

6. Dapic V, Abdomerovic V, Marrington R, et al. Biophysical and biological properties of quadruplex oligodeoxyribonucleotides. Nucleic Acids Res 2003;31:2097-107.
7. Girvan AC, Teng Y, Casson LK, et al. AGRO100 inhibits activation of nuclear factor-kappaB (NF-kappaB) by forming a complex with NF-kappaB essential modulator (NEMO) and nucleolin. Mol Cancer Ther 2006;5:1790-9.
8. Laber D, Bates P, Trent J, Barnhart K, Taft B, Miller D. Long term clinical response in renal cell carcinoma patients treated with quadruplex forming oligonucleotides. Clin Cancer Res 2005;11:9088S
9. Miller D, Laber D, Bates P, Trent J, Taft B, Kloecker GH. Extended phase I study of AS1411 in renal and non-small cell lung cancers. Ann Oncol. 2006;17(Suppl 8):ix147-8.
10. Srivastava M, Pollard HB. Molecular dissection of nucleolin's role in growth and cell proliferation: new insights. FASEB J 1999;13:1911-22.
11. Storck S, Shukla M, Dimitrov S, Bouvet P. Functions of the histone chaperone nucleolin in diseases. Subcell Biochem. 2007;41:125-44.
12. Mongelard F, Bouvet P. Nucleolin: a multiFACeTed protein. Trends Cell Biol 2007;17:80-6.
13. Sirri V, Roussel P, Gendron MC, Hernandez-Verdun D. Amount of the two major Ag-NOR proteins, nucleolin, and protein B23 is cell-cycle dependent. Cytometry 1997;28:147-56.
14. Derenzini M, Sirri V, Trere D, Ochs RL. The quantity of nucleolar proteins nucleolin and protein B23 is related to cell doubling time in human cancer cells. Lab Invest 1995;73:497-502.
15. Mi Y, Thomas SD, Xu X, Casson LK, Miller DM, Bates PJ. Apoptosis in leukemia cells is accompanied by alterations in the levels and localization of nucleolin. J Biol Chem 2003;278:8572-9.
16. Hovanessian AG, Puvion-Dutilleul F, Nisole S, et al. The cell-surface-expressed nucleolin is associated with the actin cytoskeleton. Exp Cell Res 2000;261:312-28.
17. Dumler I, Stepanova V, Jerke U, et al. Urokinase-induced mitogenesis is mediated by casein kinase 2 and nucleolin. Curr Biol 1999;9:1468-76.
18. Legrand D, Vigie K, Said EA, et al. Surface nucleolin participates in both the binding and endocytosis of lactoferrin in target cells. Eur J Biochem 2004;271:303-17.
19. Shibata Y, Muramatsu T, Hirai M, et al. Nuclear targeting by the growth factor midkine. Mol Cell Biol 2002;22:6788-96.
20. Larrucea S, Cambronero R, Gonzalez-Rubio C, et al. Internalization of factor J and cellular signalization after factor J-cell interaction. Biochem Biophys Res Commun 1999;266:51-7.
21. Christian S, Pilch J, Akerman ME, Porkka K, Laakkonen P, Ruoslahti E. Nucleolin expressed at the cell surface is a marker of endothelial cells in angiogenic blood vessels. J Cell Biol 2003;163:871-8.
22. Huang Y, Shi H, Zhou H, Song X, Yuan S, Luo Y. The angiogenic function of nucleolin is mediated by vascular endothelial growth factor and nonmuscle myosin. Blood 2006;107:3564-71.

23. Takagi M, Absalon MJ, McLure KG, Kastan MB. Regulation of p53 translation and induction after DNA damage by ribosomal protein L26 and nucleolin. Cell 2005;123:49-63.

24. Otake Y, Soundararajan S, Sengupta TK, et al. Overexpression of nucleolin in chronic lymphocytic leukemia cells induces stabilization of bcl2 mRNA. Blood. 2007;109:3069-75.

25. Grinstein E, Wernet P, Snijders PJ, et al. Nucleolin as activator of human papillomavirus type 18 oncogene transcription in cervical cancer. J Exp Med 2002;196:1067-78.

26. Fu Z, Fenselau C. Proteomic evidence for roles for nucleolin and poly(ADP-ribosyl) transferase in drug resistance. J Proteome Res 2005;4:1583-91.

27. Powell DW, Rane MJ, Joughin BA, et al. Proteomic identification of 14-3-3zeta as a mitogen-activated protein kinase-activated protein kinase 2 substrate: role in dimer formation and ligand binding. Mol Cell Biol 2003;23:5376-87.

28. Hanakahi LA, Sun H, Maizels N. High affinity interactions of nucleolin with G-G-paired rDNA. J Biol Chem 1999;274:15908-12.

29. Pal S, Vishwanath SN, Erdjument-Bromage H, Tempst P, Sif S. Human SWI/SNF-associated PRMT5 methylates histone H3 arginine 8 and negatively regulates expression of ST7 and NM23 tumor suppressor genes. Mol Cell Biol 2004;24:9630-45.

30. Sun A, Shanmugam I, Song J, Terranova PF, Thrasher JB, Li B. Lithium suppresses cell proliferation by interrupting E2F-DNA interaction and subsequently reducing S-phase gene expression in prostate cancer. Prostate 2007;67:976-88.

31. Bedford MT, Richard S. Arginine methylation an emerging regulator of protein function. Mol Cell 2005;18:263-72.

32. Pahlich S, Zakaryan RP, Gehring H. Protein arginine methylation: Cellular functions and methods of analysis. Biochim Biophys Acta. 2006;1764:1890-903.

33. Krause CD, Yang ZH, Kim YS, Lee JH, Cook JR, Pestka S. Protein arginine methyltransferases: Evolution and assessment of their pharmacological and therapeutic potential. Pharmacol Ther 2007;113:50-87.

34. Blanchet F, Schurter BT, Acuto O. Protein arginine methylation in lymphocyte signaling. Curr Opin Immunol 2006;18:321-8.

35. McBride AE, Silver PA. State of the arg: protein methylation at arginine comes of age. Cell 2001;106:5-8.

36. Boisvert FM, Cote J, Boulanger MC, Richard S. A proteomic analysis of arginine-methylated protein complexes. Mol Cell Proteomics 2003;2:1319-30.

37. Yanagida M, Shimamoto A, Nishikawa K, Furuichi Y, Isobe T, Takahashi N. Isolation and proteomic characterization of the major proteins of the nucleolin-binding ribonucleoprotein complexes. Proteomics 2001;1:1390-404.

38. Cimato TR, Tang J, Xu Y, et al. Nerve growth factor-mediated increases in protein methylation occur predominantly at type I arginine methylation sites and involve protein arginine methyltransferase 1. J Neurosci Res 2002;67:435-42.

39. Raman B, Guarnaccia C, Nadassy K, et al. N(omega)-arginine dimethylation modulates the interaction between a Gly/Arg-rich peptide from human nucleolin and nucleic acids. Nucleic Acids Res 2001;29:3377-84.

40. Pellar GJ, DiMario PJ. Deletion and site-specific mutagenesis of nucleolin's carboxy GAR domain. Chromosoma 2003;111:461-9.

41. Lefebvre S, Burlet P, Viollet L, et al. A novel association of the SMN protein with two major non-ribosomal nucleolar proteins and its implication in spinal muscular atrophy. Hum Mol Genet 2002;11:1017-27.

42. Mikhaylova LM, Boutanaev AM, Nurminsky DI. Transcriptional regulation by Modulo integrates meiosis and spermatid differentiation in male germ line. Proc Natl Acad Sci U S A 2006;103:11975-80.

43. Gonsalvez GB, Rajendra TK, Tian L, Matera AG. The Sm-protein methyltransferase, dart5, is essential for germ-cell specification and maintenance. Curr Biol 2006;16:1077-89.

44. Fabbrizio E, El Messaoudi S, Polanowska J, et al. Negative regulation of transcription by the type II arginine methyltransferase PRMT5. EMBO Rep 2002;3:641-5.

45. Angelov D, Bondarenko VA, Almagro S, et al. Nucleolin is a histone chaperone with FACT-like activity and assists remodeling of nucleosomes. EMBO J 2006;25:1669-79.

46. Masumi A, Fukazawa H, Shimazu T, et al. Nucleolin is involved in interferon regulatory factor-2-dependent transcriptional activation. Oncogene 2006;25:5113-24.

47. Grinstein E, Du Y, Santourlidis S, Christ J, Uhrberg M, Wernet P. Nucleolin regulates gene expression in CD34-positive hematopoietic cells. J Biol Chem 2007;282:12439-49.

48. Kim JM, Sohn HY, Yoon SY, et al. Identification of gastric cancer-related genes using a cDNA microarray containing novel expressed sequence tags expressed in gastric cancer cells. Clin Cancer Res 2005;11:473-82.

49. Ancelin K, Lange UC, Hajkova P, et al. Blimp1 associates with Prmt5 and directs histone arginine methylation in mouse germ cells. Nat Cell Biol 2006;8:623-30.

50. Hooi CF, Blancher C, Qiu W, et al. ST7-mediated suppression of tumorigenicity of prostate cancer cells is characterized by remodeling of the extracellular matrix. Oncogene 2006;25:3924-3.

51. Pal S, Baiocchi RA, Byrd JC, Grever MR, Jacob ST, Sif S. Low levels of miR-92b/96 induce PRMT5 translation and H3R8/H4R3 methylation in mantle cell lymphoma. EMBO J. 2007; [Epub ahead of print]

**FIGURE LEGENDS**

**Figure 1. Identification of a PRMT5-nucleolin complex and the effect of AS1411 on its location.** *A,* DU145 prostate cancer cells were transiently transfected with FLAG-tagged nucleolin (pFLAG-Nucleolin) or empty vector (pFLAG). Immunofluorescent staining with antibodies to nucleolin (left) or FLAG (right) confirms that the epitope-tagged protein has a distribution similar to endogenous nucleolin. *B,* Transiently transfected cells were treated with AS1411 or control oligonucleotide (CRO), or left untreated. The nucleolin complex was isolated from nuclear extracts by FLAG immunoprecipitation and then analyzed by electrophoresis followed by silver staining. *Lane 1,* cells were transfected with empty vector. The image shows part of a silver-stained gel and the band that was subsequently identified as PRMT5 (indicated by the arrow). *C,* MALDI-TOF analysis of tryptic peptides from the band shown in panel B. *D,* Endogenous nucleolin was immunoprecipitated (nucleolin IP) from nuclear or cytoplasmic extracts from non-transfected DU145 cells that were untreated (-), AS1411-treated (1411), or control-treated (CRO). Non-specific mouse IgG (mock IP) was used in parallel as a control for specificity. Precipitated proteins were analyzed by western blotting for PRMT5 or nucleolin and the amount of nucleolin-associated PRMT5 was quantified by densitometry. The intensity of the PRMT5 band in each sample was normalized to the corresponding nucleolin band and expressed relative to untreated extracts. The bars represent the mean and standard error of three independent experiments.

**Figure 2. AS1411 alters subcellular distribution of PRMT5 in a time-dependent, dose-dependent and nucleolin-dependent manner.** Nuclear and cytoplasmic extracts were prepared from DU145 cells that had been treated with either AS1411 (A) or control oligonucleotide (C). Extracts were analyzed by western blotting for PRMT5, then for β-actin (a control for equal loading). *A,* Cells were incubated with 10 μM of AS1411 for the times indicated. *B,* Cells were incubated for 24 h with oligonucleotide at the concentrations indicated. *C,* Cells were transfected with either nucleolin siRNA or control siRNA for 48 h before treatment with 10 μM oligonucleotide and then analyzed by western blotting after a further 24 h. All panels show representative western blots and quantification of the results using densitometry. The intensity of the PRMT5 band in each sample was normalized to the corresponding β-actin band and expressed relative to the untreated sample. Where error bars are shown, the data points represent the mean and standard error of three independent experiments.

**Figure 3. AS1411 alters the distribution of sDMA-modified proteins, including sDMA-nucleolin.** Nuclear and cytoplasmic extracts were prepared from DU145 cells that were untreated (-) or had been treated with either AS1411 (1411) or control oligonucleotide (CRO). *A,* Extracts were analyzed by western blotting for sDMA or aDMA, as indicated. The intensities of representative bands, which were normalized to the loading control (β-actin) and expressed relative to untreated cells, are shown below each blot. *B,* sDMA-modified proteins were captured from extracts by immunoprecipitation using anti-sDMA antibody and precipitated proteins were then western blotted using a nucleolin antibody. Immunoprecipitation with non-specific IgG was performed in parallel as a control. The relative amount of nucleolin that was precipitated by sDMA antibody was quantified by densitometry of western blots. Levels were expressed relative to the untreated sDMA IP in each blot and the bars represent the mean and standard error of three independent experiments. *C,* The proportion of total PRMT5 that is associated with nucleolin was estimated by

comparing levels of PRMT5 and nucleolin in extracts before and after immunoprecipitation with nucleolin antibody. The blots show 10 μg of nuclear or cytoplasmic extract compared with the total immunoprecipitate (IP) obtained from 50 μg of the same extract using a nucleolin antibody (NCL) or non-specific control (IgG). The fraction of protein precipitated was calculated by dividing the intensity of the relevant IP band by 5× the intensity of the corresponding extract band. The proportion of PRMT5 associated with nucleolin is the fraction of co-precipitated PRMT5 divided by the fraction of precipitated nucleolin. *D*, A similar experiment was performed to estimate the percentage of nucleolin that is sDMA-modified.

**Figure 4. Interaction with PRMT5 involves the RBD1,2 and RGG domains of nucleolin**. *A*, Schematic representation of nucleolin and the different recombinant proteins produced in *E. coli* for use in these interaction studies. Polypeptides representing the RNA binding domains (RBD1,2) and/or the arginine/glycine-rich domain (RGG) of nucleolin fused to maltose binding protein (MBP) tag at their N termini were used. *B*, Whole cell lysate from DU145 cells was incubated with purified MBP-tagged polypeptides, which were then captured using amylose-linked magnetic beads. After extensive washing, bound proteins were eluted and analyzed by western blotting for with anti-PRMT5 (*top*) and anti-MBP, as a control for loading (*bottom*). As a negative control, purified MBP-tagged RGG was incubated with amylose beads in the absence of cell lysate (*lane 5*).

**Figure 5. Transcription of tumor suppressor gene *ST7* and cell cycle regulator *cyclin E2* are increased in AS1411-treated prostate cancer cells due to decreased chromatin-associated PRMT5.** *A*, The levels of selected PRMT5 target genes were analyzed by real-time quantitative RT-PCR using mRNA from DU145 cells that were untreated or treated for 24 h with 10 μM AS1411 or control oligonucleotide (CRO). Bars represent the mean and standard error of three separate experiments and mRNA levels are shown relative to expression in untreated cells. *B*, DU145 cells treated as indicated were subjected to chromatin IP (ChIP) assay using PRMT5 antibody. Mock ChIP (using non-specific IgG in place of anti-PRMT5) and the reaction without cell lysate were performed as controls. PCR products corresponding to the promoter regions of *ST7* or *cyclin E2* were electrophoresed on agarose gels, visualized by ethidium bromide staining and analyzed by densitometry. Bars represent the mean and standard error of three separate experiments and are shown relative to expression in untreated cells. *C*, Cell cycle profiles of DU145 cells showing histograms and percentage of cells in each phase after 24 h of treatment, as indicated. Analysis was performed on 10,000 events per sample and bars represent the mean and standard error of four separate experiments.

## Figure 1

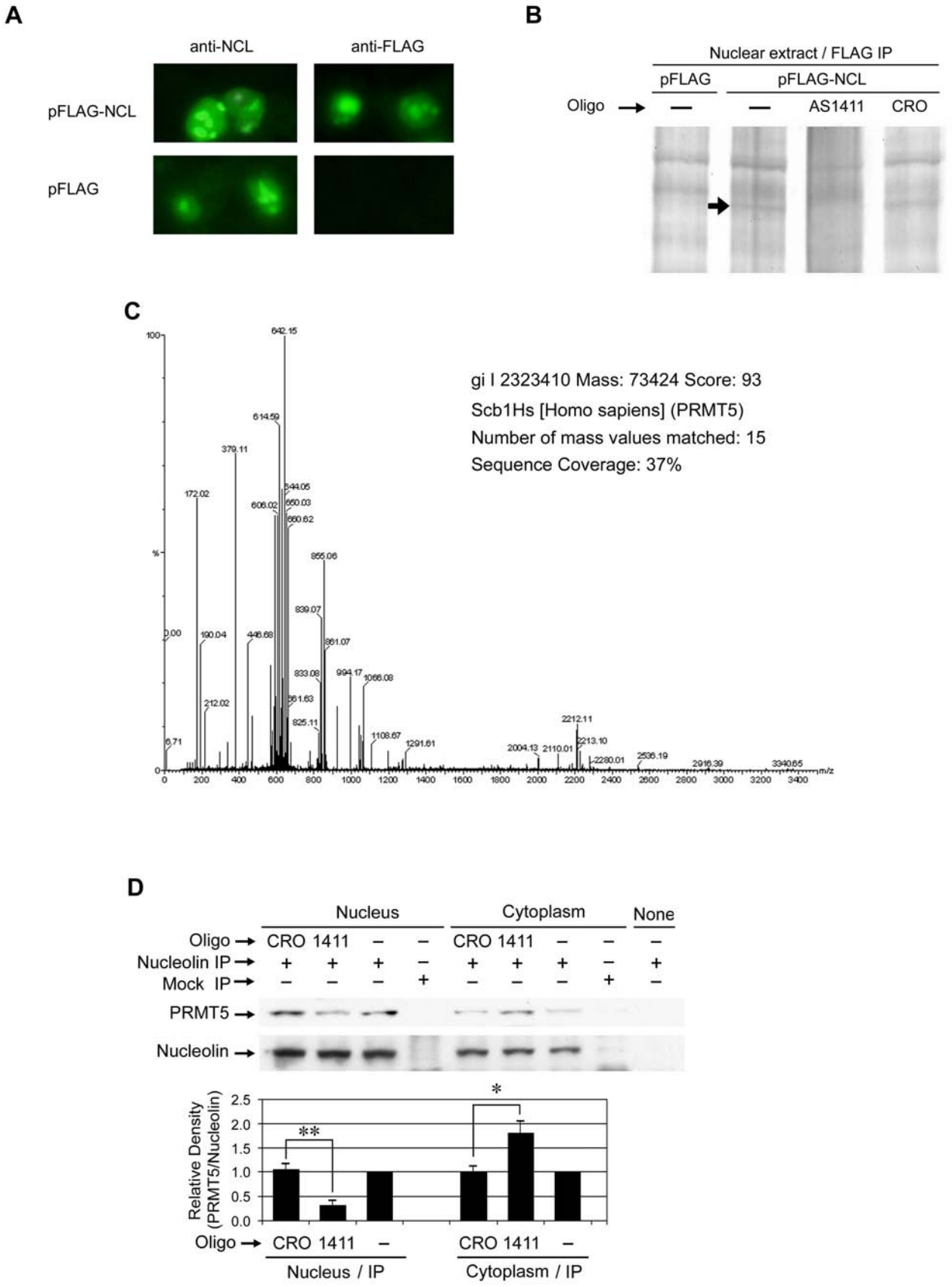
A
anti-NCL
anti-FLAG
pFLAG-NCL
pFLAG
B
Nuclear extract / FLAG IP
pFLAG
pFLAG-NCL
Oligo
—
—
AS1411
CRO
C
gi I 2323410 Mass: 73424 Score: 93
Scb1Hs [Homo sapiens] (PRMT5)
Number of mass values matched: 15
Sequence Coverage: 37%
D
Nucleus
Cytoplasm
None
Oligo
CRO 1411
Nucleolin IP
Mock IP
PRMT5
Nucleolin
Relative Density (PRMT5/Nucleolin)
Nucleus / IP
Cytoplasm / IP

## Figure 2

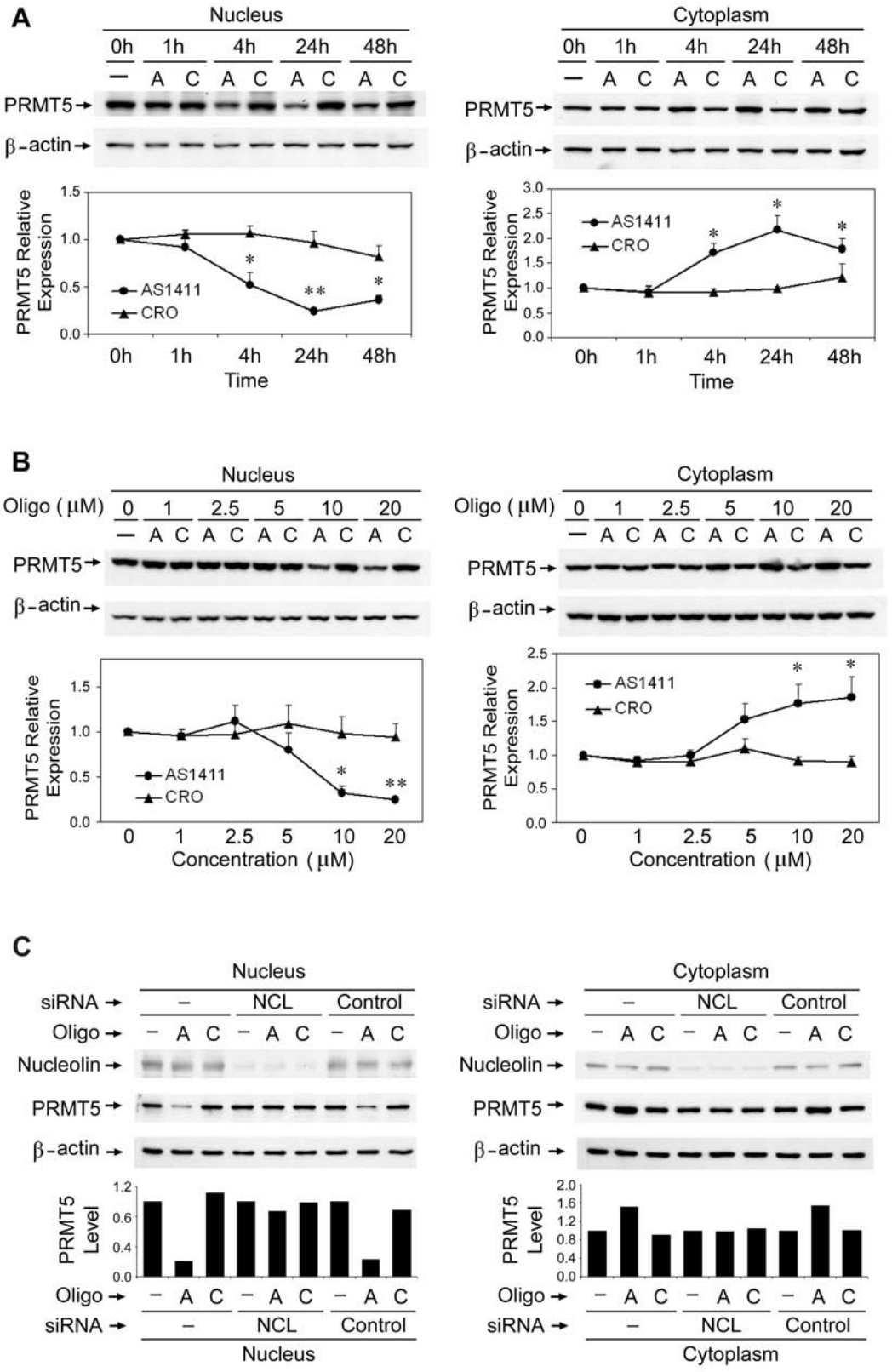
A
Nucleus
Cytoplasm
0h 1h 4h 24h 48h
— A C A C A C A C
PRMT5
β-actin
PRMT5 Relative Expression
AS1411
CRO
Time
B
Nucleus
Cytoplasm
Oligo (μM) 0 1 2.5 5 10 20
Concentration (μM)
C
siRNA
Oligo
Nucleolin
PRMT5 Level
NCL
Control

**Figure 3**

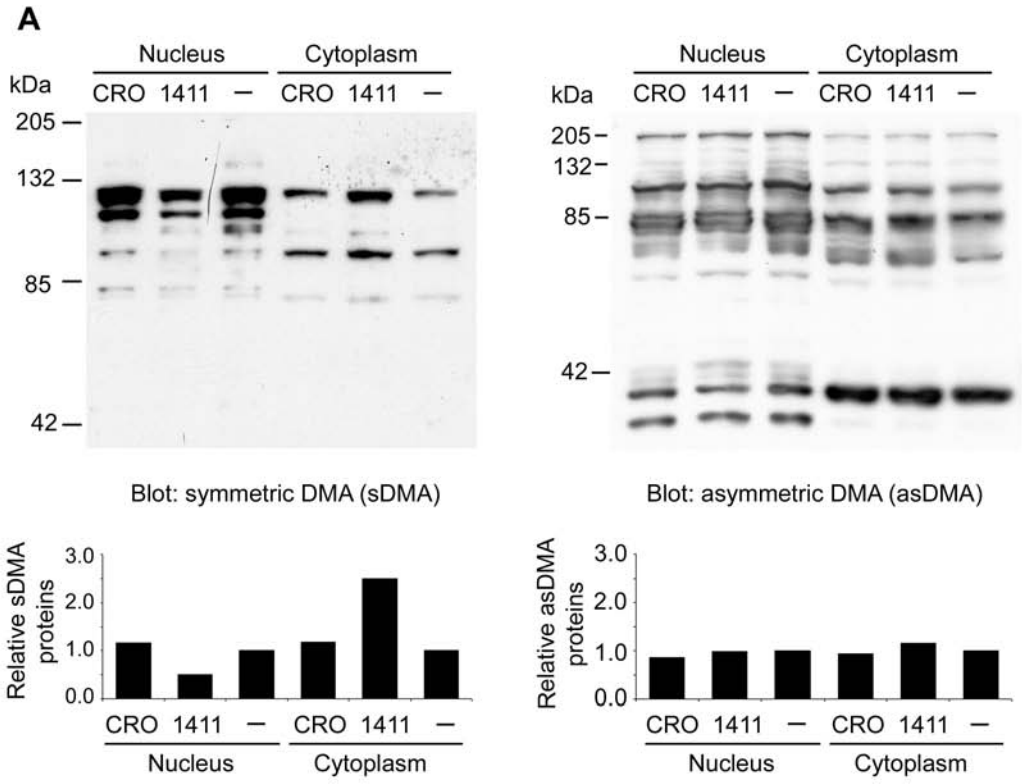
A
Nucleus
Cytoplasm
kDa
CRO 1411 – CRO 1411 –
205
132
85
42
Blot: symmetric DMA (sDMA)
Blot: asymmetric DMA (asDMA)
Relative sDMA proteins
Relative asDMA proteins
3.0
2.0
1.0
0.0
CRO 1411 – CRO 1411 –
Nucleus
Cytoplasm

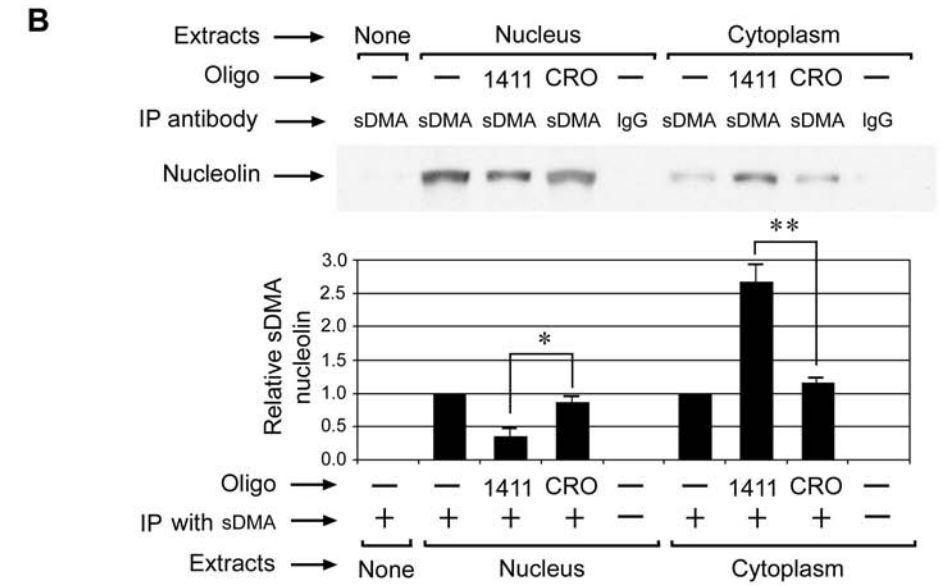
B
Extracts → None Nucleus Cytoplasm
Oligo → – – 1411 CRO – – 1411 CRO –
IP antibody → sDMA sDMA sDMA sDMA IgG sDMA sDMA sDMA IgG
Nucleolin →
Relative sDMA nucleolin
3.0
2.5
2.0
1.5
1.0
0.5
0.0
*
**
Oligo → – – 1411 CRO – – 1411 CRO –
IP with sDMA → + + + + – + + + –
Extracts → None Nucleus Cytoplasm

**C**

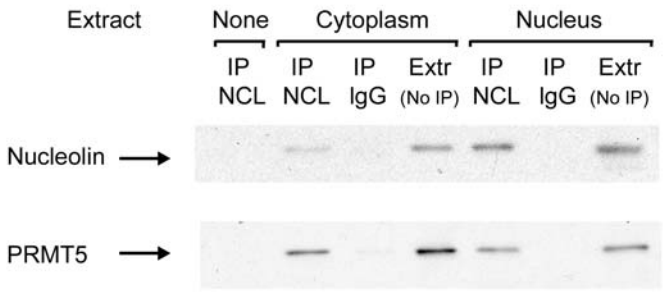


| Extracts | Fraction of Total Nucleolin Precipitated | Fraction of Total PRMT5 Co-precipitated | Fraction of Total PRMT5 Associated with NCL |
|---|---|---|---|
| Nucleus | 18.5 % | 14.5 % | 78.4 % |
| Cytoplasm | 8.3 % | 7.3 % | 88.8 % |

**D**

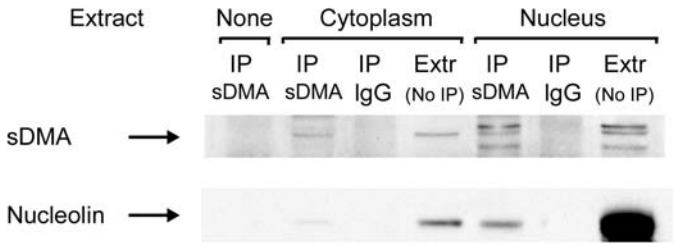


| Extracts | Fraction of sDMA Precipitated | Fraction of Total Nucleolin Co-precipitated | Fraction of Total Nucleolin with sDMA modification |
|---|---|---|---|
| Nucleus | 13.5 % | 0.7 % | 5.0 % |
| Cytoplasm | 14.2 % | 0.8 % | 5.6 % |

**Figure 4**

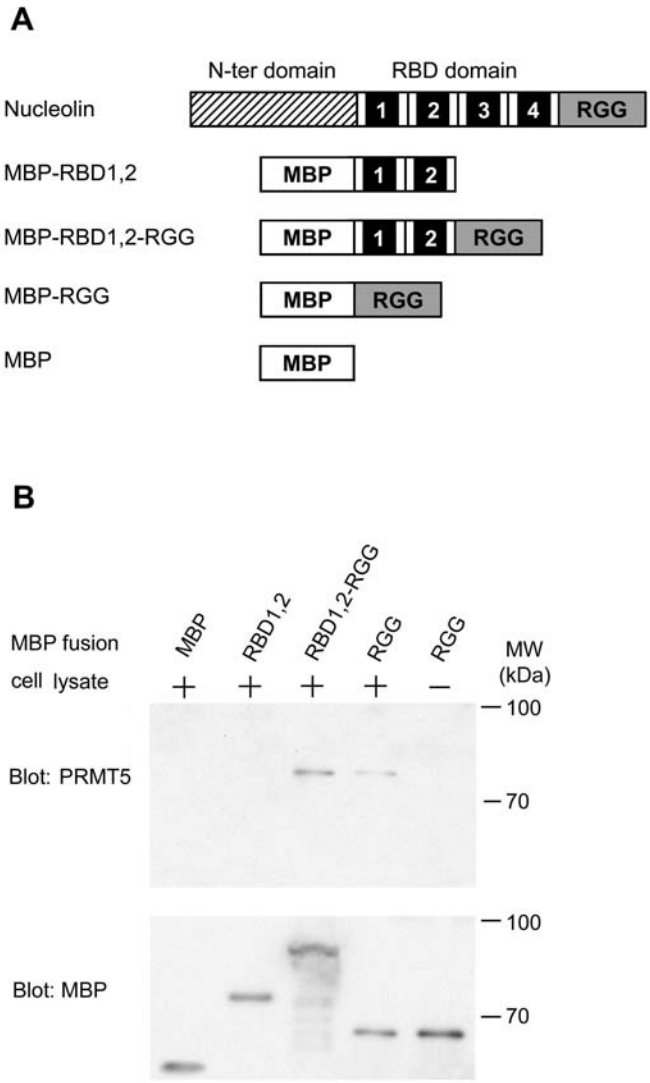
A
N-ter domain
RBD domain
Nucleolin
1
2
3
4
RGG
MBP-RBD1,2
MBP
1
2
MBP-RBD1,2-RGG
MBP
1
2
RGG
MBP-RGG
MBP
RGG
MBP
MBP
B
MBP fusion
cell lysate
MBP
RBD1,2
RBD1,2-RGG
RGG
RGG
MW
(kDa)
+
+
+
+
−
100
70
Blot: PRMT5
100
70
Blot: MBP

**Figure 5**

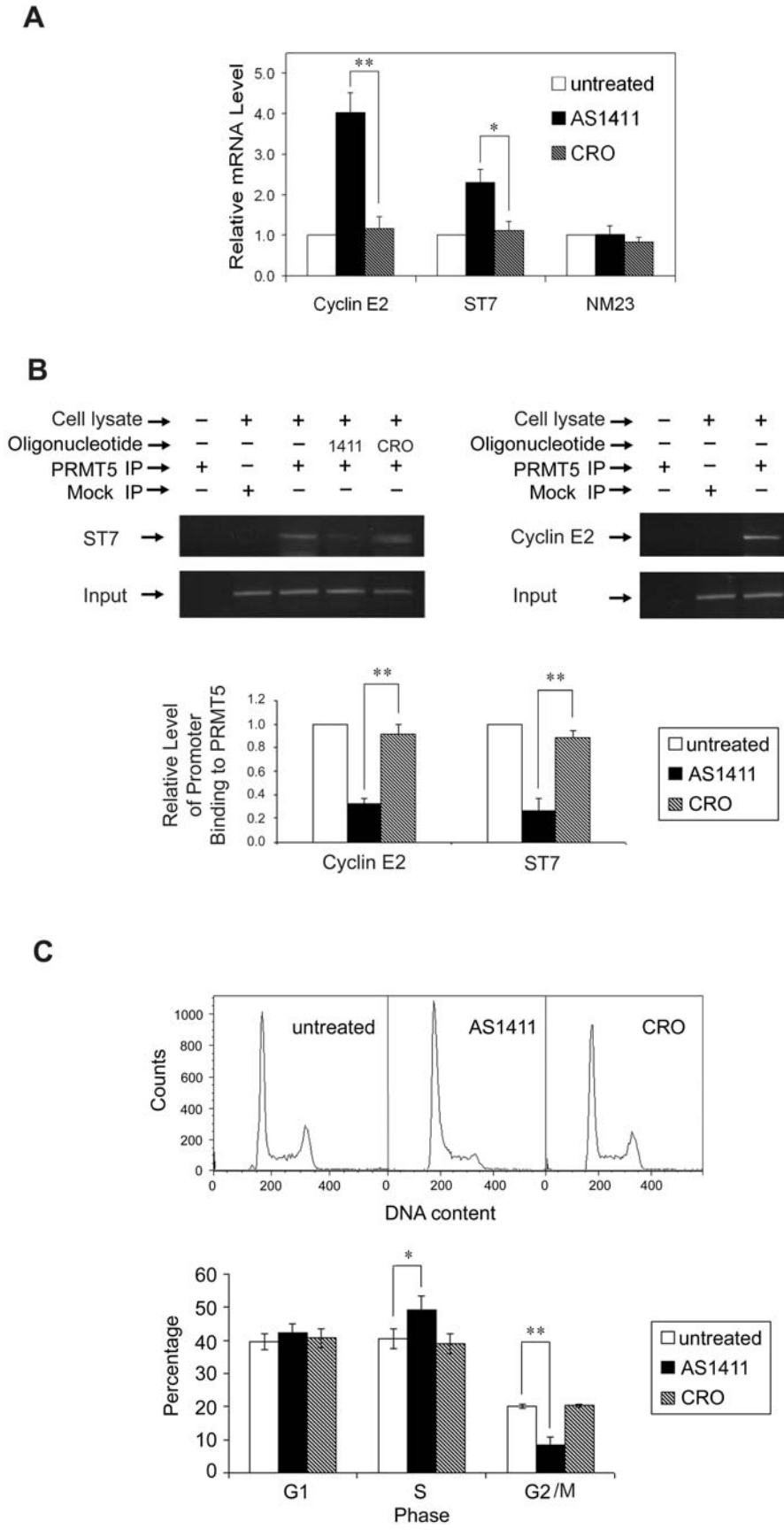
A
Relative mRNA Level
5.0
4.0
3.0
2.0
1.0
0.0
**
*
untreated
AS1411
CRO
Cyclin E2
ST7
NM23
B
Cell lysate
Oligonucleotide
PRMT5 IP
Mock IP
1411
CRO
ST7
Input
Cyclin E2
Input
Relative Level of Promoter Binding to PRMT5
1.2
1.0
0.8
0.6
0.4
0.2
0.0
**
**
Cyclin E2
ST7
untreated
AS1411
CRO
C
Counts
1000
800
600
400
200
0
untreated
AS1411
CRO
0
200
400
DNA content
Percentage
60
50
40
30
20
10
0
*
**
G1
S
G2/M
Phase
untreated
AS1411
CRO